Heavy-Quark QCD Exotica

Richard F. Lebed[a,*], Ryan E. Mitchell[b], Eric S. Swanson[c]

[a] *Department of Physics, Arizona State University, Tempe, Arizona 85287-1504, USA*
[b] *Department of Physics, Indiana University, Bloomington, Indiana 47405, USA*
[c] *Department of Physics and Astronomy, University of Pittsburgh, Pennsylvania 15260, USA*

Abstract

This review presents an overview of the remarkable progress in the field of heavy-quark exotic hadrons over the past 15 years. It seeks to be pedagogical rather than exhaustive, summarizing both the progress and specific results of experimental discoveries, and the variety of theoretical approaches designed to explain these new states.

Contents

*Corresponding author
Email addresses: richard.lebed@asu.edu (Richard F. Lebed), remitche@indiana.edu (Ryan E. Mitchell), swansone@pitt.edu (Eric S. Swanson)

1. Introduction

1.1. Overview

When one considers all the elementary particles discovered in the past two decades, the Higgs boson rightly takes center stage as the most significant example, not only by virtue of its eminent role of completing the Standard Model, but also in capturing the attention of both the scientific community and the public. However, most of the particles discovered in the current era were almost completely unexpected, and they seem to be broadly interrelated. Quite remarkably, though, no scientific consensus has yet emerged to explain all of them by means of a single, universal theoretical principle. These particles are, of course, the 30 or so observed candidate *exotic hadrons* (*i.e.*, ones that do not fit into the paradigms of either $q\bar{q}$ bosonic *mesons* or qqq fermionic *baryons* [q being a generic quark]). Most of these states have masses in the same region as conventional charmonium states (hadrons consistent with a $c\bar{c}$ bound-state structure), and indeed have so far never been observed to decay into hadrons not containing charm—and hence are called *charmoniumlike*). Almost all of the other candidate exotic hadrons appear in the $b\bar{b}$ bound-state sector and are *bottomoniumlike*. In addition, a few states have recently been observed in the lighter-quark sectors that are good candidate exotics; however, the most unambiguous candidates for exotic hadrons observed to date appear in the $c\bar{c}$ and $b\bar{b}$ sectors, and their formation, properties, and structure comprise the subject of this review.

Quantum Chromodynamics (QCD) has long been the accepted quantum field theory of the strong nuclear force responsible for holding atomic nuclei together. The three interaction charges, called *colors*, are carried by elementary strongly interacting spin-$\frac{1}{2}$ particles called *quarks*, which interact through the exchange of massless force-carrying *gauge bosons* called *gluons*. In these respects, QCD is very similar to Quantum Electrodynamics (QED), the quantum field theory of electricity and magnetism, for which the interaction charge is simply electric charge, and the gauge bosons are photons. However, QCD is much more complicated in several ways: The presence of three distinct color charges and the non-Abelian nature of the gauge group means that the gluons themselves carry color and therefore can interact with other gluons (in contrast to charge-neutral photons). More significantly, no particle—quark or gluon—carrying a net color charge has ever been experimentally isolated, a phenomenon called *color confinement*. The contrast with QED could not be more pronounced, in which it is effortless to produce free charged particles, such as electron beams. Instead, colored particles are only found in color-neutral compounds called *hadrons*, and until very recently, it was possible to classify every known hadron as a conventional meson or baryon.

The mathematical structure of the *gauge symmetry* describing the 3 color charges is that of the group SU(3), which produces an easily enumerated list of possible color-singlet combinations, and hence of possible hadron structures. The rule is very simple: Any net number of quarks (N_q quarks minus $N_{\bar{q}}$ antiquarks) that is divisible by 3, plus any number N_g of valence gluons (except for a single gluon with no quarks) can form a color singlet. Mesons have $N_q = N_{\bar{q}} = 1$, $N_g = 0$, while baryons have $N_q = 3$, $N_{\bar{q}} = 0$, $N_g = 0$ (and antibaryons of course swap $N_q \leftrightarrow N_{\bar{q}}$). "Valence" here refers just to those gluons—or, if one prefers, the total gluonic field of the hadron—affecting the overall spin (J), parity (P), and charge conjugation parity (C) quantum numbers J^{PC} of the hadron, because real QCD is so strong that innumerable gluons (not to mention virtual $q\bar{q}$ *sea quark* pairs) are constantly created and destroyed in any hadron. Then a hadron with valence structure $q\bar{q}g$ ($N_q = N_{\bar{q}} = 1$, $N_g \geq 1$) is called a *hybrid* meson, and a hadron with valence gluons ($N_g \geq 2$) but no valence quarks is called a *glueball*. Multiquark hadrons are also possible, the smallest two options being $q\bar{q}q\bar{q}$ *tetraquarks* and $qqqq\bar{q}$ *pentaquarks*. All of these hadrons except conventional mesons and baryons are called exotics.

The possibility of exotic hadrons was anticipated even before the advent of the color charge degree of freedom or of QCD, in the seminal works by Gell-Mann [1] (which introduced quarks) and Zweig [2, 3] (which introduced the equivalent "aces"). The development of the quark model provides a special intellectual resonance with the current state of affairs in exotics studies: The quark model was developed as a simple paradigm that brought order to the confusing proliferation of hadrons discovered in the 1950s and 1960s, and the current era awaits the development of an analogous resolution for exotics. As of the time of this writing, several paradigms or physical pictures have been developed to understand the known exotics, such as *hadronic molecules*, *diquarks*, and so on, and we will discuss the successes and shortcomings of each of these pictures in detail in this review. But one should be under no illusion that any single one of these pictures has yet accommodated all of the experimental data on masses, production mechanisms, decay modes, and decay rates of the exotics. Of course, it is likely that no single picture will suffice to explain all of the new data.

Even so, some interesting patterns have begun to emerge, and we will offer some opinions on the directions that the data and theory appear to be heading.

Speaking of the data, the very first charmoniumlike exotic was discovered by the Belle collaboration at KEK in 2003 [4], and although a great deal is now known about this state, it is still called $X(3872)$ to indicate its fundamentally unknown nature. It was just the first of many unforeseen states to be observed in subsequent years, some at multiple facilities and some (so far) only at one. Several of the most important experiments for uncovering these exotics are still in operation (*e.g.*, BESIII, LHCb, CMS), some are undergoing upgrades for future runs (*e.g.*, JLab12, Belle II), and yet others are in the planning/development stages (*e.g.*, $\bar{\text{P}}$ANDA). The full story of exotics is an ongoing one: It is a rich,

data-driven field producing numerous new and surprising results every year, in which novel theoretical ideas compete and are continually tested.

Our purpose in this review is to summarize and clarify the field of heavy-quark QCD exotics for non-experts. It is not meant to be completely exhaustive; dozens of experimental papers and on the order of 1000 theoretical papers have already contributed to the study of these states. Nor is it the first review dedicated to heavy-quark exotics, which date back as far as 2006 [5, 6, 7, 8, 9, 10, 11, 12, 13, 14]. In addition, several previous reviews whose subject is heavy quarkonium, or exotics in general, discuss exotics [15, 16, 17, 18, 19, 20]. We intend to paint a detailed picture, accessible to non-expert researchers, on the discovery history, current status, and future prospects of these remarkable states.

The remainder of Sec. 1 presents the key theoretical underpinnings of the states and an overview of the methods used to analyze them; Sec. 2 provides a semi-historical account (organized by physical process) of the key experimental findings on the exotics; Sec. 3 describes the leading theoretical pictures for the exotics in greater detail; Sec. 4 offers a discussion of the possible future directions for exotics studies; and Sec. 5 concludes. Appendix A summarizes the exotic candidates individually.

1.2. Distinguishing Conventional from Exotic Hadrons

In order to substantiate a claim that an exotic state has been observed, one must first ask two questions: how does one know that a state has been observed, and second, how does one know that it is exotic?

First, with regard to observation, a sufficiently long-lived charged state leaves a measurably long track in a detector, while a sufficiently long-lived neutral state leaves a measurable gap between its production point and its decay via charged particles or observed absorption in a calorimeter. Kinematical reconstruction is then used to identify the energy, momentum, and ultimately mass, of the particle. A short-lived particle is identified via the energy-time uncertainty principle as a resonant peak in the production amplitude, its mean lifetime given as the reciprocal of the full width at half maximum, Γ. The idealized form representing such a resonant state is the *Breit-Wigner amplitude*,

$$f(s) = \frac{\Gamma/2}{M - \sqrt{s} - i\Gamma/2}\,, \tag{1}$$

where $\sqrt{s} = E_{\rm CM}$ is the center-of-momentum (CM) frame energy and M is the resonant-state mass parameter (to be specific, this is a Lorentz-invariant expression of the nonrelativistic form). The absolute square $|f(s)|^2$, which is the quantity observed in a scattering cross section, gives a Lorentzian peak at $\sqrt{s} = M$ of the same type that is familiar from multiple branches of physics. However, in a physical situation one finds that the parameter Γ can assume an energy dependence, that closely spaced resonances do not assume the simple form of a sum of Breit-Wigners [21], and that other amplitude effects, such as the opening of thresholds for the formation of on-shell particles, can severely obscure the idealized form of Eq. (1). One cannot assume that every bump in a cross section corresponds to a new resonance. Fortunately, Eq. (1) also presents one additional handle for discerning resonant behavior, through the phase $\delta = \arg f(s)$ (the phase shift of scattering theory). In the neighborhood of $\sqrt{s} = M$, δ increases rapidly from 0 to π, passing through $\frac{\pi}{2}$ precisely at $\sqrt{s} = M$. The amplitude $f(s)$ exhibits a counterclockwise "looping" behavior in the Argand plane, which is taken as the standard indicator of resonant behavior, idealized Breit-Wigner or not.

Second, the procedure for deciding whether a state is conventional or exotic can be carried out at several levels. The simplest is by means of J^{PC} quantum numbers. In a nonrelativistic quark model, a $q\bar{q}$ meson with total spin angular momentum S and relative orbital angular momentum L has $P = (-1)^{L+1}$ and $C = (-1)^{L+S}$. The case $J^{PC} = 0^{--}$ and the series $J^{P=(-1)^J,\, C=(-1)^{J+1}} \in \{0^{+-},\, 1^{-+}, \ldots\}$, cannot be reached for any values of S and L, and are therefore manifestly exotic. No manifestly exotic baryon J^{PC} value occurs, however.

The known electric charges of quarks (or alternately, their isospin [for u, d] and other quark flavor [s, c, or b]) content provide another signal for exotics. A bosonic hadron with charge +2, for example, cannot be formed as a $q\bar{q}$ state, and therefore is at minimum a tetraquark. Charmoniumlike states with nonzero charge are necessarily exotic, since they must contain more valence quarks than just the (neutral) pair $c\bar{c}$; for example, the $Z_c(3900)^+$, which was the first state of this type with its discovery confirmed (in 2013) [22, 23], is believed to be a $c\bar{c}u\bar{d}$ state.

More typically, however, an exotic candidate carries the same J^{PC} and charge as some conventional state. In such circumstances, one expects the states to mix quantum-mechanically, making identification even trickier. However, even in those cases, one can make headway. If one has a principle for deciding how many states of a given J^{PC} should occur in a certain mass range and finds extras—so-called *supernumerary* states—then one can be sure that the set of these states contains an exotic component; we shall see such examples in the $J^{PC} = 1^{--}$ charmoniumlike sector. Second, a state may have the same J^{PC} and approximately the expected mass of a conventional state, but it may be difficult to produce in the expected way, or it may decay into unexpected channels or have suppressed decay rates into the expected channels. For instance, the $X(3872)$ has the same $J^{PC} = 1^{++}$ as a yet-unseen $c\bar{c}$ state, $\chi_{c1}(2P)$, but its behavior is inconsistent with expectations for the $\chi_{c1}(2P)$ in a variety of ways. In particular, its width is quite small, $\Gamma < 1.2$ MeV. The $\chi_{c1}(1P)$ state for which $\chi_{c1}(2P)$ is a radial excitation is well known, and despite being hundreds of MeV lighter and therefore having much less available phase space for decays, it has a width only slightly smaller (840 keV) than the $X(3872)$ upper bound.

1.3. Heavy Quarkonium

In order to predict a spectrum of hadronic bound states, one must make certain assumptions about quark and gluon interactions to solve their equation of motion. The complexity of the strong interaction, both in its magnitude and in the intricacies of gluon self-coupling and sea-quark production, makes for a problem that cannot be completely solved analytically, and even reliable numerical solutions (in the form of *lattice QCD* simulations) remain difficult to achieve. These effects are particularly prominent in the light-quark (u, d, s) sector, in which the quarks are manifestly relativistic. However, in the heavy-quark (c, b) sector[1], one can consider the quarks to be slowly moving color sources interacting with a background field of gluons and sea quarks—a *Born-Oppenheimer* scale separation. The typical energies associated with light quarks and glue are given by the QCD scale $\Lambda_{\rm QCD} = O(200\ {\rm MeV})$, which is larger than $m_{u,d,s}$ but much smaller than $m_{c,b}$. The production of $c\bar{c}$, $b\bar{b}$ sea-quark pairs in hadrons is also known to be suppressed, which justifies treating the $c\bar{c}$ in charmoniumlike states (or $b\bar{b}$ in bottomoniumlike states) to be valence quarks.

One can thus obtain a substantial simplification by treating the heavy quarks as interacting nonrelativistically via a chosen potential $V(r)$. The best known such example is the *Cornell potential* [24, 25] for heavy quarkonium,

$$V(r) = -\frac{\kappa}{r} + br\,, \tag{2}$$

where the first term represents the short-distance Coulomb-like one-gluon exchange interaction, while the second represents the confinement potential, ever-increasing with separation. The Cornell model has been enhanced over the years, its most thorough application being Ref. [26]. One may then solve the Schrödinger equation with the heavy-quark pair interacting through $V(r)$ just as one does for e^-p in hydrogen, thus obtaining a complete spectrum of conventional $c\bar{c}$ or $b\bar{b}$ states. The results are quite impressive: 14 $c\bar{c}$ and 17 $b\bar{b}$ states predicted by this quark-potential model have already been observed. Several of these states lie above the threshold for producing open-flavor heavy hadrons (*i.e.*, $c\bar{q} + \bar{c}q$ for $c\bar{c}$), which is the analogue to the ionization threshold for hydrogen; in other words, confinement allows for the production of prominent above-threshold resonances, which have been experimentally seen. Solving the Schrödinger equation also produces specific eigenstate wave functions, which can then be used to predict hadronic and radiative transition rates, and in turn provide comparisons to data in order to confirm a state's conventional quarkonium status.

1.4. Quarkoniumlike Exotics

The level diagram for neutral $c\bar{c}$-containing states is presented in Fig. 1. Conventional $c\bar{c}$ states are solid (black) lines labeled by Greek-letter particle names, while the lowest predicted but yet-unobserved $c\bar{c}$ states are represented by dashed (blue) lines (clusters indicating the predictions of variant models). The stunning result of the years since 2003 is the observation of all the levels marked in red and labeled as X, Y, or Z, the exotic candidates. The states of the charged charmoniumlike sector, which as noted above are manifestly exotic, are presented in Fig. 2. These figures should be considered a snapshot in time, as some of the states may disappear under closer scrutiny, while additional ones will doubtlessly be discovered. In the higher-energy (and thus not quite as easily accessible through current experiments) $b\bar{b}$ sector, 2 neutral and 2 charged exotic candidates have been observed.

The naming scheme currently in use for the new states is still not entirely settled. The labels currently employed are X, Y, Z, and P_c. The original $X(3872)$ was first seen [4] as a $J/\psi\,\pi^+\pi^-$ resonance in the decay $B^\pm \to K^\pm J/\psi\,\pi^+\pi^-$, and therefore X has generically been used to denote neutral resonances appearing in B-meson decays. However, not only has $X(3872)$ been since observed in other processes (such as at hadron colliders [27, 28]), but also some states appearing in B decays [*e.g.*, $Y(4140)$] are labeled as Y, and some states appearing so far only in other production processes [*e.g.*, $X(4350)$ in $\gamma\gamma$ fusion] are labeled as X.

The first new state observed in the *initial-state radiation* (ISR) process $e^+e^- \to \gamma_{\rm ISR}Y$ pioneered at the BaBar experiment at SLAC was seen in 2005 and named $Y(4260)$ [29]. Currently, all such states produced this way are labeled Y, but as noted above, so are a few others.

The first charged charmonium-like state was observed by Belle in 2008 [30] and was named $Z_c(4430)$. Since then, the label Z has been used for all charged quarkoniumlike bosons, but since all such states are expected to have neutral isospin partners (*e.g.*, $Z_c(3900)^+$ has an observed $Z_c(3900)^0$ partner [31, 32, 33]), the label now has come to mean exotic candidates in an isospin multiplet that has a charged member.

Bottomoniumlike states are labeled with a b subscript (Y_b, Z_b).

The Particle Data Group (PDG) [34] currently avoids the naming ambiguities in the meson sector simply by calling all charmoniumlike bosons X.

Only the label P_c is, as yet, completely unambiguous. It is used for baryonic charmoniumlike exotics (first observed in 2015 at LHCb [35]). Certainly, a clearer naming scheme for the new states is highly desirable.

[1] t quarks are so heavy that they decay weakly to b quarks long before they could form hadrons.

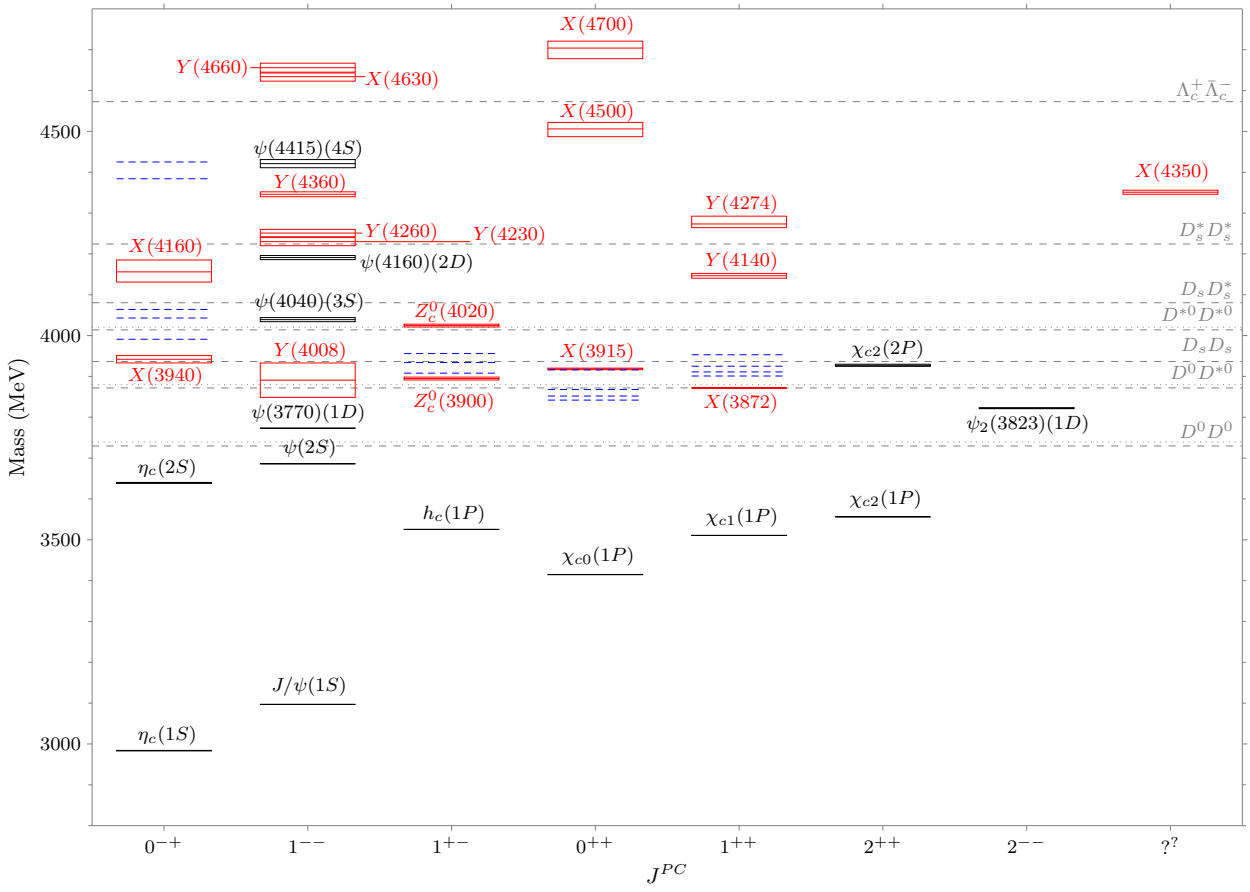

Figure 1: Level diagram for the neutral $c\bar{c}$ sector. Conventional, observed $c\bar{c}$ states are solid (black) lines labeled by Greek letters, the lowest predicted yet-unobserved conventional $c\bar{c}$ states are labeled with dashed (blue) lines (the clusters indicating predictions of several variant model calculations), and the solid (red) lines labeled by X, Y, or Z indicate exotic charmoniumlike candidates. Each measured state mass, including its central value and uncertainty, is presented as a rectangle (lines simply indicating very thin rectangles). Relevant thresholds are given by gray dashed lines; if a gray dotted line is nearby, it indicates the threshold isospin partner to the labeled dashed line. In some cases, likely quantum numbers have been assigned to states for which some uncertainty remains; this is the case, for example, for the $X(3940)$ and $X(4160)$, which have been studied as $\eta_c(3S)$, $\eta_c(4S)$ candidates. The actual known quantum numbers are listed in Table 2.

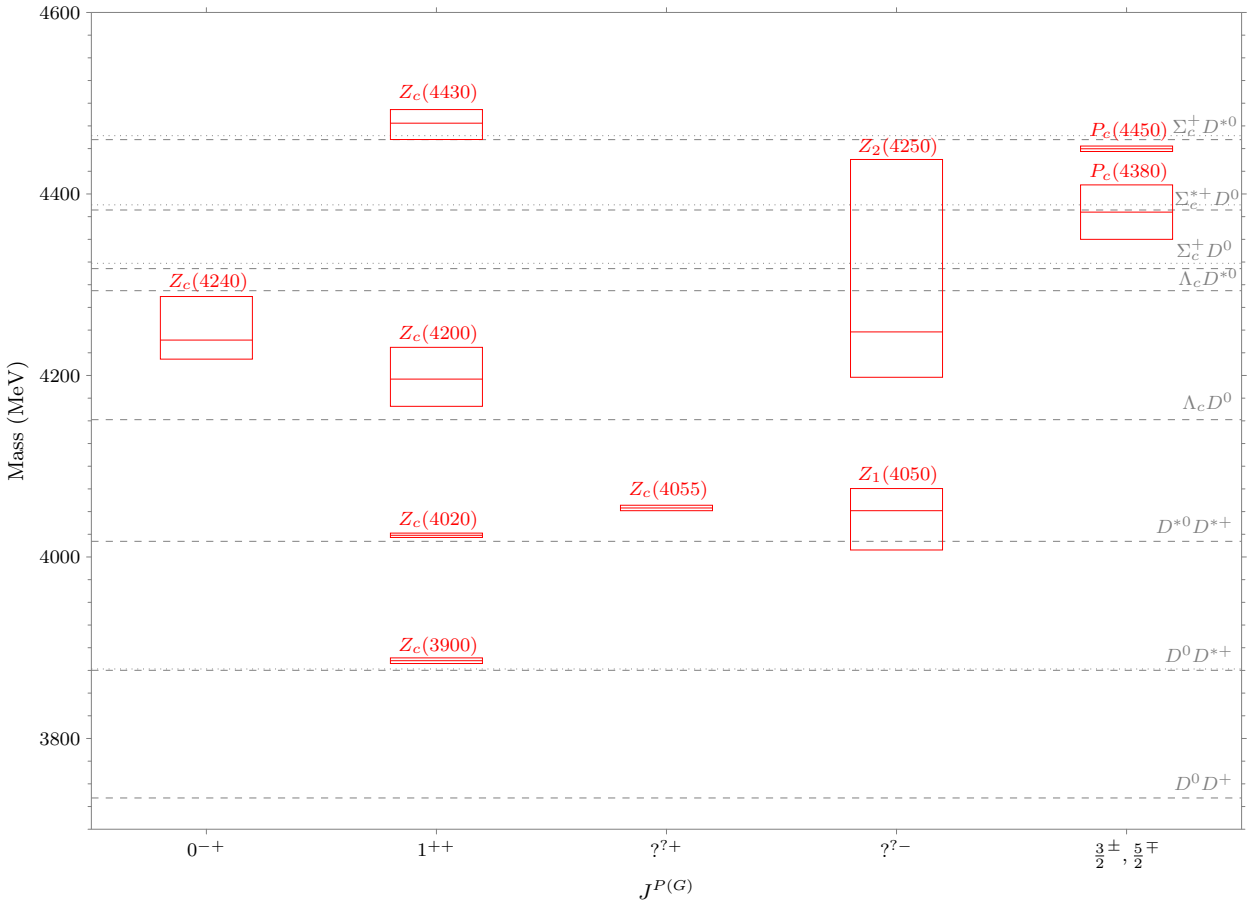

Figure 2: Charged charmoniumlike states, both bosonic and fermionic. Each measured state mass, including its central value and uncertainty, is presented as a rectangle. Relevant thresholds are given by gray dashed lines; if a gray dotted line is nearby, it indicates the threshold isospin partner to the labeled dashed line.

1.5. Overview: Models and Pictures for Exotics

The large amount of data on candidate exotic states has spawned a number of potential theoretical explanations that are summarized here and described in greater detail in the following sections. It should be emphasized that no single picture naturally accommodates all the observed states; some might turn out to be of a molecular nature, some of a hybrid nature, and so on, or a given state could easily be a quantum-mechanical mixture of more than one type. Furthermore, distinctions between some of the pictures can sometimes blur, depending upon dynamical assumptions.

1.5.1. Molecular Picture

Upon first glance, the most obvious interpretation of a tetraquark (pentaquark) state is that of a hadronic molecule of two mesons (one meson and one baryon). In this picture, each component meson is bound internally by strong QCD color forces, while the mesons bind to each other by means of a much weaker color-neutral residual QCD force, the analogue of the van der Waals attraction in chemistry. Molecules formed of separate color-neutral hadrons are of course plentiful in nature—after all, all atomic nuclei beyond hydrogen have this structure. Supporting the molecular interpretation is a mathematical fact of color algebra: A 2-quark 2-antiquark system can be assembled into a color singlet in only two independent ways; in the case of $c\bar{c}q'\bar{q}$, the combinations are $(c\bar{c})(q'\bar{q})$ and $(c\bar{q})(\bar{c}q')$, *i.e.*, either the color structure of charmonium plus a light meson, or a pair of open-charm mesons (with analogous results for pentaquarks). Indeed, the original proposal of molecules formed from charmed-meson pairs is almost as old as QCD itself [36, 37]. Similar comments hold for pentaquarks, charmed or not [38, 39]. Of course, this result alone does not necessarily imply that the quarks segregate themselves inside the tetraquark to resemble two separate hadrons. The color-singlet pairs can be completely delocalized within the tetraquark in a variety of interesting ways, the specifics of which define the other physical pictures to be described below.

The plausibility of the molecular picture is greatly substantiated by two further facts. First, a number of exotic candidates lie remarkably close to two-meson thresholds. The most impressive example is provided by the original exotic candidate, $X(3872)$, whose mass obeys $m_{X(3872)} - m_{D^{*0}} - m_{D^0} = +0.01 \pm 0.18$ MeV. This value suggests a state *at least 10 times* more weakly bound than a deuteron, which itself is already considered a weakly bound hadronic molecule. Second, the absence of evidence for near-degenerate quartets of exotic candidates containing $u\bar{u}$, $u\bar{d}$, $d\bar{u}$, and $d\bar{d}$ forming $I = 0$ and $I = 1$ isospin multiplets, despite a dedicated search [40] in this energy region, suggests a preference for binding in certain isospin channels. Such a result is natural when one supposes that the necessary molecular binding is the result of meson exchanges, and recalls that the lightest mesons π have $I = 1$. Indeed, a significant part of the binding of the $I = 0$ deuteron is accomplished through π exchange. Moreover, no prominent resonant structure seems to occur at the $D^0\bar{D}^0$ threshold [41], which is consistent with a molecular picture in which the binding is accomplished through the exchange of $J^P = 0^-$ mesons like π, since the invariance of strong interactions under rotations plus parity forbids a three-pseudoscalar coupling such as $D^0\bar{D}^0\pi$.

Not every exotic candidate lies just below a suitable threshold, however. For example, the $Z_c(3900)^+$ lies about 20 MeV above the nearest $(D\bar{D}^*)$ threshold and dominantly decays through this mode. In this case, one faces the awkward problem of attempting to form a bound state out of components into which it can freely decay. It is also worth remembering that the deuteron, unlike all charm molecules, faces no such stability issues.

In addition, the production rate of $X(3872)$ at high-energy collider experiments in the primary interaction region ("prompt" production) is observed to be comparable to that of ordinary charmonium states [27, 28]. If $X(3872)$ is a purely molecular $D^0\bar{D}^{*0} + \bar{D}^0 D^{*0}$ state (subsequently we write just the first term, the charge conjugate being understood), then presumably the two mesons form in the collision first, and they must furthermore possess a sufficiently small relative momentum—a rare occurrence in a high-energy collision—to allow their subsequent coalescence into a molecule. The large measured prompt production rate of $X(3872)$ argues against this state having a purely molecular nature [42, 43].

1.5.2. Hadrocharmonium Picture

In the *hadrocharmonium* (or more generally, *hadroquarkonium*) picture for multiquark exotics, the heavy-quark pair $Q\bar{Q}$ forms a compact core about which the light $q\bar{q}$ or qqq forms a quantum-mechanical cloud [18, 44]. The $Q\bar{Q}$ in the simplest variant of the picture forms a color singlet, in which case the light-quark cloud does as well, and their mutual binding again occurs through weak color van der Waals forces, like in molecular models. Alternately, both the core and the cloud can occur in the color-adjoint representation, thereby creating a much stronger mutual binding, but this configuration lies outside the original hadrocharmonium proposal.

The hadrocharmonium picture was originally motivated by the strong preference of several exotics to decay to conventional charmonium [*e.g.*, J/ψ, $\psi(2S)$, and χ] rather than to heavy open-flavor hadrons (D, D^*), which can naturally be viewed as the dissociation of the charmonium core from the light cloud. If the dynamics is such that the heavy degrees of freedom largely decouple from the light ones, as expected from *heavy-quark spin symmetry* [45], then the spin and wave function of the $Q\bar{Q}$ within the exotic should leave an imprint on the final-state quarkonium. For example, the preference of $Z_c(4430)$ to decay to $\psi(2S)$ rather than the $1S$ state J/ψ [46] may indicate a radially excited $c\bar{c}$ core in $Z_c(4430)$. Decays of a particular exotic state into final states with more than one $c\bar{c}$ spin [*e.g.*, both J/ψ ($s_{c\bar{c}} = 1$) and h_c ($s_{c\bar{c}} = 0$)] need not violate heavy-quark spin symmetry, as long as the exotic contains an admixture of the two spin states [47].

On the other hand, hadroquarkonium also has conceptual drawbacks. If the forces holding the state together are sufficiently weak, it is unclear why the system would persist long enough to be identified as a distinct state. If the forces are sufficiently strong, it is unclear why the quarkonium and light components would remain largely decoupled, rather than immediately rearranging into two heavy open-flavor hadrons. Indeed, the exotics that decay prominently into open-flavor pairs, such as $X(3872)$ into $D^0\bar{D}^{*0}$, do not appear to admit a satisfactory hadrocharmonium interpretation.

1.5.3. Diquark Picture

The binding of color-singlet hadrons through the triplet ($\mathbf{3}$)-antitriplet ($\bar{\mathbf{3}}$) $q\bar{q}$ combination is so familiar from the ubiquity of mesons that it is easy to forget certain other color combinations are also attractive. Of course, the baryon qqq combination also forms color-singlet hadrons, and since each of the quarks transforms as a $\mathbf{3}$, each complementary quark pair must form a color-conjugate $\bar{\mathbf{3}}$. The *diquark* combination $\mathbf{3}\otimes\mathbf{3}\to\bar{\mathbf{3}}$ must therefore be attractive in order for the baryon to be bound. Indeed, it is straightforward to compute the color dependence of the short-distance coupling of particles in $\mathrm{SU}(3)_c$ representations R_1 and R_2, whose color generators appearing at the interaction vertices are T_1^a and T_2^a, respectively, to the product representation R. The trick is precisely the one used to compute spin-spin couplings for SU(2): $\mathbf{s}_1\cdot\mathbf{s}_2=\frac{1}{2}[(\mathbf{s}_1+\mathbf{s}_2)^2-\mathbf{s}_1^2-\mathbf{s}_2^2]$. For an arbitrary group, the squares define the quadratic Casimirs $C_2(R)\equiv T_R^aT_R^a$,

$$\mathcal{C}(R,R_1,R_2)\equiv C_2(R)-C_2(R_1)-C_2(R_2)\,. \tag{3}$$

From Eq. (3), one may compute the relative size of short-distance color couplings for all qq or $q\bar{q}$ systems:

$$\mathcal{C}(R,R_1,R_2)=\frac{1}{3}(-8,-4,+2,+1)\text{ for }R=(\mathbf{1},\bar{\mathbf{3}},\mathbf{6},\mathbf{8})\,, \tag{4}$$

respectively. Unsurprisingly, the most attractive coupling is that of the color-singlet $q\bar{q}$ combination. However, the diquark $\bar{\mathbf{3}}$ coupling is also quite large, being half as strong at short distance, while the two repulsive couplings are rather weaker.

Diquarks therefore provide a promising potential source of substructure in hadronic physics, and have long been studied as such [48], particularly in the baryon sector. In the tetraquark sector, the structure is that of a bound state of a diquark and antidiquark, although such systems are often confusingly dubbed "tetraquark models" in the literature. Originally suggested for the light-quark scalar mesons $a_0(980)$ and $f_0(980)$ [49], the diquark picture was applied to the charmoniumlike exotics in Ref. [50] by means of a constituent-quark Hamiltonian including spin couplings between the quarks. Due to the equal importance of each colored quark in determining the structure of the full state (as opposed to molecular models, in which the $q\bar{q}$ pairs are first combined into color singlets), diquark models predict a rich spectrum of states. Indeed, when the pattern of observed exotics became more apparent in the past few years, the original model of [50] was found to predict too many states, and was modified through the *Ansatz* that the only significant spin couplings are the ones within each diquark [51]. In such models, the Y exotics are understood as $L=1$ orbital excitations of lower states such as $X(3872)$ (which is supported by possible observation of the decay $Y(4260)\to\gamma X(3872)$ [52]), while the lighter Z states [$Z_c(3900)$, $Z_c(4020)$] are related to the $X(3872)$ through different diquark spins and relative orientations, and $Z_c(4430)$ is a radial excitation of the $Z_c(3900)$. The P_c states can be considered analogously [53]. Even with these successes, the diquark model of [51] still predicts many more states than have yet been observed.

Additionally, a Hamiltonian treatment suggests an (approximately) common rest frame for all the components, since it implies a single, shared time coordinate. If the diquark-antidiquark $(cq)(\bar{c}\bar{q})$ pair form a relatively static molecule, then the question of stability again arises: Why should the system not simply reorganize itself into the more tightly bound open-flavor heavy-meson molecule $(c\bar{q})(\bar{c}q)$? The *dynamical diquark picture* [54] addresses this question by proposing that the diquark-antidiquark pair are created with a large relative momentum and, if below the threshold for creating extra $q\bar{q}$ pairs, can only hadronize through the long-distance tails of meson wave functions stretching between the quarks and antiquarks, providing an explanation of exotics' relatively small widths. The large diquark pair separation also gives a natural explanation for the spin *Ansatz* of Ref. [51]. The pentaquarks P_c can be constructed by an extension of the dynamical diquark attraction [55] to the color-triplet attraction of *triquarks*, $\bar{c}_{\bar{\mathbf{3}}}(qq)_{\bar{\mathbf{3}}}\to[\bar{c}(qq)]_{\mathbf{3}}$, thus describing the P_c as diquark-triquark states. However, the dynamical diquark picture has not yet been developed as a fully predictive model.

1.5.4. Hybrids

The previous sections have focused on quark dynamics for conventional and novel hadrons. As noted, an alternative way to construct novel hadrons is by admitting explicit gluonic degrees of freedom, in addition to quarks, in the state. These states are called *hybrids* [56], while states that are dominated by gluonic degrees of freedom are called *glueballs*.

The history of the development the quark model and QCD illustrates that discovering explicit nonperturbative glue can be difficult. As stated above, all the well-established mesons have J^{PC} equal to 0^{-+}, 0^{++}, 1^{++}, *etc.*, which can be created with $q\bar{q}$ pairs in a given orbital momentum state. The $q\bar{q}$ picture is supported further by the absence of mesons with isospin or strangeness greater than unity. Thus it appears that quarks are spin-$\frac{1}{2}$ entities, while the spectrum ordering suggests that energy eigenvalues increase with orbital angular momentum. In this way, the simple quark model of mesons (and baryons) was partly motivated by the *absence* of "exotic" hadrons such as multiquark or gluonic states. It is therefore perhaps no surprise that QCD exotics have been difficult to observe.

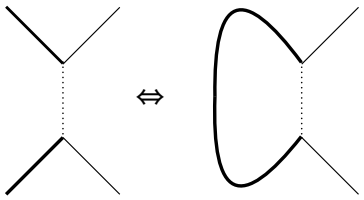

Figure 3: The relationship of scattering and self-energy amplitudes.

The simplest explanation for this absence is that gluonic degrees of freedom are somewhat "stiff" and therefore difficult to excite. Of course, with the increasing energy, luminosity, and capabilities of modern accelerators and detectors, one might hope that this impediment can be overcome.

Historically, the nonperturbative gluonic degrees of freedom have been analyzed in the context of two broad ideas: They are some sort of *string* or *flux tube*, or they manifest as an effective constituent confined by a *bag* or potential [57, 58]. Alternatively, nonperturbative glue can be thought of as either collective, nonlocal degrees of freedom, or as a local *quasiparticle* degree of freedom. More recently, lattice gauge theory computations have provided compelling evidence that nonperturbative gluons are effectively chromomagnetic quasiparticles of quantum numbers $J^{PC} = 1^{+-}$ [59] with an excitation energy of approximately 1 GeV. Thus, the lightest charmonium hybrid multiplet is expected near 4180 MeV, with quantum numbers $J^{PC} = (0, 1, 2)^{-+}$ and 1^{--}. In addition, effective field theories have been developed for hybrids that place on a rigorous footing some of the lore of the field [60].

Hybrid mesons are every bit as "hadronic" as conventional mesons, and thus convincingly identifying them will rely on developing a robust and reliable model of their spectrum and production and decay characteristics. This effort profits greatly from recent algorithmic and computational advances in lattice gauge field theory. These developments, coupled with the nascent GlueX experiment and the forthcoming $\bar{\mathrm{P}}$ANDA experiment, provide much hope for dramatic progress in the subfield.

1.5.5. Kinematical Effects

As stated above, many of the XYZ states lie near threshold and are therefore naturally associated with weakly bound molecular interpretations. Intriguingly, several of the new states lie just *above* threshold: $Z_c(3900)$ $[D\bar{D}^*]$, $Z_c(4020)$ $[D^*\bar{D}^*]$, $Z_b(10610)$ $[B\bar{B}^*]$, and $Z_b(10650)$ $[B^*\bar{B}^*]$. This fact strongly suggests that these experimental enhancements may be due to threshold rescattering rather than quark-level dynamics.

That something nontrivial can happen at a threshold can be seen with the following two-channel nonrelativistic example. Consider $a \to a$ and $a \to b$ scattering (the letters refer to channels) described by the S matrix:

$$S = \begin{pmatrix} \sqrt{1-\rho^2}\, e^{2i\delta_a} & i\rho\, e^{i(\delta_a+\delta_b)} \\ i\rho\, e^{i(\delta_a+\delta_b)} & \sqrt{1-\rho^2}\, e^{2i\delta_b} \end{pmatrix}. \tag{5}$$

Near an s-wave threshold at $E = E_0$, $\rho^2 \approx 2ck$, where c is a constant, and

$$k^2 = 2\mu_b(E - E_0). \tag{6}$$

Under these conditions,

$$\sigma(a \to a) \approx \frac{4\pi}{2\mu_a E} \left| \frac{(1-ck)\, e^{2i\delta_a} - 1}{2i} \right|^2 \approx \frac{4\pi}{2\mu_a E}(1-ck)\, \sin^2 \delta_a. \tag{7}$$

As E_0 is approached from above, $\sigma(E)$ is well behaved, but $d\sigma/dE \to -\infty$, indicating a slope discontinuity. Continuing $\sigma(E)$ below E_0 shows that this discontinuity can appear as a cusp. This effect was first pointed out by Wigner in 1948 [61] and was studied further by Baz' and Okun [62] and Nauenberg and Pais [63] in the late 1950s.

Two-particle scattering can be mapped to a two-point function by cutting a propagator (Fig. 3). Thus, the opening-channel singularity is related to the self-energy threshold singularity. Because of these connections, terms such as "threshold effect", "rescattering effect", and "cusp effect" all refer to similar dynamics, and tend to be used interchangeably.

We illustrate the two-point function behavior with a simple nonrelativistic expression for the self-energy of a scalar particle coupled to an intermediate state AB, dropping overall coefficients:

$$\Pi(s) = \int \frac{d^3q}{(2\pi)^3} \frac{\exp\left(-2q^2/\beta^2\right)}{\sqrt{s} - m_A - m_B - q^2/(2\mu_{AB}) + i\epsilon}. \tag{8}$$

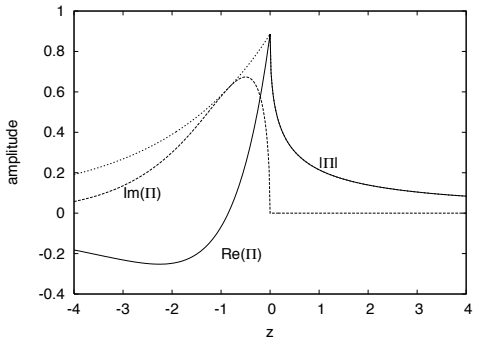

Figure 4: Self-energy $\Pi(z)$ vs. z. $|\Pi|$ for $z < 0$ is given by the dotted line.

A phenomenological exponential "form factor" with scale β has been included in the expression to account for the spatial extent of the hadrons in the process. The integral can be evaluated in closed form and is given by

$$\Pi(s) = -\frac{\mu_{AB}\beta}{(2\pi)^{3/2}} \left[1 - \sqrt{\pi z}\exp(z)\mathrm{erfc}(\sqrt{z})\right] , \tag{9}$$

with

$$z = \frac{4\mu_{AB}}{\beta^2}(m_A + m_B - \sqrt{s}). \tag{10}$$

The behavior of the self-energy [in units of the prefactor of Eq. (9)] is shown in Fig. 4. The imaginary part of the amplitude is zero for positive z (*i.e.*, below threshold) and turns on rapidly once the intermediate-state threshold is crossed. The real part of the amplitude also exhibits singular behavior near threshold [as required by the complex analyticity of $\Pi(s)$], and it is no surprise that the rate can display large enhancements just above threshold. Furthermore, the "cusp" produces phase motion that is similar to that of a Breit-Wigner amplitude (but differs in that the motion follows the real axis until threshold is reached).

Törnqvist [64] and Bugg [65, 66] have stressed the importance of this simple phenomenon for interpreting hadronic reactions for many years, highlighting, among other effects, the mechanism by which resonances are "attracted" to threshold cusps.

1.6. Theoretical Techniques

1.6.1. Quark Potential Models

Attempts to understand hadrons with potential models date from shortly after quarks were introduced by Gell-Mann [1] and Zweig [2, 3], and were based on a simple-minded extension of the quantum-number coupling techniques of nuclear physics. Early problems with the apparent lack of free quarks and fermionic quark statistics were obviated by the introduction of QCD (or, more accurately, were replaced with the color-confinement problem), which in turn led to a renaissance of the field [67, 68]. In the modern treatment, the application of simple quantum-mechanical models to the structure of hadrons is underpinned by potential nonrelativistic QCD (pNRQCD), which builds a systematic description of low-lying heavy hadrons by integrating out (*à la* Wilson) a series of large energy scales in QCD [69].

Typical quark potential models of heavy quarkonia assume a central confinement potential, often taken to be linear, a Coulombic interaction [or both, as in the Cornell potential of Eq. (2)], and supplemental QCD-motivated spin-dependent interactions. The agreement with the established charmonium and bottomonium spectra can be startling, and it is in fact difficult to understand why it continues to work for states above the open-flavor threshold. For example, a four-parameter nonrelativistic model [26] obtains the masses of the 12 charmonium masses known at the time with an average error of 0.26%.

The application of quark potential models to highly excited heavy hadrons and light hadrons is a *model* of QCD, in the sense that it is not justified by an expansion in an identifiable small parameter. Nevertheless, in the same way that Landau's *quasiparticles* emerge from strongly interacting fermionic systems, the hope is that many phenomena can be subsumed into model parameters. We remark that the potential concept is often stated to be inapplicable in the light-quark regime. However, the QCD Hamiltonian can be defined in Coulomb gauge, which induces an explicit instantaneous interaction. The presence of light quarks can greatly modify this interaction, but does not eliminate it.

Important conceptual problems nevertheless do occur once light quarks are included. For example, light quarks permit transitions between Fock sectors, and these transitions are expected to play a large role in hadronic properties high in the spectrum. Gluonic degrees of freedom must also have an impact once excitations of the order of the effective gluon mass are reached (around 1 GeV). Finally, chiral symmetry breaking is the dominant dynamical feature of QCD in the very low-energy regime, but is impossible to incorporate into simple nonrelativistic potential models.

We remark that all of these problems can be overcome with generalizations of the potential model approach: coupled-channel models can be used to model transitions, gluonic degrees of freedom can be explicitly included, relativistic kinematics and dynamics can be assumed, and chiral symmetry breaking can be incorporated with simple many-body physics techniques.

1.6.2. Meson Exchange Models

The idea that meson exchange is relevant to nuclear structure dates to a seminal paper by Yukawa in 1935 [70]. In just over a decade, Yukawa's suggestion was confirmed with the discovery of the pion. By modern standards, this saga is something of a fluke: Baryons are made of quarks, and quarks strongly interact via gluon exchange. Had Yukawa known this, he would have arrived at an infinite-ranged NN interaction—which he knew could not be right, because real nuclei have a finite size. Alternatively, had he known of color charge and confinement as well, he would have arrived at an interaction range that is too small. In fact, obtaining the correct interaction requires spontaneous chiral symmetry breaking *and* the correct amount of explicit chiral symmetry breaking in order to achieve a pion of the "correct" physical mass. This circumstance conspires to make the pion unnaturally light, and therefore ubiquitous in hadronic interactions.

Yukawa's idea has been taken to its limit by the Nijmegen [71], Bonn [72], and Argonne [73] groups, who have built extensive models of nucleon-nucleon interactions based upon the exchange of many mesons. Of course QCD is a theory of quarks and gluons, and presumably the short-range nucleon-nucleon interaction is dominated by these degrees of freedom. Since mesons couple to quarks, it is also natural to consider meson-exchange contributions to the interquark interaction, and a phenomenology of the baryon spectrum has been based on this idea [74]. We add, however, that this idea has been heavily criticized as inapplicable to mesons and incompatible with baryon phenomenology [75].

Since pion exchange provides an essential source of binding for the deuteron, it might be relevant to other hadronic interactions. The first to treat this idea seriously was Törnqvist, who found many possible bound-states of combinations of D, D^*, B, or B^* mesons [76]. The idea has found many applications to novel hadrons, especially those that couple to heavy-meson pairs in an s wave and have masses just below the decay-channel threshold.

In spite of the enthusiasm for meson-exchange dynamics, several conceptual difficulties bedevil the field. The standard approach is to consider the nonrelativistic limit of pion (or other meson) exchange for the process $AB \to AB$. For pion exchange, the resulting scattering amplitude is of the form

$$\mathcal{M} \propto \frac{(\boldsymbol{\sigma}_A \cdot \boldsymbol{q})\,(\boldsymbol{\sigma}_B \cdot \boldsymbol{q})}{\boldsymbol{q}^2 + \mu^2}\,\boldsymbol{\tau}_A \cdot \boldsymbol{\tau}_B\,,$$

where $\mu^2 = m_\pi^2 - (m_A - m_B)^2$. Here $\boldsymbol{q}$ is the momentum exchange in the process, and $\boldsymbol{\sigma}$ and $\boldsymbol{\tau}$ refer to spin and isospin. Fourier transforming this expression yields a central potential with a delta function and a tensor function that is not an admissable quantum-mechanical interaction because of its singular nature. These problems are addressed by introducing a regulator that modifies the interaction at short distance. This modification can be drastic: It is typically of the opposite sign to the central Yukawa potential and very strong at the origin. In the case of the deuteron, the regulator "core" is useful because it matches expectations for the repulsive NN core interaction. However, in general the regulator dependence is arbitrary and cannot be expected to match to reality. This problem is especially visible when repulsive Yukawa interactions are considered, since these correspond to an (unphysical) attractive core.

An additional problem arises when the masses of hadrons A and B are not equal. If the difference is large enough, μ and the interaction become imaginary. Such a result may be a reasonable analytic continuation for the amplitude, but it implies that the system should be considered as a three-body problem (A-B-π) to capture the essential dynamics.

1.6.3. Heavy Quark Symmetry

Were quarks degenerate in mass and electric charge, they would give rise to hadron multiplets degenerate in masses and couplings. This effect is well illustrated by the phenomenon of isospin symmetry, since the few-MeV difference between m_u and m_d and the QED-induced energies are small compared to the strong-interaction energy scale $\Lambda_{\rm QCD}$. In the opposite limit $\epsilon_Q \equiv \Lambda_{\rm QCD}/m_Q \to 0$, different heavy quark flavors Q become interchangeable static sources of color charge. Moreover, since the spin-dependent interactions of these quarks are suppressed by powers of ϵ_Q, one finds a near degeneracy between different spin states of heavy quarks (as seen, *e.g.*, from the relative smallness of the difference $m_{D^*} - m_D$ compared to its average, since the D and D^* differ only by the flip of the c-quark spin). Taken together, this *heavy-quark spin-flavor symmetry* [77, 78] gives rise to the powerful *heavy-quark effective theory* [79, 80], which has ϵ_Q as its expansion parameter; for a review, see [45].

Heavy-quark spin symmetry (HQSS) also plays an important role in the spectra and decays of the multiquark exotics, generally producing nearly degenerate multiplets of different spin, analogous to the D-D^* pair. Each theoretical picture

produces a distinctive set of constraints on the spectrum, once HQSS is imposed [81]. For example, the spin of the heavy $c\bar{c}$ pair in hadrocharmonium should be a conserved quantum number, so that if the $Y(4260)$ is a $J^{PC} = 1^{--}$ hadrocharmonium state, it should have a slightly lighter 0^{-+} partner, while molecular models based upon single-pion exchange should have multiplets in which a given spin state has either isospin 0 or 1 (but not both), and static diquark models should produce multiplets with dozens of states.

From the perspective of heavy-quark physics, the chief difference between the $c\bar{c}$ and $b\bar{b}$ spectra lies in the fact that $\epsilon_c \simeq 3\epsilon_b$, leading to the open-flavor threshold $(Q\bar{q})(\bar{Q}q)$ falling in a different location with respect to the conventional quarkonium states, depending upon the quark flavor. For example, the $D\bar{D}$ threshold occurs only slightly above the $\psi(2S)$, while the $B\bar{B}$ threshold occurs slightly below the $\Upsilon(4S)$, a fact used to great effect at the B factory experiments BaBar and Belle. The location of exotics with respect to open-flavor thresholds are similarly expected to be flavor dependent.

1.6.4. Chiral Unitary Models

Effective Lagrangians can also be formulated in terms of certain hadronic degrees of freedom by exploiting the *chiral symmetry* of the QCD Lagrangian under transformations $q \to \exp(i\theta\gamma_5)q$ for massless quarks q, which is broken spontaneously by quantum effects and leads, by means of *Goldstone's theorem*, to the appearance of a multiplet of massless $J^P = 0^-$ mesons. In the real world, the masses m_u, m_d (and to a lesser extent, m_s) are small but nonzero, leading to the lightness of pions (and to a lesser extent, K and η). An expansion in inverse powers of the scale $\Lambda_\chi \simeq 1$ GeV of chiral symmetry breaking, or more accurately, in powers of the typical momenta p of physical hadronic processes in the combination $\epsilon_\chi \equiv p/\Lambda_\chi$, leads to the rather successful *chiral perturbation theory* (χPT) [82].

However, χPT is only valid for $p \ll \Lambda_\chi$. As p approaches Λ_χ, the number of terms in the effective Lagrangian contributing significantly to the process increases rapidly (just like the number of terms of a Taylor series needed for the accurate representation of a function near its radius of convergence), degrading the predictive power of χPT. The key physical ingredient one can use to extend the range of usefulness of such calculations is the unitarity of the scattering matrix [83].

One such unitarization approach, called the Inverse Amplitude Method (IAM), uses χPT to fix constants that appear in a dispersion relation for the physical amplitude (which, by construction, acts as a Padé resummation of the perturbative series and satisfies unitarity). The amplitude, when re-expanded, not only reproduces the low-energy input of χPT, but can generate nonperturbative resonant poles as well. The IAM was first described for elastic scattering in [84] and for coupled-channel systems in [85].

The other common approach [86] uses the N/D method [87] and allows one to incorporate explicitly the existence of known resonant poles. Here, the numerator N and denominator D functions for a partial-wave amplitude are separately defined so as to isolate the contributions of branch cuts in various regions of the complex momentum plane corresponding to scattering processes and their crossed channels. Such an approach is advantageous in that it allows one to probe whether a given resonance has an existence independent of its couplings to other hadrons, or only appears as the dynamical effect of the rescattering of lighter hadrons. This distinction is especially interesting for multiquark exotics, where even the most basic questions of their structure remain unanswered.

1.6.5. QCD Sum Rules

The *operator product expansion* (OPE) of a two-point correlation Green's function at some momentum transfer q^2,

$$\Pi(q^2) \equiv i \int d^4x\, e^{iqx} \left\langle 0 \left| TJ(x)J^\dagger(0) \right| 0 \right\rangle , \tag{11}$$

for a quark current J of some chosen quantum numbers, forms the starting point of the *QCD sum rule* method [88]. One writes $\Pi(q)$ in two ways: as a sum of Wilson coefficients $C_n(q^2)$ times vacuum expectation values of local operators $\hat{O}_n$ that are expressed in terms of the fundamental quark and gluon degrees of freedom (the operator product side), and as a dispersion integral over the imaginary part of $\Pi(q)$, which (reminiscent of the optical theorem) can in turn can be written in terms of the hadronic spectral density function $\rho(s)$, a function of measurable masses M, decay constants f, and continuum-state form-factor contributions for all hadronic states that can couple to J:

$$\Pi(q) = \sum_n C_n \left\langle \hat{O}_n \right\rangle = \int ds\, \frac{\rho(s)}{s - q^2 + i\epsilon} , \tag{12}$$

where

$$\rho(s) = \sum_n \delta(s - M_n^2) \left\langle 0 \left| J \right| n \right\rangle \left\langle n \left| J^\dagger \right| 0 \right\rangle + \rho_{\text{cont}} = \sum_n f_n^2 \delta(s - M_n^2) + \rho_{\text{cont}} . \tag{13}$$

Choosing a value $s = s_0$ above which continuum and higher resonance ($n > 0$) contributions are expected to dominate, and performing an integral transform on both sides of the equation that gives extra weight to the lower-energy

contributions where the lightest resonance occurs (a *Borel transformation* with mass parameter M^2), one obtains a result for the lowest resonance mass M_0:

$$M_0^2 = \frac{\int_0^{s_0} ds\, e^{-s/M^2}\, s\, \rho^{\rm OPE}(s)}{\int_0^{s_0} ds\, e^{-s/M^2}\, \rho^{\rm OPE}(s)}\,. \tag{14}$$

The quantity $\rho^{\rm OPE}(s)$ here is the spectral function computed from the OPE.

A good deal of artistry is needed to achieve successful application of QCD sum rules. For example, one can obtain numerically stable results only by a careful choice of the current J, the operators $\hat{O}_n$ to include, and the values of s_0 and M. Early applications of QCD sum rules to the charmoniumlike exotics are reviewed in [89], and more recent ones in [13].

1.6.6. Lattice QCD

In 1974 Ken Wilson examined the strong-coupling behavior of QCD by discretizing the theory on a spacetime grid (called a *lattice* in the community) [90]. It was soon realized that this approach provides a representation of QCD (really, a regularization) suitable for carrying out Monte Carlo simulations [91, 92], thereby spawning the discipline of *lattice gauge field theory*. The intervening four decades have seen tremendous advances in computational abilities, with commensurate improvements in the quality of lattice calculations. At the same time, software and algorithms have progressed from an era where a single investigator could write a complete simulation in a few days, to one in which suites of sophisticated code are maintained by large collaborations.

Lattice gauge field theory computations are typically set up with scalar and spinor fields on lattice sites, and gauge fields appear on *links*, which connect two spatially separated sites, $\boldsymbol{x}$ and $\boldsymbol{x}+\boldsymbol{\mu}$. Link variables map to the gauge field $A_\mu(\boldsymbol{x})$ in the continuum limit, and provide a convenient way to maintain QCD gauge invariance. Monte Carlo computations of observables then amount to executing Markov-chain processes that iteratively equilibrate to the normalized exponentiated Euclidean action S_E,

$$\frac{\exp(-S_E)}{\int D\phi \exp(-S_E[\phi])}\,.$$

It is necessary that this factor defines a real probability density, and thus Grassmann-valued fields (spinors corresponding to dynamical fermions) must be integrated out explicitly. This integration gives rise to a determinant that must be included in the Markov process, which unfortunately introduces substantial numerical noise in the computation. Because of this limitation, early calculations either were performed in the pure gauge theory, or simply ignored the determinant (the *quenched approximation*). This impediment has been overcome in the last few years, and all modern lattice computations are now performed with dynamical quarks of varying types.

Measuring correlation functions permits the extraction of particle masses, via expressions like

$$\langle T\phi(x)\phi(0)\rangle = \frac{\int D\phi\, \phi(x)\phi(0)\, \exp(-S_E)}{\int D\phi\, \exp(-S_E)} = \sum_n |\langle n|\phi(0)|0\rangle|^2\, \exp[-(E_n - E_0)x]. \tag{15}$$

Similarly, measuring three-point or higher correlation functions permits the extraction of hadronic couplings. The matrix elements in Eq. (15) also provide information on the structure of states, although the values obtained in a simulation must be interpreted with care, since they depend upon the regularization scale.

The accomplishments of the field are impressive; among them are the establishment of color confinement, a precision computation of the pure-glue spectrum, the computation of the proton mass—along with the masses of other low-lying mesons and baryons in each flavor sector—and a convincing demonstration of the independent existence of hybrid mesons. Recently, the resonance structure of hadrons has started to be explored, the extraction of scattering parameters for simple processes has been achieved, and beyond-Standard Model physics is being explored.

We remark that hadronic properties that feature "unnatural" scales (*i.e.*, scales much smaller than the scale $\Lambda_{\rm QCD} \sim$ 200 MeV), such as in nuclear physics (*e.g.*, the deuteron binding energy 2.2 MeV), or the properties of weakly bound exotic states, remain stubbornly out of reach.

1.6.7. Born-Oppenheimer Approximation

The presence of heavy quarks in many of the exotic hadrons suggests that the Born-Oppenheimer approximation is a useful tool in the study of these systems. This approach was introduced by Born and Oppenheimer in 1927 [93] in an effort to understand atomic binding in molecules. The method relies on the large ratio of electron to nuclear masses to separate their temporal scales. Thus, electron motion can be considered in the potential created by static nuclear Coulombic sources. The energy of these systems can then be traced as a function of the positions of the nuclei, thereby generating *Born-Oppenheimer potentials*. Finally, masses can be obtained by studying nuclear dynamics in the Born-Oppenheimer potentials.

The first lattice gauge theory computation of the Born-Oppenheimer potentials for meson was made in 1983 by Griffiths *et al.* [94]. In the static limit, the quark and antiquark serve as a color source and sink, and the gluonic field

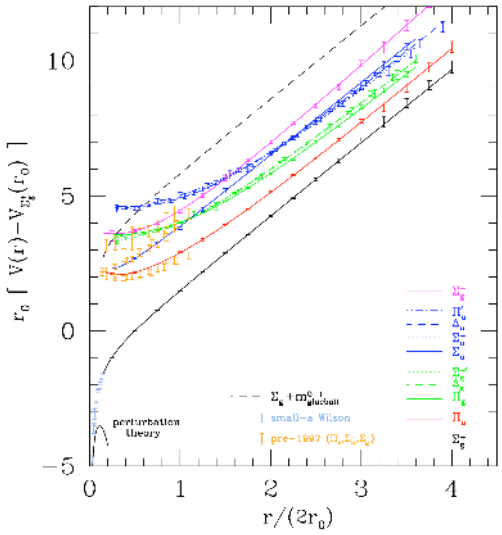

Figure 5: Lattice adiabatic hybrid potentials. The curves are labeled with diatomic quantum numbers Λ_η^Y, where Λ is the projection of the gluonic angular momentum on the quark-antiquark axis, Y represents parity under reflection through a plane containing this axis, and η is the product of gluonic parity (through the midpoint of the quark-antiquark pair) and charge conjugation. The quantity r_0 is approximately 0.5 fm. Figure courtesy of C. Morningstar.

arranges itself into configurations described by the quantum numbers of diatomic molecules. These potentials were traced in great detail in the quenched approximation by Juge *et al.* [95], and are displayed in Fig. 5.

Once nontrivial quark dynamics are permitted, the resulting mesons are interpreted as hybrids with their gluonic degrees of freedom in the appropriate representation. These energies were compared to the corresponding meson masses in a full lattice calculation by Juge *et al.*, with agreement at the 10% level. It is thus likely that the Born-Oppenheimer approximation is a useful guide to properties of (spin-averaged) heavy-quark hadrons. Subsequent work has extended the method to heavy baryons [96, 97, 98], heavy four-quark systems [99, 100, 101], and pentaquark systems [102, 103]. The use of Born-Oppenheimer techniques for the XYZ mesons is discussed in Ref. [104].

2. Experimental Foundations

2.1. Historical Sketch and Overview

A new era in the study of QCD exotica began in 2003 with the accidental discovery of the $X(3872)$. While studying the process $B \to K\psi(2S)$ with $\psi(2S) \to \pi^+\pi^- J/\psi$, the Belle Collaboration noticed a narrow peak in the invariant mass spectrum of the $\pi^+\pi^- J/\psi$ system higher than the $\psi(2S)$ mass (Fig. 6a) [4]. The peak was surprisingly narrow and did not correspond to any of the expected charmonium states from potential models. We remark that, in a not atypical happenstance, the X had previously been sighted by the E705 Collaboration at Fermilab; however, the significance of the novel peak was not appreciated at the time [105].

Immediate efforts to clarify the nature of the $X(3872)$ focused on searching for other decay modes and other production mechanisms. However, these searches only led to new experimental discoveries. It is this pattern of one unexpected result after another, with the emergence of desperately few connections, that has characterized the last 14 years of experimental studies in this field. A brief historical sketch of a few of the discoveries between 2003 and 2007 illustrates this rapidly expanding collection of QCD exotica.

(1) In the initial discovery of the $X(3872)$ with $X(3872) \to \pi^+\pi^- J/\psi$, it was noticed that the $\pi^+\pi^-$ system appears to originate from a ρ. If so, either the $X(3872)$ is an isovector (which cannot be the case for ordinary charmonium), or the $X(3872) \to \rho J/\psi$ decay violates isospin. Assuming it is the latter, a natural place to search for the $X(3872)$ is in $B \to K(\omega J/\psi)$, since the $X(3872) \to \omega J/\psi$ decay would conserve isospin. This search was quickly performed in 2005 by the Belle Collaboration, but instead of finding the $X(3872)$, a broader peak was found at a higher mass (Fig. 6b) [106]. This peak became known as the $Y(3940)$.

(2) Since the quantum numbers of the $X(3872)$ were still unknown after its discovery, it became important to search for it using several different production mechanisms. If the $X(3872)$ had $J^{PC} = 1^{--}$, it should be produced in e^+e^- annihilation. The BaBar Collaboration searched for $e^+e^- \to X(3872) \to \pi^+\pi^- J/\psi$ using *Initial State Radiation* (ISR),

where the initial e^+e^- beams had center-of-mass energy around 10 GeV, but radiated photons before colliding, thus allowing the search to cover a wide range of collision energies. Rather than finding evidence for the $X(3872)$ [107], a different peak was discovered in 2005, referred to as the $Y(4260)$ (Fig. 6c) [29].

(3) After the discovery of the $Y(4260)$ in $e^+e^- \to Y(4260) \to \pi^+\pi^- J/\psi$, it was natural to search for the $Y(4260)$ in other decay modes. Since the $Y(4260)$ decayed to $\pi^+\pi^- J/\psi$, it is expected also to decay to $\pi^+\pi^-\psi(2S)$. However, a 2007 search for the $Y(4260)$ in $e^+e^- \to \pi^+\pi^-\psi(2S)$ by the BaBar Collaboration, using the same ISR technique used in the discovery of the $Y(4260)$, did not find the $Y(4260)$, but instead found a peak at an even higher mass (Fig. 6d) [108]. This peak became known as the $Y(4360)$.

Thus, by 2007, the collection of QCD exotica had already grown to a half-dozen or so. Attempts to understand the existing peaks had only led to further peaks and puzzles. This pattern of discovery, attempts to clarify, and then new discovery, has largely continued to the present. The timeline in Fig. 7 shows a steady stream of new discoveries. While a few patterns have emerged, such as between the Z_c states (in the charmonium region) and the Z_b states (in the bottomonium region) both being observed in $e^+e^- \to \pi Z_{c,b}$, there are still many states that appear in only one production mechanism. For example, it is still not clear why the Z_c states observed in $e^+e^- \to \pi Z_c$ [such as $Z_c(3900)$] and the Z_c states observed in $B \to K Z_c$ [such as $Z_c(4430)$] are apparently mutually exclusive.

Because there have been so few connections made between different production mechanisms, this section is organized by production mechanism. Table 1 sorts the XYZ states according to production mechanism and serves as a loose outline for the following discussions. For reference, Table 2 also lists the XYZ states organized (roughly) by mass. A glossary of all observed exotic states (Appendix A) also serves as a reference.

As a final note, all of the results covered in the following are experimentally robust, unless otherwise stated.

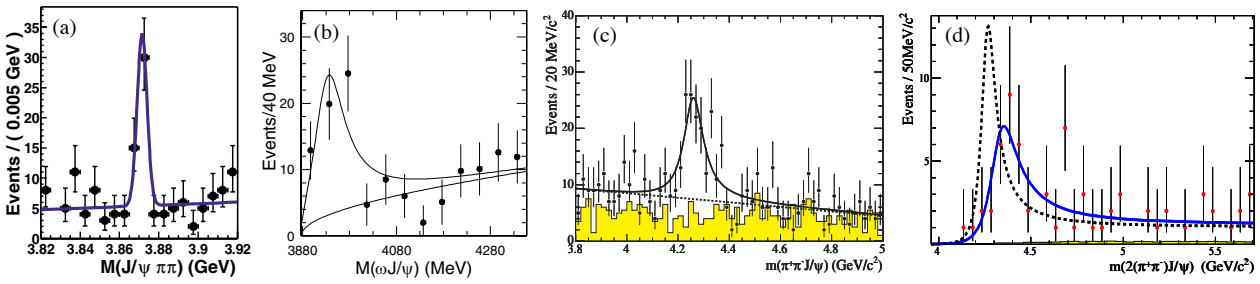

Figure 6: Earliest observations of the XYZ. (a) The $X(3872)$ was discovered in $B \to K X(3872)$ with $X(3872) \to \pi^+\pi^- J/\psi$ [4]. The $\pi^+\pi^- J/\psi$ mass spectrum is shown (from [4]). (b) The $Y(3940)$ was discovered in $B \to K Y(3940)$ with $Y(3940) \to \omega J/\psi$ [106], as part of a search for $X(3872) \to \omega J/\psi$. The $\omega J/\psi$ mass spectrum is shown (from [106]). (c) The $Y(4260)$ was discovered in $e^+e^- \to Y(4260)$ with $Y(4260) \to \pi^+\pi^- J/\psi$ [29], following a search for $e^+e^- \to X(3872)$. The $\pi^+\pi^- J/\psi$ mass spectrum is shown, along with the background estimation from J/ψ sidebands (from [29]). (d) The $Y(4360)$ was discovered in $e^+e^- \to Y(4360)$ with $Y(4360) \to \pi^+\pi^-\psi(2S)$ [108], as part of a search for $Y(4260) \to \pi^+\pi^-\psi(2S)$. The $\pi^+\pi^-\psi(2S)$ mass spectrum is shown (from [108]). The solid curve is the $Y(4360)$ and the dotted curve is how the $Y(4260)$ would appear if it decayed to $\pi^+\pi^-\psi(2S)$.

2.2. Experiments and Production Mechanisms

Before describing the individual candidates for QCD exotica, it is useful to survey a few of the general features of the experimental mechanisms used to produce them. Two of these production mechanisms, weak decays of the B and Λ_b and e^+e^- annihilation, have proven to be particularly rich in new phenomena. The experiments using each technique are listed in each of the following sections, but more detailed information on the experimental collaborations driving this field is given in Table 3.

2.2.1. B and Λ_b Decays

Mesons and baryons containing a single bottom (b) quark, such as a B meson or the Λ_b baryon, provide a good source of charmonium through the weak decay $b \to W^- c$ followed by $W^- \to s\bar{c}$. This decay of the b quark generates the decays $B \to K\psi$ and $\Lambda_b \to Kp\psi$, where ψ stands for any state containing a $c\bar{c}$ pair. With e^+e^- center-of-mass energies near the $\Upsilon(4S)$ mass (which dominantly decays to $B\bar{B}$), the BaBar and Belle experiments have traditionally led these studies. The LHCb experiment, however, using B mesons and Λ_b baryons produced in pp collisions, has recently exceeded the statistics of Belle and BaBar. Belle II, an upgrade of the Belle experiment, will also start collecting data soon.

For the decay $B \to K\psi$, the "ψ" can either be electrically neutral or charged. In the case it is neutral, and if it does not correspond to a traditional state of charmonium, it is generally referred to as an "X". This is the case for the $X(3872)$ seen to decay to $\pi^+\pi^- J/\psi$ [4]. For historical reasons, it is also sometimes called a "Y", such as for the $Y(3940)$, found decaying to $\omega J/\psi$ [106].

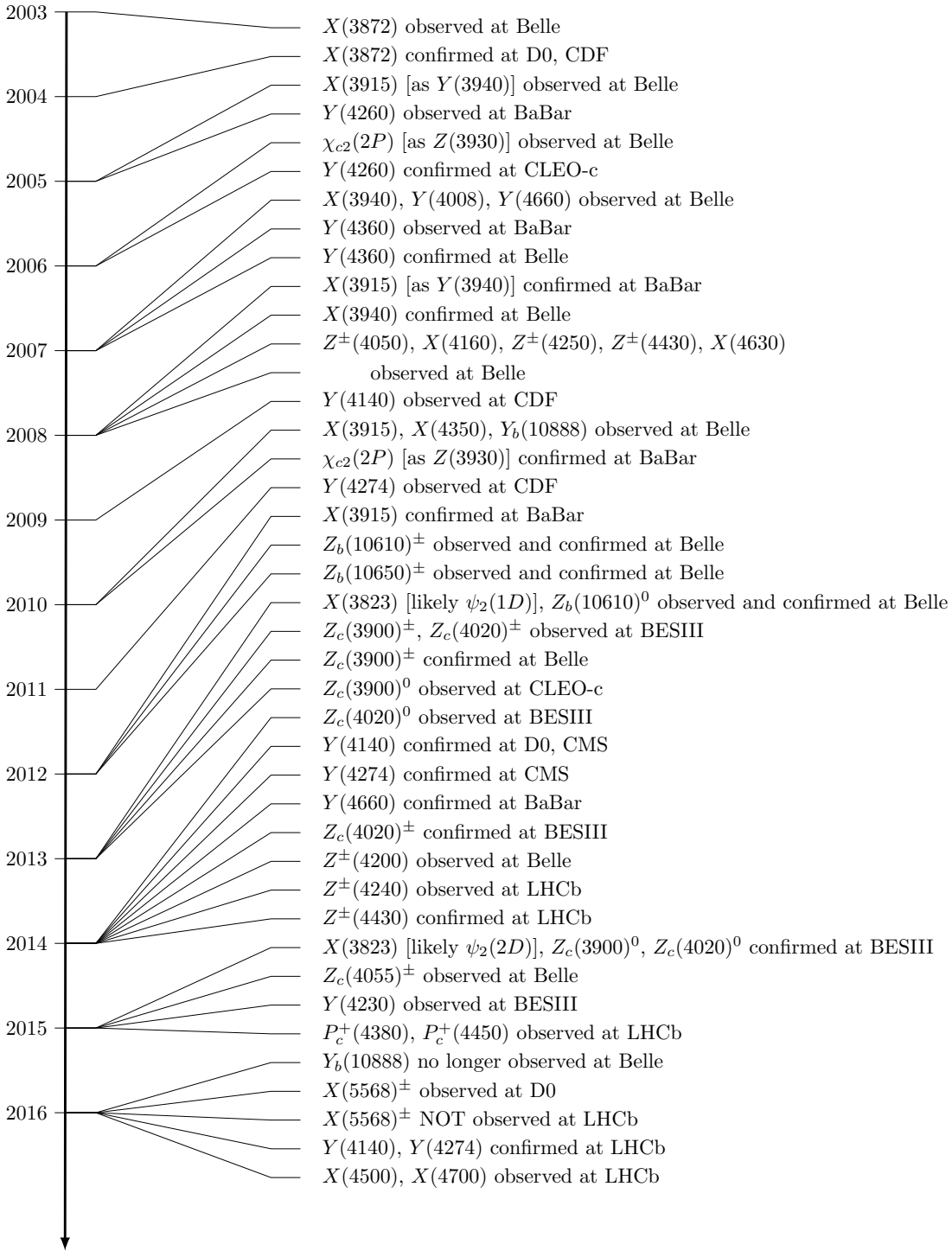

Figure 7: Timeline of discoveries of heavy-quark exotic candidates.

Table 1: Exotica organized by the way they are produced. References are given in the decay column.

Process	Production	Decay	Particle
B and Λ_b Decays	$B \to K + X$	$X \to \pi^+\pi^- J/\psi$ [4, 109, 110, 111, 112, 113, 114] $X \to D^{*0}\bar{D}^0$ [115, 116, 117] $X \to \gamma J/\psi$ [118, 119, 120, 121] $X \to \gamma\psi(2S)$ [118, 120]	$X(3872)$
		$X \to \omega J/\psi$ [106, 122, 123]	$X(3872)$ $Y(3940)$
		$X \to \gamma\chi_{c1}$ [124]	$X(3823)$
		$X \to \phi J/\psi$ [125, 126, 127, 128, 129, 130, 131, 132]	$Y(4140)$ $Y(4274)$ $X(4500)$ $X(4700)$
	$B \to K + Z$	$Z \to \pi^\pm\chi_{c1}$ [133, 134]	$Z_1(4050)$ $Z_2(4250)$
		$Z \to \pi^\pm J/\psi$ [46, 135]	$Z_c(4200)$ $Z_c(4430)$
		$Z \to \pi^\pm\psi(2S)$ [30, 135, 136, 137, 138, 139]	$Z_c(4240)$ $Z_c(4430)$
	$B \to K\pi + X$	$X \to \pi^+\pi^- J/\psi$ [140]	$X(3872)$
	$\Lambda_b \to K + P_c$	$P_c \to pJ/\psi$ [35]	$P_c(4380)$ $P_c(4450)$
e^+e^- Annihilation	$e^+e^- \to Y$	$Y \to \pi\pi J/\psi$ [23, 29, 141, 142, 143, 144, 145]	$Y(4008)$ $Y(4260)$
		$Y \to \pi\pi\psi(2S)$ [108, 146, 147, 148]	$Y(4360)$ $Y(4660)$
		$Y \to \omega\chi_{c0}$ [149]	$Y(4230)$
		$Y \to \Lambda_c\bar{\Lambda}_c$ [150]	$X(4630)$
		$Y \to \pi\pi\Upsilon(1S, 2S, 3S)$ [151, 152] $Y \to \pi\pi h_b(1P, 2P)$ [153]	$Y_b(10888)$
	$e^+e^- \to \pi + Z$	$Z \to \pi J/\psi$ [22, 23, 31, 32] $Z \to D^*\bar{D}$ [33, 154, 155]	$Z_c(3900)$
		$Z \to \pi h_c$ [156, 157] $Z \to D^*\bar{D}^*$ [158, 159]	$Z_c(4020)$
		$Z \to \pi^\pm\psi(2S)$ [148]	$Z_c(4055)$
		$Z \to \pi\Upsilon(1S, 2S, 3S)$ [160, 161, 162] $Z \to \pi h_b(1P, 2P)$ [160]	$Z_b(10610)$ $Z_b(10650)$
		$Z \to B\bar{B}^*$ [163]	$Z_b(10610)$
		$Z \to B^*\bar{B}^*$ [163]	$Z_b(10650)$
	$e^+e^- \to \gamma + X$	$X \to \pi^+\pi^- J/\psi$ [52]	$X(3872)$
	$e^+e^- \to \pi^+\pi^- + X$	$X \to \gamma\chi_{c1}$ [164]	$X(3823)$
	$e^+e^- \to J/\psi + X$	$X \to D\bar{D}^*$ [41, 165]	$X(3940)$
		$X \to D^*\bar{D}^*$ [41]	$X(4160)$
$\gamma\gamma$ Collisions	$\gamma\gamma \to X$	$X \to \omega J/\psi$ [166, 167]	$X(3915)$
		$X \to D\bar{D}$ [168, 169]	$Z(3930)$
		$X \to \phi J/\psi$ [170]	$X(4350)$
Hadron Collisions	pp or $p\bar{p} \to X+$ anything	$X \to \pi^+\pi^- J/\psi$ [27, 171, 172, 173]	$X(3872)$
		$X \to \phi J/\psi$ [174]	$Y(4140)$
		$X \to B_s\pi^\pm$ [175]	$X(5568)$

Table 2: Candidates for QCD exotica roughly organized by mass. Quantum numbers that have not been measured, but are assumed, are listed in parentheses. Unknown quantum numbers are left blank or are indicated with a question mark. References for mass and width values are given in the mass column. When only a single value has been measured or there is one dominant measurement, the value from the original reference is used. Otherwise, we quote the PDG average. References for the production processes and decay modes are given in Table 1.

Particle	$I^G J^{PC}$	Mass [MeV]	Width [MeV]	Production and Decay
$X(3823)$ $(\psi_2(1D))$	(0^-2^{--})	3822.2 ± 1.2 [176]	< 16	$B \to KX$; $X \to \gamma\chi_{c1}$ $e^+e^- \to \pi^+\pi^- X$; $X \to \gamma\chi_{c1}$
$X(3872)$	0^+1^{++}	3871.69 ± 0.17 [176]	< 1.2	$B \to KX$; $X \to \pi^+\pi^- J/\psi$ $B \to KX$; $X \to D^{*0}\bar{D}^0$ $B \to KX$; $X \to \gamma J/\psi, \gamma\psi(2S)$ $B \to KX$; $X \to \omega J/\psi$ $B \to K\pi X$; $X \to \pi^+\pi^- J/\psi$ $e^+e^- \to \gamma X$; $X \to \pi^+\pi^- J/\psi$ pp or $p\bar{p} \to X$ + any.; $X \to \pi^+\pi^- J/\psi$
$Z_c(3900)$	1^+1^{+-}	3886.6 ± 2.4 [176]	28.1 ± 2.6	$e^+e^- \to \pi Z$; $Z \to \pi J/\psi$ $e^+e^- \to \pi Z$; $Z \to D^*\bar{D}$
$X(3915)$	0^+0^{++}	3918.4 ± 1.9 [176]	20 ± 5	$\gamma\gamma \to X$; $X \to \omega J/\psi$
$Y(3940)$				$B \to KX$; $X \to \omega J/\psi$
$Z(3930)$ $(\chi_{c2}(2P))$	0^+2^{++}	3927.2 ± 2.6 [176]	24 ± 6	$\gamma\gamma \to Z$; $Z \to D\bar{D}$
$X(3940)$		$3942^{+7}_{-6} \pm 6$ [41]	$37^{+26}_{-15} \pm 8$	$e^+e^- \to J/\psi + X$; $X \to D\bar{D}^*$
$Y(4008)$	1^{--}	$3891 \pm 41 \pm 12$ [23]	$255 \pm 40 \pm 14$	$e^+e^- \to Y$; $Y \to \pi^+\pi^- J/\psi$
$Z_c(4020)$	$1^+?^{?-}$	4024.1 ± 1.9 [176]	13 ± 5	$e^+e^- \to \pi Z$; $Z \to \pi h_c$ $e^+e^- \to \pi Z$; $Z \to D^*\bar{D}^*$
$Z_1(4050)$	$1^-?^{?+}$	$4051 \pm 14^{+20}_{-41}$ [133]	82^{+21+47}_{-17-22}	$B \to KZ$; $Z \to \pi^\pm \chi_{c1}$
$Z_c(4055)$	$1^+?^{?-}$	$4054 \pm 3 \pm 1$ [148]	$45 \pm 11 \pm 6$	$e^+e^- \to \pi^\mp Z$; $Z \to \pi^\pm \psi(2S)$
$Y(4140)$	0^+1^{++}	$4146.5 \pm 4.5^{+4.6}_{-2.8}$ [125]	$83 \pm 21^{+21}_{-14}$	$B \to KY$; $Y \to \phi J/\psi$ pp or $p\bar{p} \to Y$ + any.; $Y \to \phi J/\psi$
$X(4160)$		$4156^{+25}_{-20} \pm 15$ [41]	$139^{+111}_{-61} \pm 21$	$e^+e^- \to J/\psi + X$; $X \to D^*\bar{D}^*$
$Z_c(4200)$	1^+1^{+-}	4196^{+31+17}_{-29-13} [46]	$370^{+70+70}_{-70-132}$	$B \to KZ$; $Z \to \pi^\pm J/\psi$
$Y(4230)$	0^-1^{--}	$4230 \pm 8 \pm 6$ [149]	$38 \pm 12 \pm 2$	$e^+e^- \to Y$; $Y \to \omega\chi_{c0}$
$Z_c(4240)$	1^+0^{--}	$4239 \pm 18^{+45}_{-10}$ [138]	$220 \pm 47^{+108}_{-74}$	$B \to KZ$; $Z \to \pi^\pm \psi(2S)$
$Z_2(4250)$	$1^-?^{?+}$	$4248^{+44+180}_{-29-35}$ [133]	$177^{+54+316}_{-39-61}$	$B \to KZ$; $Z \to \pi^\pm \chi_{c1}$
$Y(4260)$	0^-1^{--}	4251 ± 9 [176]	120 ± 12	$e^+e^- \to Y$; $Y \to \pi\pi J/\psi$
$Y(4274)$	0^+1^{++}	$4273.3 \pm 8.3^{+17.2}_{-3.6}$ [125]	$52 \pm 11^{+8}_{-11}$	$B \to KY$; $Y \to \phi J/\psi$
$X(4350)$	$0^+?^{?+}$	$4350.6^{+4.6}_{-5.1} \pm 0.7$ [170]	$13^{+18}_{-9} \pm 4$	$\gamma\gamma \to X$; $X \to \phi J/\psi$
$Y(4360)$	1^{--}	4346 ± 6 [176]	102 ± 10	$e^+e^- \to Y$; $Y \to \pi^+\pi^-\psi(2S)$
$Z_c(4430)$	1^+1^{+-}	4478^{+15}_{-18} [176]	181 ± 31	$B \to KZ$; $Z \to \pi^\pm J/\psi$ $B \to KZ$; $Z \to \pi^\pm \psi(2S)$
$X(4500)$	0^+0^{++}	$4506 \pm 11^{+12}_{-15}$ [125]	$92 \pm 21^{+21}_{-20}$	$B \to KX$; $X \to \phi J/\psi$
$X(4630)$	1^{--}	4634^{+8+5}_{-7-8} [150]	92^{+40+10}_{-24-21}	$e^+e^- \to X$; $X \to \Lambda_c\bar{\Lambda}_c$
$Y(4660)$	1^{--}	4643 ± 9 [176]	72 ± 11	$e^+e^- \to Y$; $Y \to \pi^+\pi^-\psi(2S)$
$X(4700)$	0^+0^{++}	$4704 \pm 10^{+14}_{-24}$ [125]	$120 \pm 31^{+42}_{-33}$	$B \to KX$; $X \to \phi J/\psi$
$P_c(4380)$		$4380 \pm 8 \pm 29$ [35]	$205 \pm 18 \pm 86$	$\Lambda_b \to KP_c$; $P_c \to pJ/\psi$
$P_c(4450)$		$4449.8 \pm 1.7 \pm 2.5$ [35]	$39 \pm 5 \pm 19$	$\Lambda_b \to KP_c$; $P_c \to pJ/\psi$
$X(5568)$		$5567.8 \pm 2.9^{+0.9}_{-1.9}$ [175]	$21.9 \pm 6.4^{+5.0}_{-2.5}$	$p\bar{p} \to X$ + anything; $X \to B_s\pi^\pm$
$Z_b(10610)$	1^+1^{+-}	10607.2 ± 2.0 [176]	18.4 ± 2.4	$e^+e^- \to \pi Z$; $Z \to \pi\Upsilon(1S, 2S, 3S)$ $e^+e^- \to \pi Z$; $Z \to \pi h_b(1P, 2P)$ $e^+e^- \to \pi Z$; $Z \to B\bar{B}^*$
$Z_b(10650)$	1^+1^{+-}	10652.2 ± 1.5 [176]	11.5 ± 2.2	$e^+e^- \to \pi Z$; $Z \to \pi\Upsilon(1S, 2S, 3S)$ $e^+e^- \to \pi Z$; $Z \to \pi h_b(1P, 2P)$ $e^+e^- \to \pi Z$; $Z \to B^*\bar{B}^*$
$Y_b(10888)$	0^-1^{--}	10891 ± 4 [176]	54 ± 7	$e^+e^- \to Y$; $Y \to \pi\pi\Upsilon(1S, 2S, 3S)$ $e^+e^- \to Y$; $Y \to \pi\pi h_b(1P, 2P)$

Table 3: Major experiments in the past, present, and future of heavy-quark exotics studies.

Experiment	Highlights	Accelerator	Years	Institute	Production
BaBar	$Y(4260)$ [29] $Y(4360)$ [108]	PEP-II	1999–2008	SLAC (Menlo Park, California, USA)	e^+e^- annihilation ($E_{\rm CM} \approx 10$ GeV): $e^+e^- \to B\bar{B}$; $B \to KX$ $e^+e^- \to Y_b$ $e^+e^- \to \pi Z_b$ $e^+e^-(\gamma_{\rm ISR}) \to Y$ $e^+e^-(\gamma_{\rm ISR}) \to \pi Z_c$ $e^+e^- \to J/\psi + X$ $\gamma\gamma \to X$
Belle	$X(3872)$ [4] $Y(3940)$ [106] $X(3915)$ [166] $Z_c(4430)$ [30, 136, 137] $Z_b(10610)$, $Z_b(10650)$ [160, 162, 163] $Y_b(10888)$ [151, 152]	KEKB	1998–2010	KEK (Tsukuba, Japan)	
Belle II	Upcoming continuation of Belle	SuperKEKB	2018–		
CLEO-c	$Y(4260)$ [142] $\pi^+\pi^- h_c$ [177]	CESR-c	2003–2008	Cornell U. (Ithaca, New York, USA)	e^+e^- annihilation ($E_{\rm CM} \approx 4$ GeV): $e^+e^- \to Y$ $e^+e^- \to \pi Z$ $e^+e^- \to \gamma X$
BESIII	$Z_c(3900)$ [22, 154] $Z_c(4020)$ [156, 158] $Y(4230)$ [149] $X(3872)$ [52]	BEPCII	2008–	IHEP (Beijing, China)	
CDF	$Y(4140)$ [126] $Y(4274)$ [132] $X(3872)$ [178, 179, 172]	Tevatron	1985–2011	Fermilab (Batavia, Illinois, USA)	$p\bar{p}$ collisions ($E_{\rm CM} \approx 2$ TeV): $p\bar{p} \to X$ + any $p\bar{p} \to B$ + any; $B \to KX$
D0	$X(3872)$ [171] $Y(4140)$ [174] $X(5568)$ [175]				
ATLAS	$\chi_b(3P)$ [180]	LHC	2010–	CERN (Geneva, Switzerland)	pp collisions ($E_{\rm CM} = 7$, 8, 13 TeV): $pp \to X$ + any $pp \to B$ + any; $B \to KX$ $pp \to \Lambda_b$ + any; $\Lambda_b \to KP_c$
CMS	$X(3872)$ [28] $Y(4140)$, $Y(4274)$ [130]				
LHCb	$Z_c(4430)$ [138, 139] $X(3872)$ [109] $P_c(4380)$, $P_c(4450)$ [35] $Y(4140)$, $Y(4274)$ [125, 131]				
COMPASS	photoproduction [181] $a_1(1420)$ [182]	SPS	2002-2011		μ/π beam on N target ($p_{beam} \approx 160$, 200 GeV) $\pi N \to XN$ $\gamma N \to XN$
$\bar{\rm P}$ANDA	Upcoming	HESR		GSI (Darmstadt, Germany)	$\bar{p}$ beam on p target ($p_{beam} \approx 1.5$–15 GeV): $p\bar{p} \to X$ $p\bar{p} \to X$ + any
GlueX	Beginning (searches for light quark hybrid mesons)	CEBAF	2016–	Jefferson Lab (Newport News, Virginia, USA)	γ beam on p target ($E_{beam} \leq 11$ GeV): $\gamma p \to Xp$
CLAS12					

By rearranging the light quarks in the decay $B \to K\psi$, the "ψ" can also be electrically charged. In this case it is usually referred to as a "Z". These electrically charged Z states are especially interesting since, if they are truly states, they must contain quarks in addition to the neutral $c\bar{c}$ pair. Prominent examples are the $Z_c(4430)$ decaying to $\pi^{\pm}\psi(2S)$ [30] and the $Z_1(4050)$ and $Z_2(4250)$ decaying to $\pi\chi_{c1}$ [133].

Similarly, in the decay $\Lambda_b \to KpJ/\psi$, there appears to be non-trivial structure in the pJ/ψ system, which cannot originate from a traditional three-quark baryon [35] (See the discussion of the $P_c(4380)$ and the $P_c(4450)$ in Sec. 2.4.3 for more detail). Other decays of the form $\Lambda_b \to Kp\,\psi$ are yet to be thoroughly explored.

2.2.2. e^+e^- Annihilation

Both the charmonium and bottomonium systems can be conveniently accessed through e^+e^- annihilation in a number of ways. The simplest is direct production through a virtual photon. In this way, the $J^{PC} = 1^{--}$ states (the ψ states in charmonium and the Υ states in bottomonium) can be produced. Using this method, BESIII and CLEO-c can produce charmonium states and BaBar, Belle, and Belle II can produce bottomonium states. Resonances typically appear as peaks in the cross section as a function of e^+e^- center-of-mass energy.

As a powerful extension of the above technique, e^+e^- annihilation experiments can also use Initial State Radiation (ISR) to probe e^+e^- collisions below the nominal center-of-mass energy. In this process, a photon is radiated by the initial e^+ or e^-, effectively lowering the center-of-mass energy of the collision. One advantage of this method is that it provides access to a whole range of e^+e^- center-of-mass energies. This improvement has allowed BaBar and Belle to survey a number of cross sections in the charmonium region, despite having nominal center-of-mass energies in the bottomonium region. In addition to the expected ψ states, a number of unexpected ones have been found as well, such as the $Y(4260)$ in $e^+e^- \to Y(4260) \to \pi^+\pi^- J/\psi$ [29]. A disadvantage of the ISR method is that the rate is severely suppressed with respect to direct production by the extra power of $\alpha_{\rm EM}$.

In e^+e^- annihilation, one can also analyze the decay products of the directly produced ψ, Υ, or Y. This approach has led to, for example, the discovery of the electrically charged Z_c and Z_b states in the process $e^+e^- \to \pi^{\mp}Z^{\pm}_{b,c}$. Using e^+e^- collisions in the bottomonium region, the states $Z_b(10610)$ and $Z_b(10650)$ were found [160], while e^+e^- collisions in the charmonium region led to the discovery of the $Z_c(3900)$ [22, 23] and the $Z_c(4020)$ [156]. It is still unclear if the e^+e^- annihilation in these processes proceeds through traditional ψ or Υ states, or through exotic Y states, or neither. Similarly, one can look for radiative transitions, such as the process $e^+e^- \to \gamma X(3872)$ [52], or for dipion transitions, such as the process $e^+e^- \to \pi^+\pi^- X(3823)$ [164].

Another method used in e^+e^- annihilation is the double-charmonium production process $e^+e^- \to J/\psi X$, where X also contains charm, and the initial e^+e^- collision energy is in the bottomonium region. Using this technique, Belle has been able to observe traditional charmonium states, such as the $\eta_c(1S, 2S)$, recoiling against the J/ψ, but has also seen the possibly exotic $X(3940)$ and $X(4160)$ [165, 41]. This technique remains relatively unexplored.

2.2.3. $\gamma\gamma$ Collisions

The e^+e^- experiments with center-of-mass energies in the bottomonium region (BaBar, Belle, and Belle II) can explore $\gamma\gamma$ collisions in the charmonium region through the process $e^+e^- \to e^+e^-X$. This technique has proven to be a powerful way to produce conventional charmonium states. For example, the BaBar Collaboration has been able to make precision measurements of the mass and width of the $\eta_c(2S)$, as well as measure new decay modes of the $\eta_c(2S)$, using $\gamma\gamma$ collisions [183, 184]. But there are several more observations that are yet to be fully understood. The $X(3915)$ (decaying to $\omega J/\psi$ [166, 167]) and the $Z(3930)$ (decaying to $D\bar{D}$ [168, 169]) are both seen clearly and are often identified with the $\chi_{c0}(2P)$ and $\chi_{c2}(2P)$ states of charmonium, respectively (although the former assignment is more controversial). The $X(4350)$ (decaying to $\phi J/\psi$ [170]) needs further experimental confirmation.

2.2.4. Hadron Collisions

The CDF and D0 experiments at Fermilab and the CMS, ATLAS, and LHCb experiments at CERN have had success producing QCD exotica in very high-energy $p\bar{p}$ (Fermilab) and pp (CERN) collisions. Direct production of particles from the initial collision (*prompt* production) is generally separated from production from subsequent B decays (*nonprompt* production) using the position of the decay vertex. The $X(3872)$ appears to have a significant prompt cross section when compared to prompt production of the $\psi(2S)$ [28]. Other states seen in hadron collisions include the $Y(4140)$ (decaying to $\phi J/\psi$ [174]) and the recently reported $X(5568)$ (decaying to $B_s\pi$ [175]).

2.3. The $X(3872)$ as the First of the XYZ

As the first of the XYZ states to be discovered, the $X(3872)$ is also the most ubiquitous and thoroughly studied. But even in 2003, after its initial discovery by Belle in the process $B \to KX(3872)$ with $X(3872) \to \pi^+\pi^- J/\psi$ [4], it was already known that the $X(3872)$ was out of the ordinary. It was narrow and had a mass suspiciously close to the $D^{*0}\bar{D}^0$ threshold. Even while its quantum numbers were not yet known, it was difficult to fit the $X(3872)$ into any of the unoccupied places in the charmonium spectrum. For example, the ${}^3D_2$ ($J^{PC} = 2^{--}$) state of charmonium could be ruled out because the upper limit on the ratio of branching fractions $B(X(3872) \to \gamma\chi_{c1})/B(X(3872) \to \pi^+\pi^- J/\psi)$ was too

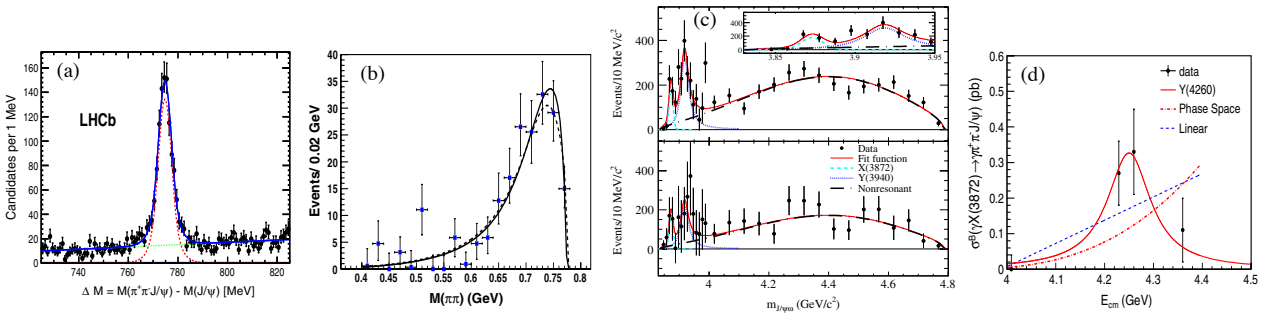

Figure 8: Properties of the $X(3872)$. (a) The latest observation of the $X(3872)$ in $B \to K(\pi^+\pi^- J/\psi)$ from LHCb [109]. Compare the size of the data sample to the earliest observation of the $X(3872)$ (Fig. 6a). This sample was used in the determination of the J^{PC} of the $X(3872)$. (b) The $\pi^+\pi^-$ mass spectrum from the decay $X(3872) \to \pi^+\pi^- J/\psi$ from Belle [110], showing the $\pi^+\pi^-$ system originates from a ρ. The two lines are for different assumptions about the orbital angular momentum in the decay to $\rho J/\psi$. (c) Observation of the decay $X(3872) \to \omega J/\psi$ from BaBar [122]. The top plot is for $B^+ \to K^+(\omega J/\psi)$ and the bottom is for $B^0 \to K^0(\omega J/\psi)$. The $X(3872)$ appears just below the $Y(3940)$. (d) The cross section as a function of center-of-mass energy for $e^+e^- \to \gamma X(3872)$ from BESIII [52]. The $Y(4260)$ assumption (solid line) is more consistent with the data than phase space or linear (dashed lines) assumptions. With only four data points, more data is required.

restrictive. And it was also too light to be the $\chi_{c1}(2P)$. Furthermore, the $\pi^+\pi^-$ system in the decay $X(3872) \to \pi^+\pi^- J/\psi$ appeared to come from a ρ, making the $X(3872)$ either isospin 1, or meaning that the $X(3872)$ has significant isospin violation in its decay. Rather than trace the historical development of facts, below we list a number of results that we currently know about the $X(3872)$ and how we know them.

1. **The $X(3872)$ exists.** The initial observation of the $X(3872)$ [discovered in $B \to KX(3872)$ with $X(3872) \to \pi^+\pi^- J/\psi$] already had a statistical significance of 10.3σ (Fig. 6a) [4]. Later observations, including using the same process used in its discovery, but with a massive increase in the size of the data sample (compare Figs. 6a and 8a) [109], have put the existence of the $X(3872)$ beyond any doubt.
2. **The mass of the $X(3872)$ is close to the $D^{*0}\bar{D}^0$ threshold.** The average value of all measurements of the $X(3872)$ mass is currently 3871.69 ± 0.17 MeV [176]. Using the current value for the D^{*0} mass, 2006.85 ± 0.05 MeV, and the D^0 mass, 1864.83 ± 0.05 MeV, the $D^{*0}\bar{D}^0$ threshold is 3871.68 ± 0.07 MeV [176]. The difference between the $X(3872)$ mass and the $D^{*0}\bar{D}^0$ threshold is therefore remarkably small, 0.01 ± 0.18 MeV. Notice that the error is dominated by the error on the $X(3872)$ mass.
3. **The $X(3872)$ is narrow.** The upper limit on the width of the $X(3872)$ is currently 1.2 MeV. This value was set by the Belle experiment in an analysis of $B \to KX(3872)$ with $X(3872) \to \pi^+\pi^- J/\psi$ [110]. Using a simultaneous fit to the B mass, the B energy, and the $\pi^+\pi^- J/\psi$ mass spectrum, they were able to overconstrain the area of the $X(3872)$ peak in the $\pi^+\pi^- J/\psi$ mass spectrum. This technique improved sensitivity to the width of the $X(3872)$, allowing for such a tight upper limit, even though the detector resolution for the mass of the $\pi^+\pi^- J/\psi$ system was around 4 MeV.
4. **The $X(3872)$ has no isospin partners.** The electrically neutral $X(3872)$ has been well-established in both of the processes, $B^+ \to K^+X(3872)$ and $\bar{B}^0 \to \bar{K}^0X(3872)$, with $X(3872) \to \pi^+\pi^- J/\psi$. If the $X(3872)$ had an electrically charged isospin partner, it would be evident in the related processes $B^+ \to K^0X^+$ and $\bar{B}^0 \to K^-X^+$ with $X^+ \to \pi^+\pi^0 J/\psi$, according to predictable isospin ratios. However, only upper limits have been determined for these related processes, inconsistent with the predicted isospin ratios [40, 110].
5. **The $X(3872)$ radiatively decays to both $\gamma J/\psi$ and $\gamma\psi(2S)$.** The LHCb experiment has made the most precise measurements of both radiative decays $X(3872) \to \gamma J/\psi$ and $X(3872) \to \gamma\psi(2S)$ [118]. The current average value for the ratio of branching fractions is $B(X(3872) \to \gamma\psi(2S))/B(X(3872) \to \gamma J/\psi) = 2.6 \pm 0.6$ [176].
6. **The $X(3872)$ decays to $\rho J/\psi$.** Once the radiative decays $X(3872) \to \gamma J/\psi$, $\gamma\psi(2S)$ are established, it follows that the $X(3872)$ has $C = +$. In the decay $X(3872) \to \pi^+\pi^- J/\psi$, the $\pi^+\pi^-$ system must then have $C = -$. Since the $\pi^+\pi^-$ system must have $C = P = (-1)^L = (-1)^J$, the only J^{PC} possibilities are 1^{--}, 3^{--}, *etc.*, of which the only plausible combination, considering the low $\pi^+\pi^-$ mass, is 1^{--}. This result is consistent with analyses of the $\pi^+\pi^-$ mass distribution, showing $X(3872) \to \rho^0 J/\psi$ (Fig. 8b) [28, 110, 178]. Note that this decay violates isospin if the $X(3872)$ has isospin 0.
7. **The $X(3872)$ has $J^{PC} = 1^{++}$.** The LHCb experiment conclusively determined the J^{PC} of the $X(3872)$ to be 1^{++} using a five-dimensional angular analysis of the process $B^+ \to K^+X(3872)$ with $X(3872) \to \rho^0 J/\psi$ and $\rho^0 \to \pi^+\pi^-$ [109]. The analysis was based on a large sample of $X(3872)$ decays (Fig. 8a), and built upon earlier J^{PC} analyses [179, 111].
8. **The $X(3872)$ decays to $\omega J/\psi$.** The BaBar experiment found evidence for the decay $B \to KX(3872)$ with $X(3872) \to \omega J/\psi$ [122]. The mass spectrum of the $\omega J/\psi$ system is dominated by the $Y(3940)$; the $X(3872)$ appears

just below it (Fig. 8c). Comparing $X(3872)$ decays to $\omega J/\psi$ with its decays to $\pi^+\pi^- J/\psi$, where the $X(3872)$ is produced in $B \to KX(3872)$ in both cases, one can determine the ratio of branching fractions, $\mathcal{B}(X(3872) \to \omega J/\psi)/\mathcal{B}(X(3872) \to \pi^+\pi^- J/\psi) = 0.8 \pm 0.3$ [118]. Note that the presence of both of these decays implies that there is isospin violation.

9. **The $X(3872)$ decays to $D^{*0}\bar{D}^0 + c.c.$** The $X(3872)$ appears as a peak just above $D^{*0}\bar{D}^0$ threshold in the process $B \to KX(3872)$ with $X(3872) \to D^{*0}\bar{D}^0 + c.c.$ [115, 116, 117]. Because of the limited available phase space, it is difficult to determine if there is a continuum $X(3872) \to D^0\bar{D}^0\pi^0$ decay in addition to the $X(3872) \to D^{*0}\bar{D}^0$ decay. Using the latest value of $\mathcal{B}(B^+ \to X(3872)K^+) \times \mathcal{B}(X(3872) \to \pi^+\pi^- J/\psi) = (0.84 \pm 0.15 \pm 0.07) \times 10^{-5}$ [112] and the latest value of $\mathcal{B}(B^+ \to X(3872)K^+) \times \mathcal{B}(X(3872) \to D^{*0}\bar{D}^0 + c.c.) = (7.7 \pm 1.6 \pm 1.0) \times 10^{-5}$ [117], one obtains the ratio $\mathcal{B}(X(3872) \to D^{*0}\bar{D}^0 + c.c.)/\mathcal{B}(X(3872) \to \pi^+\pi^- J/\psi) = 9.2 \pm 2.9$, where statistical and systematic errors have been added in quadrature.
10. **There are lower limits on $X(3872)$ branching fractions.** The BaBar experiment set an upper limit $\mathcal{B}(B^+ \to K^+X(3872)) < 3.2 \times 10^{-4}$ in a search for inclusive decays of the $X(3872)$ [185]. This upper limit, combined with measured product branching fractions, such as $\mathcal{B}(B^+ \to K^+X(3872)) \times \mathcal{B}(X(3872) \to \pi^+\pi^- J/\psi)$, allows lower limits to be calculated for $X(3872)$ branching fractions. In this way, we know $\mathcal{B}(X(3872) \to \pi^+\pi^- J/\psi) > 2.6\%$ and $\mathcal{B}(X(3872) \to D^{*0}\bar{D}^0 + c.c.) > 24\%$.
11. **The $X(3872)$ is produced in hadron collisions.** The $X(3872)$ has been seen in $p\bar{p}$ collisions with $\sqrt{s} = 1.96$ TeV at the Tevatron [27, 178, 171, 172] and in pp collisions with $\sqrt{s} = 7$ TeV at the LHC [28, 173]. The CMS experiment studied the production of the $X(3872)$ in relation to the production of the $\psi(2S)$, and found the ratio

$$R = \frac{\sigma(pp \to X(3872) + \text{anything}) \times \mathcal{B}(X(3872) \to \pi^+\pi^- J/\psi)}{\sigma(pp \to \psi(2S) + \text{anything}) \times \mathcal{B}(\psi(2S) \to \pi^+\pi^- J/\psi)} = 0.0656 \pm 0.0029 \pm 0.0065\,, \tag{16}$$

in a region of rapidity ($|y| < 1.2$) and transverse momentum ($10 < p_T < 50$ GeV) [28]. They also determined the fraction of these $X(3872)$ produced in B decays to be $0.263 \pm 0.023 \pm 0.016$, the remainder being the so-called "prompt" production. In the kinematic region studied, the ratio R appears to have no dependence on p_T.
12. **The $X(3872)$ is possibly produced in radiative decays of the $Y(4260)$.** The BESIII experiment found clear evidence for $e^+e^- \to \gamma X(3872)$ with $X(3872) \to \pi^+\pi^- J/\psi$, where the e^+e^- center-of-mass energy was in the region of the $Y(4260)$ [52]. The cross section of this process as a function of center-of-mass energy is suggestive that it proceeds through a $Y(4260)$ (Fig. 8d), which would imply the existence of the radiative decay $Y(4260) \to \gamma X(3872)$, but more data is needed before this prospect can be determined definitively.

2.4. Structure in B and Λ_b Decays

Besides the $X(3872)$, a series of other structures have been observed in B decays through $B \to KX$, where the "X" decays to charmonium and can be either electrically charged or neutral. Two of these additional structures, the $X(3823)$ decaying to $\gamma\chi_{c1}$ and the $Y(3940)$ decaying to $\omega J/\psi$, are relatively narrow and can likely be accommodated in the traditional spectrum of $c\bar{c}$ states. These will be discussed in Section 2.6. In this section we discuss the more exotic remaining structures.

Recall that if the "X" is charged [as is the case with, for example, the $Z_c(4430)$], and if the peak is not generated by a dynamical effect, then that state must be composed of at least four quarks, since additional quarks are needed beyond the neutral $c\bar{c}$ pair to give a unit of electric charge. It is the presence of this signature for an exotic state that has brought so much attention to many of these processes. But even the neutral "X" [such as the $Y(4140)$] do not fit in the traditional spectrum of $c\bar{c}$ states.

These additional "X" structures appearing in $B \to KX$ are broad, unlike the $X(3872)$, with widths ranging from roughly 100 to 400 MeV. And, with the possible exception of the $Z_c(4430)$, each has been seen in only one decay channel. It is also interesting, but possibly only a coincidence, that these structures seem to appear in pairs. The $Z_c(4430)$ and $Z_c(4240)$ are observed decaying to $\pi^\pm\psi(2S)$; the $Y(4140)$, $Y(4274)$, $X(4500)$, and $X(4700)$ are observed in $\phi J/\psi$; the $Z_1(4050)$ and $Z_2(4250)$ are reported in $\pi^\pm\chi_{c1}$; and the $Z_c(4200)$ and $Z_c(4430)$ [perhaps the same $Z_c(4430)$ as seen in $\pi^\pm\psi(2S)$] are reported in $\pi^\pm J/\psi$.

This section also includes a discussion of the decay $\Lambda_b \to K(pJ/\psi)$, since there are many similarities between this process and $B \to KX$. The physical process is similar (both including a weak decay of the bottom quark, $b \to sc\bar{c}$), and the methods used to analyze them are similar. Because anything decaying to pJ/ψ is electrically charged, contains a $c\bar{c}$ pair, and is a baryon, it must contain at least five quarks. Here again, a pair of broad states is seen decaying to pJ/ψ, the $P_c(4380)$ and $P_c(4450)$.

In the case of $B \to KX(3872)$ with $X(3872) \to \pi^+\pi^- J/\psi$ discussed above, the $X(3872)$ was sufficiently narrow to allow the neglect of interference with any possible structure in, for example, the $K\pi$ system. To determine the properties of the $X(3872)$, a one-dimensional fit to the $\pi^+\pi^- J/\psi$ mass spectrum was therefore reliable. This is not the case for the wider "X" structures produced in $B \to KX$, which require more complex methods. For example, in the decay $B \to K[\pi^\pm\psi(2S)]$, in addition to any exotic structure in the $\pi^\pm\psi(2S)$ system, one has to also contend with the K^*

resonances in the $K\pi^\pm$ system. In fact, these resonances are generally larger than the interesting structure in, for example, the $\pi^\pm\psi(2S)$ system. And, due to their non-trivial angular momenta, the K^* decays can populate the $K\pi^\pm\psi(2S)$ Dalitz plot in a way that affects the projections onto the $\pi^\pm\psi(2S)$ mass, leading to pollution by *kinematical reflections*. A number of methods have been employed to handle this problem, such as full-amplitude analyses or methods that attempt to parameterize all reasonable angular structure in the $K\pi^\pm$ system. Since many methods have been used to analyze the $Z_c(4430)$ [decaying to $\pi^\pm\psi(2S)$], they will be discussed in the following section.

2.4.1. $B \to K\pi\psi(2S)$ and the $Z_c(4430)$ Tetraquark Candidate

The $Z_c(4430)$ was first reported by the Belle experiment in the process $B \to KZ_c(4430)$ with $Z_c(4430) \to \pi^\pm\psi(2S)$ [30]. It was the first claim of an electrically charged state in the charmonium region and therefore received a lot of attention. Rather than presenting a full analysis of the Dalitz plot and angular distributions, this initial observation dealt with K^* contributions by vetoing $K\pi^\pm$ combinations with a mass within 100 MeV of the $K^*(890)$ or $K_2^*(1430)$. After applying this K^* veto, the $\pi^\pm\psi(2S)$ mass distribution was fit with a smooth background function and a Breit-Wigner distribution. The resulting $Z_c(4430)$ had a significance of 6.5σ.

The BaBar experiment objected to this method, arguing that there are many other K^* resonances besides the $K^*(890)$ and $K_2^*(1430)$ that could have an influence on the $\pi^\pm\psi(2S)$ mass spectrum. To explore the influence of these other $K\pi^\pm$ resonances, BaBar analyzed its own sample of data, which was of a comparable size to the Belle sample, using a model-independent approach [135]. They first described the angular distributions of the $K\pi^\pm$ system in bins of $K\pi^\pm$ mass, using a series of Legendre polynomials $P_l(\cos\theta)$, where θ is the angle in the $K\pi^\pm$ rest frame between the K momentum and the boost direction that takes the $K\pi^\pm$ to its lab-frame momentum. They used polynomials up to $l = 6$, which allowed for $K\pi^\pm$ resonances with spin ≤ 3. This series of Legendre polynomials has the feature that the coefficients, called moments, can be determined without needing to fit the data. BaBar then generated a Dalitz plot based upon these moments and projected it onto the $\pi^\pm\psi(2S)$ mass. They found that this projection described the $\pi^\pm\psi(2S)$ mass spectrum well, and therefore found no need for the $Z_c(4430)$ state, despite the Belle and BaBar data sets being statistically consistent.

The Belle experiment quickly improved upon the one-dimensional analysis of the $\pi^\pm\psi(2S)$ system by performing a two-dimensional Dalitz plot analysis, simultaneously analyzing both the $\pi^\pm\psi(2S)$ and $K\pi^\pm$ systems [136]. They later also performed a full amplitude analysis (four-dimensional) of the $B \to K\pi^\pm\psi(2S)$ decay, also taking into account angular distributions [137]. Both analyses, using data sets that were almost the same as the original data set, confirmed the existence of the $Z_c(4430)$. The latter found evidence that the $Z_c(4430)$ had a J^P of 1^+.

While Belle and BaBar collected samples of a few thousand $B \to K\pi^\pm\psi(2S)$ events, the LHCb experiment was able to analyze a sample roughly an order of magnitude larger. With this increase in statistics, the LHCb experiment performed a full four-dimensional amplitude analysis, confirmed the existence of the $Z_c(4430)$, and conclusively showed its J^P to be 1^+ (Fig. 9a) [138]. They also observed a lighter and wider structure in the $\pi^\pm\psi(2S)$ amplitude, the $Z_c(4240)$, with a significance of 6σ and a preferred J^P of 0^-. In addition, LHCb was able to analyze the phase motion of the $Z_c(4430)$ by replacing the $Z_c(4430)$ Breit-Wigner amplitude with a piece-wise complex constant as a function of $\pi^\pm\psi(2S)$ mass. The motion in the complex plane (the Argand diagram) is consistent with what one would expect for a resonance (Fig. 9b). As a final test, LHCb also repeated the moments method used by the BaBar experiment and found that the $\pi^\pm\psi(2S)$ mass spectrum could not be described by using reflections from the $K\pi^\pm$ system; the $Z_c(4430)$ was still needed [138, 139]. In this moments study, the existence of the broader $Z_c(4240)$ was not addressed.

2.4.2. $B \to K\phi J/\psi$ and the $Y(4140)$ and More

Like the $Z_c(4430)$, produced in $B \to KZ_c(4430)$ with $Z_c(4430) \to \pi^\pm\psi(2S)$, the $Y(4140)$, produced in $B \to KY(4140)$ with $Y(4140) \to \phi J/\psi$, had a controversial beginning. It was first reported by the CDF experiment [126], but with a significance of only 3.8σ from a sample of fewer than 100 B^+ decays. It was not confirmed by the LHCb [127] and BaBar [128] experiments, but it was confirmed by the D0 experiment [129], each using samples of a few hundred B decays. The CMS experiment [130], using a sample of around 2000 B decays, found a 5σ-significance signal for the $Y(4140)$. Complicating the situation, both the original CDF analysis [126] and the higher-statistics CMS analysis [130] also reported the existence of a higher-mass state, the $Y(4274)$, although the masses reported for the state were significantly different. All of these initial analyses were performed by fitting only the one-dimensional $\phi J/\psi$ mass spectrum, neglecting any influence from the $K\phi$ system.

Similar to the story of the $Z_c(4430)$, the status of the $Y(4140)$ remained in limbo until a higher-statistics analysis from the LHCb experiment was performed [125, 131]. Using more than 4000 B^+ decays with relatively small backgrounds, the LHCb experiment in fact not only confirmed the existence of the $Y(4140)$ and the $Y(4274)$, with significances of 8.4σ and 6.0σ, respectively, but also reported another pair of peaks, the $X(4500)$ and $X(4700)$, with significances greater than 5σ (Fig. 9c). Using a full six-dimensional amplitude analysis, including K^* resonances in the $K\phi$ system and descriptions of all decay angular distributions, the J^{PC} of the $Y(4140)$ and the $Y(4274)$ were both determined to be 1^{++}. The J^{PC} values of the higher-mass $X(4500)$ and $X(4700)$ were both found to be 0^{++}.

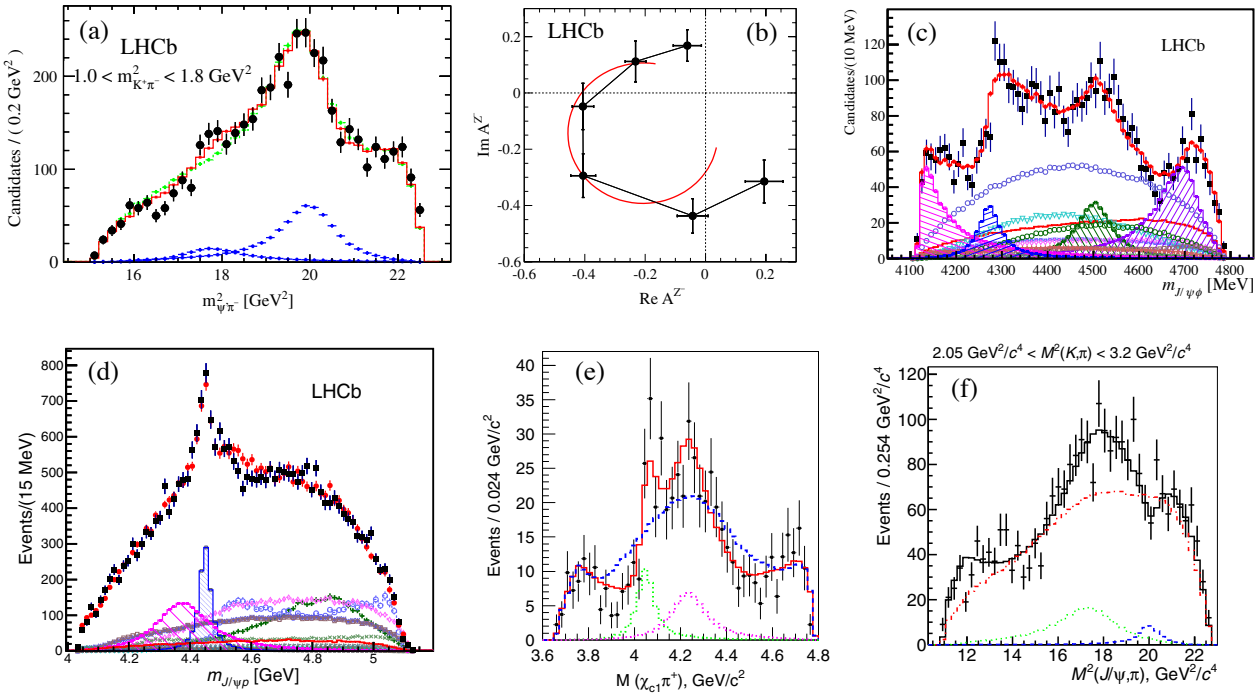

Figure 9: QCD exotica found in B and Λ_b decays. (a) Observation of the $Z_c(4200)$ and $Z_c(4430)$ at LHCb in $B \to K(\pi^\pm\psi(2S))$ [138]. (b) Argand diagram for the $Z_c(4430)$ [138]. (c) Observation of the $Y(4140)$, $Y(4274)$, $X(4500)$, and $X(4700)$ by LHCb in $B \to K(\phi J/\psi)$ [125]. (d) Observation of the $P_c(4380)$ and $P_c(4450)$ by LHCb in $\Lambda_b \to K(pJ/\psi)$ [35]. (e) Observation of the $Z_1(4050)$ and $Z_2(4250)$ by Belle in $B \to K(\pi^\pm\chi_{c1})$ [133]. (f) Observation of the $Z_c(4200)$ and evidence for the $Z_c(4430)$ by Belle in $B \to K(\pi^\pm J/\psi)$ [46].

2.4.3. $\Lambda_b \to KpJ/\psi$ and the P_c Pentaquark Candidates

The experimental analysis of the decay $\Lambda_b \to K(pJ/\psi)$ is very similar to that of $B \to K[\pi^\pm\psi(2S)]$ and $B \to K(\phi J/\psi)$ discussed above. Using a sample of around 26,000 Λ_b decays, LHCb performed a full amplitude analysis of the process $\Lambda_b \to K(pJ/\psi)$, which included all known Λ states decaying to Kp [35]. Two additional amplitudes in the pJ/ψ system were needed to describe the data, both found with more than 9σ significance (Fig. 9d). The lighter one, the $P_c(4380)$, was wide, with a width around 200 MeV; the heavier one, the $P_c(4450)$, was narrow, with a width around 40 MeV. The favored J^P of the $P_c(4380)$ and $P_c(4450)$ were found to be $\frac{3}{2}^-$ and $\frac{5}{2}^+$, respectively, although the combinations $(\frac{3}{2}^+, \frac{5}{2}^-)$ and $(\frac{5}{2}^+, \frac{3}{2}^-)$ could not be ruled out. The Argand diagram for the narrower $P_c(4450)$ was found to be consistent with a resonance; the Argand diagram for the wider $P_c(4380)$ was more uncertain and depends more upon the details of the pK amplitudes, which are not precisely known.

2.4.4. Other B Decays

Like the decays $B \to K\pi^\pm\psi(2S)$, $B \to K\phi J/\psi$, and $\Lambda_b \to KpJ/\psi$ discussed above, the decays $B \to K\pi^\pm\chi_{c1}$ and $B \to K\pi^\pm J/\psi$ also possibly show evidence for pairs of exotic structures decaying to charmonium. The $Z_1(4050)$ and $Z_2(4250)$, decaying to $\pi^\pm\chi_{c1}$, were reported by the Belle experiment in a Dalitz plot analysis of the decay $B \to K\pi^\pm\chi_{c1}$ (Fig. 9e) [133], while the $Z_c(4200)$ and $Z_c(4430)$, decaying to $\pi^\pm J/\psi$, were reported by Belle in an amplitude analysis of the decay $B \to K\pi^\pm J/\psi$ (Fig. 9f) [46]. The $Z_c(4430)$ decaying to $\pi^\pm J/\psi$ is consistent with the $Z_c(4430)$ decaying to $\pi^\pm\psi(2S)$ and is perhaps the only one of the family of Z structures to be seen in multiple decays. The three new Z structures reported by Belle were each found to have significances of greater than 5σ, while the $Z_c(4430)$ decay to $\pi J/\psi$ was found with a significance of 4.0σ.

The BaBar experiment has also analyzed both of these channels using the same moments method discussed above [135, 134]. No evidence for the Z structures was found in either case. An investigation of these two channels with higher statistics, perhaps by the LHCb experiment, is therefore needed.

2.5. Structure in e^+e^- Annihilation

When proceeding through a single virtual photon, e^+e^- annihilation should in principle be a relatively straightforward way to produce vector mesons and study their decays. The lowest-lying ψ states of charmonium, the J/ψ, $\psi(2S)$, and $\psi(3770)$, and the lowest-lying states of bottomonium, the $\Upsilon(1S)$, $\Upsilon(2S)$, $\Upsilon(3S)$, and $\Upsilon(4S)$, have been produced and

studied using e^+e^- annihilation for over 35 years. However, raising the center-of-mass energies of the e^+e^- collisions significantly above the threshold to produce open-charm or open-bottom states [the $\psi(3770)$ lies just above $D\bar{D}$ threshold and the $\Upsilon(4S)$ lies just above $B\bar{B}$ threshold] has led to a number of surprises that are yet to be understood. Before presenting more detail about the structures seen in e^+e^- annihilation, we first provide a short chronology of how these discoveries have unfolded. This narrative serves to illustrate the parallels between charmonium and bottomonium, and how developments in one have led to new studies and discoveries in the other.

(1) The surprises in e^+e^- annihilation began in 2005 with the discovery of the $Y(4260)$ by the BaBar experiment [29]. BaBar used initial-state radiation (ISR) to study the energy dependence of the cross section for $e^+e^- \to \pi^+\pi^- J/\psi$; the $Y(4260)$ appeared as an unexpected peak at 4.26 GeV. This result was soon followed by the 2007 discovery of the $Y(4360)$ by BaBar in the cross section for $e^+e^- \to \pi^+\pi^-\psi(2S)$ using the same procedure [108]. (Also see Sec. 2.1 and Figs. 6c and 6d.)

(2) In 2008, the Belle experiment, looking for a bottomonium analogue of the $Y(4260)$ or $Y(4360)$, studied the cross sections for $e^+e^- \to \pi^+\pi^-\Upsilon(1S, 2S)$ at a center-of-mass energy corresponding to the $\Upsilon(5S)$ mass [186]. The cross sections were found to be anomalously large, indicating either the presence of an underlying exotic state, or $\Upsilon(5S) \to \pi^+\pi^-\Upsilon(1S, 2S)$ partial widths several orders of magnitude larger than the measured $\Upsilon(4S) \to \pi^+\pi^-\Upsilon(1S, 2S)$ partial widths. In 2010, Belle extended this study by analyzing several center-of-mass energies in the region surrounding the $\Upsilon(5S)$ [151]. The peak in the $e^+e^- \to \pi^+\pi^-\Upsilon(1S, 2S, 3S)$ cross sections appeared to be shifted from the $\Upsilon(5S)$ mass, leading to the postulation of the $Y_b(10888)$.

(3) In 2011, the CLEO-c experiment found that the $e^+e^- \to \pi^+\pi^- h_c(1P)$ cross section in the region of the $Y(4260)$ was of a comparable size to the $e^+e^- \to \pi^+\pi^- J/\psi$ cross section [177]. This result was a surprise, because if e^+e^- proceeds through the production of a conventional $s_c = 1$ charmonium state, as expected, the process $e^+e^- \to \pi^+\pi^- h_c(1P)$ would involve a spin flip, and therefore ought to be strongly suppressed with respect to the process $e^+e^- \to \pi^+\pi^- J/\psi$, which would not involve a spin flip.

(4) In 2012, motivated by the observation of $e^+e^- \to \pi^+\pi^- h_c(1P)$, the Belle experiment performed a search for $e^+e^- \to \pi^+\pi^- h_b(1P, 2P)$ [187]. Neither the $h_b(1P)$ nor the $h_b(2P)$ had yet been discovered. Belle not only discovered both states, but also found that the $e^+e^- \to \pi^+\pi^- h_b(1P, 2P)$ cross sections in the region of the $\Upsilon(5S)$ were of comparable size to the cross sections for $e^+e^- \to \pi^+\pi^-\Upsilon(1S, 2S, 3S)$, which parallels the situation in charmonium.

(5) Also in 2012, as a follow-up to their discovery of $e^+e^- \to \pi^+\pi^- h_b(1P, 2P)$, the Belle experiment analyzed the substructure in the five processes $e^+e^- \to \pi^+\pi^- h_b(1P, 2P)$ and $e^+e^- \to \pi^+\pi^-\Upsilon(1S, 2S, 3S)$, where the e^+e^- collisions were again in the region of the $\Upsilon(5S)$ [160]. They found two electrically charged Z_b states, the $Z_b(10610)$ and the $Z_b(10650)$, in the process $e^+e^- \to \pi^\pm Z_b$, where both Z_b states decayed to all of $\pi^\pm h_b(1P, 2P)$ and $\pi^\pm\Upsilon(1S, 2S, 3S)$. The $Z_b(10610)$ has a mass near the $B\bar{B}^*$ threshold; the $Z_b(10650)$ has a mass near the $B^*\bar{B}^*$ threshold.

(6) In 2013, the BESIII experiment used e^+e^- collisions with center-of-mass energies at the $Y(4260)$ mass to study substructure in the process $e^+e^- \to \pi^+\pi^- J/\psi$ [22]. They observed the electrically charged $Z_c(3900)$ in the process $e^+e^- \to \pi^\pm Z_c(3900)$, with $Z_c(3900) \to \pi^\mp J/\psi$. This process was simultaneously discovered by the Belle experiment, except using ISR instead of direct production of the $Y(4260)$ [23]. The $Z_c(4020)$ was also discovered in 2013 by the BESIII experiment in the process $e^+e^- \to \pi^\pm Z_c(4020)$, with $Z_c(4020) \to \pi^\mp h_c(1P)$ [156]. Similar to the case of bottomonium, the charmoniumlike $Z_c(3900)$ and $Z_c(4020)$ are near the $D\bar{D}^*$ and $D^*\bar{D}^*$ thresholds, respectively.

We have therefore uncovered a number of parallels between charmonium and bottomonium. In the charmonium system, there is a series of unexplained "Y" states decaying to charmonium, such as the $Y(4260)$ and the $Y(4360)$; in bottomonium, there may be an exotic state with mass similar to the $\Upsilon(5S)$ [or at least unexpectedly large decays of the $\Upsilon(5S)$ to other bottomonium states]. In the charmonium system, the $Z_c(3900)$ and $Z_c(4020)$ lie near the $D\bar{D}^*$ and $D^*\bar{D}^*$ thresholds, respectively; in bottomonium, the $Z_b(10610)$ and $Z_b(10650)$ lie near the $B\bar{B}^*$ and $B^*\bar{B}^*$ thresholds, respectively. In the following, we discuss the bottomonium and charmonium regions separately.

2.5.1. Cross Sections in the Bottomonium Region

Above the $\Upsilon(4S)$, which has a mass just above the threshold to produce $B\bar{B}$ pairs, the inclusive $e^+e^- \to b\bar{b}$ cross section $\sigma(b\bar{b})$ clearly shows two additional peaks [151, 188, 152]. These peaks are illustrated in Fig. 10a, where $\sigma(b\bar{b})$ is normalized by the Born cross section $\sigma^0_{\mu\mu}$ (for $e^+e^- \to \mu^+\mu^-$) to form the variable $R_b \equiv \sigma(b\bar{b})/\sigma^0_{\mu\mu}$. These two peaks are the $\Upsilon(10860)$ and the $\Upsilon(11020)$, often abbreviated as the $\Upsilon(5S)$ and the $\Upsilon(6S)$, respectively, even though the $5S$ and $6S$ quark-model assignments are not certain. Determining the parameters of the $\Upsilon(5S)$ and $\Upsilon(6S)$ from the R_b spectrum is complicated by large interference effects between the resonant $\Upsilon(5S)$ and $\Upsilon(6S)$ amplitudes and the nonresonant $b\bar{b}$ amplitude (which itself is not expected to be a simple function in this region of multiple thresholds) [152]. For the same reason, it is difficult to precisely determine the electronic widths of the $\Upsilon(5S)$ and $\Upsilon(6S)$.

The exclusive cross sections for $e^+e^- \to \pi^+\pi^-\Upsilon(nS)$ (where $n = 1, 2, 3$) also show two peaks, but apparently without any of the nonresonant backgrounds (Fig. 10b) [152]. The Belle experiment has performed three separate analyses of these cross sections, with each analysis including progressively more data and more sophistication.

In the first analysis [186], completed in 2008, data at a single center-of-mass energy near the peak of the $\Upsilon(5S)$ was taken, and the cross sections for $e^+e^- \to \pi^+\pi^-\Upsilon(nS)$ were measured at this point. Assuming the entire inclusive $b\bar{b}$

cross section at the same point was from the $\Upsilon(5S)$, the $\Upsilon(5S)$ partial widths to $\pi^+\pi^-\Upsilon(nS)$ could be computed from the ratio of exclusive to inclusive cross sections. These partial widths were found to be much larger than those for the lower-lying Υ states. For example, the $\Upsilon(5S) \to \pi^+\pi^-\Upsilon(1S)$ partial width was found to be 0.59 MeV, compared to the $\Upsilon(4S) \to \pi^+\pi^-\Upsilon(1S)$ partial width of 0.0019 MeV. In fact, due to the assumption about the inclusive $b\bar{b}$ cross section, it is now thought that these $\Upsilon(5S)$ partial widths were underestimated, making the discrepancy even larger.

In the second analysis [151], completed in 2010, Belle used seven center-of-mass energies around the $\Upsilon(5S)$ to roughly map out the shape of the $e^+e^- \to \pi^+\pi^-\Upsilon(nS)$ cross sections. The peak in these exclusive cross sections was found to be at a higher mass than the $\Upsilon(5S)$ mass as it appears in the inclusive cross section. The discrepancy was 9 ± 4 MeV. This result led to the postulation of the $Y_b(10888)$ as a separate state from the $\Upsilon(5S)$.

Finally, in the third analysis [152], completed in 2016, Belle used a much larger number of center-of-mass energy points to map out the region of the $\Upsilon(5S)$ and $\Upsilon(6S)$. Here the argument shifted. Since two peaks could be seen clearly in the exclusive $e^+e^- \to \pi^+\pi^-\Upsilon(nS)$ cross sections, and with negligible backgrounds, these peaks were now used to define the parameters of the $\Upsilon(5S)$ and $\Upsilon(6S)$. The fit to the R_b spectrum yielded consistent parameters, but the interference with the nonresonant $b\bar{b}$ continuum makes the fits to the R_b spectrum unreliable. Hence the status of an exotic $Y_b(10888)$ remains unsettled, and so does the reason for the anomalously large $\pi^+\pi^-\Upsilon(nS)$ partial widths of the "$\Upsilon(5S)$".

The same two peaks are also apparent in the exclusive cross sections for $e^+e^- \to \pi^+\pi^- h_b(nP)$ with $n = 1, 2$ (Fig. 10c) [153]. Again, the $\Upsilon(5S)$ and $\Upsilon(6S)$ appear with little nonresonant background. The sizes of the cross sections are similar to those for $e^+e^- \to \pi^+\pi^-\Upsilon(nS)$.

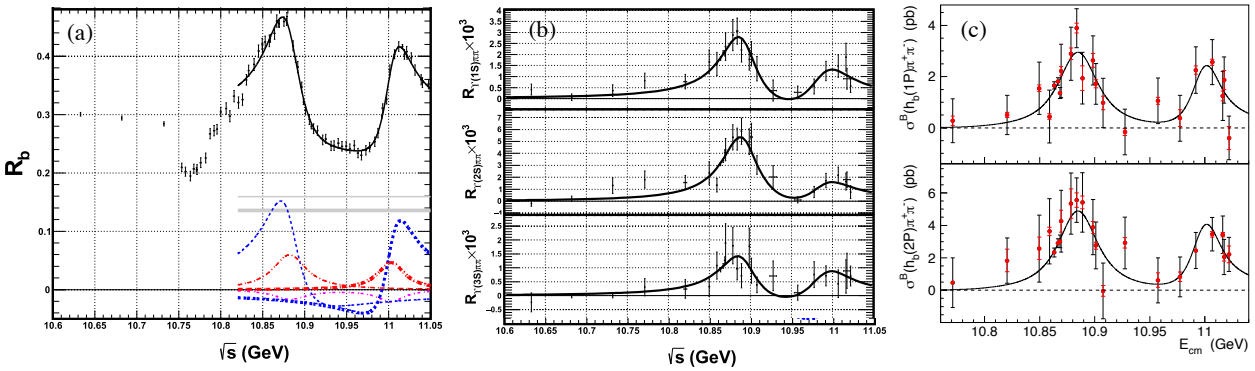

Figure 10: Inclusive and exclusive e^+e^- cross sections in the bottomonium region as a function of center-of-mass energy ($\sqrt{s}$ or E_{CM}). The $\Upsilon(5S)$ and $\Upsilon(6S)$ are present in each reaction. (a) The inclusive e^+e^- cross section (shown as $R_b \equiv \sigma(b\bar{b})/\sigma^0_{\mu\mu}$). The solid lines are for a fit that includes interfering $\Upsilon(5S)$ and $\Upsilon(6S)$ states as well as coherent and incoherent backgrounds [152]. (b) The exclusive $e^+e^- \to \pi^+\pi^-\Upsilon(1S, 2S, 3S)$ cross sections [152]. (c) The exclusive $e^+e^- \to \pi^+\pi^- h_b(1P, 2P)$ cross sections [153]. Note that all five of the exclusive cross sections are dominated by the $\Upsilon(5S)$ and $\Upsilon(6S)$. All figures are from Belle.

2.5.2. Cross Sections in the Charmonium Region

While the inclusive e^+e^- cross section at center-of-mass energies in the bottomonium region above the $\Upsilon(4S)$ shows two peaks, the $\Upsilon(5S)$ and $\Upsilon(6S)$, the inclusive e^+e^- cross section in the charmonium region above the $\psi(3770)$ shows three, the $\psi(4040)$, $\psi(4160)$, and $\psi(4415)$ (Fig. 11a) [189]. These peaks match well with potential model expectations for the $n^{2S+1}L_J = 3^3S_1$, 2^3D_1, and 4^3S_1 states of charmonium, respectively [26]. However, many complications arise when exclusive e^+e^- cross sections are considered.

The first of the puzzling exclusive e^+e^- cross sections to be measured was $e^+e^- \to \pi^+\pi^- J/\psi$, where the $Y(4260)$ appeared as a peak in the cross section around 4.26 GeV (Fig. 11b) [23, 29, 141, 142, 143, 144], and with a cross section around two orders of magnitude smaller than the inclusive cross section. The mass of the $Y(4260)$ lies between the masses of the $\psi(4140)$ and $\psi(4415)$. In fact, in the inclusive e^+e^- cross section, the region of the $Y(4260)$ has an apparently featureless depletion of events. Setting an upper limit on the inclusive decays of the $Y(4260)$ has allowed a lower limit to be calculated for the branching fraction of the decay $Y(4260) \to \pi^+\pi^- J/\psi$ of 0.6% [190], although this calculation involves a relatively difficult fit to the inclusive cross section. Besides corresponding to a dip in the inclusive cross section, the shape of the $e^+e^- \to Y(4260) \to \pi^+\pi^- J/\psi$ cross section also appears strange: It rises rapidly below the peak and falls more slowly above the peak. The Belle experiment attributed this asymmetry to interference with a lower-mass $Y(4008)$ [23, 143], although the BaBar experiment could not confirm this hypothesis [144]. The BESIII experiment has reported that the $Y(4260)$ may in fact consist of two peaks, a narrow peak around 4.22 GeV and a wider peak around 4.31 GeV, accounting for the asymmetry [145]. The shape of the $e^+e^- \to \pi^0\pi^0 J/\psi$ cross section is consistent with that of the $e^+e^- \to \pi^+\pi^- J/\psi$ cross section and is suppressed by a factor of two, consistent with expectations for an isosinglet $Y(4260)$ [32].

Finding new decay modes of the $Y(4260)$ has proven to be difficult. It is not sufficient to measure a single exclusive e^+e^- cross section at 4.26 GeV, but one must instead measure the cross section at a range of energies in order to determine whether the energy dependence of the cross section corresponds to the $Y(4260)$. For example, the CLEO-c experiment measured a non-zero cross section for $e^+e^- \to K^+K^-J/\psi$ at 4.26 GeV [142], but this single point is not sufficient to establish the existence of the decay $Y(4260) \to K^+K^-J/\psi$. Attempts to establish this decay by the Belle experiment have lacked the required statistics [191, 192].

When the data has been sufficient to map exclusive cross sections as a function of center-of-mass energy, the $Y(4260)$ has not been found. In $e^+e^- \to \pi^+\pi^-\psi(2S)$, there are two clear peaks, the $Y(4360)$ and the $Y(4660)$ (Fig. 11c) [146, 147, 148]. In $e^+e^- \to \pi^+\pi^-h_c(1P)$, the data is also clearly inconsistent with a $Y(4260)$; there is some evidence for a narrow peak around 4.23 GeV and a much wider peak at higher mass (Fig. 11d) [156, 193]. The $\omega\chi_{c0}$ cross section also shows evidence for peaking at a mass lower than that of the $Y(4260)$, a feature that has been named the $Y(4230)$ [149]. Other cross sections, such as $\eta J/\psi$ [194, 195, 196], $\omega\chi_{c1,2}$ [197], and $\Lambda_c\bar{\Lambda}_c$ [150] [where the $X(4630)$ has been reported], have also proved to be remarkably complex.

Understanding the open-charm cross sections, which are typically an order of magnitude larger than the closed-charm cross sections listed above, is likely a prerequisite for sorting out all of the structure seen in exclusive e^+e^- cross sections in the charmonium region. Many open-charm cross sections have been measured by the CLEO-c experiment [198], BaBar [199, 200, 201], and Belle [202, 203, 204, 205, 206], but higher-statistics measurements should be soon provided by the BESIII experiment.

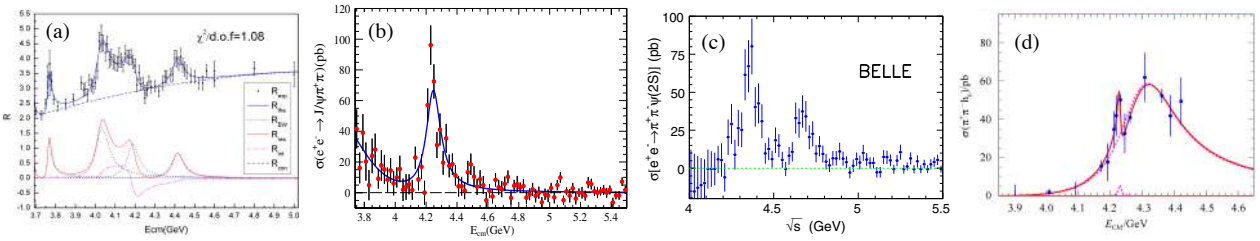

Figure 11: Inclusive and exclusive e^+e^- cross sections in the charmonium region as a function of center-of-mass energy ($\sqrt{s}$ or E_{CM}). (a) The inclusive e^+e^- cross section (shown as $R \equiv \sigma(q\bar{q})/\sigma^0_{\mu\mu}$) from BESII [189]. The solid lines are for a fit that includes interfering $\psi(3770)$, $\psi(4040)$, $\psi(4160)$, and $\psi(4415)$ states as well as a non-interfering continuum background. (b) The exclusive $e^+e^- \to \pi^+\pi^-J/\psi$ cross section from BaBar showing the $Y(4260)$ [144]. (c) The exclusive $e^+e^- \to \pi^+\pi^-\psi(2S)$ cross section from Belle showing the $Y(4360)$ and $Y(4660)$ [148]. (d) The exclusive $e^+e^- \to \pi^+\pi^-h_c(1P)$ cross section from BESIII with a fit to a narrow peak with a mass near 4.23 GeV and a wider peak at higher mass [193].

2.5.3. Substructure in the Bottomonium Region

In the bottomonium region, we have already seen that there are surprisingly large cross sections for $e^+e^- \to \pi^+\pi^-\Upsilon(1S, 2S, 3S)$ and $e^+e^- \to \pi^+\pi^-h_b(1P, 2P)$ at center-of-mass energies near the $\Upsilon(5S)$ mass (Sec. 2.5.1). Perhaps more interesting is the fact that all five of these reactions proceed, either entirely or partially, through the intermediate processes $e^+e^- \to \pi^\pm Z_b(10610)$ and $e^+e^- \to \pi^\pm Z_b(10650)$, where the $Z_b(10610)$ and $Z_b(10650)$ are electrically charged, have widths on the order of 20 MeV, and decay to $\pi^\mp\Upsilon(1S, 2S, 3S)$ and $\pi^\mp h_b(1P, 2P)$. These results were discovered by the Belle experiment in 2012 in an analysis of all five reactions [160]. In the study of $e^+e^- \to \pi^\pm Z_b$ with $Z_b \to \pi^\mp\Upsilon(nS)$, separate two-dimensional Dalitz-plot fits for $n = 1, 2, 3$ were performed (Figs. 12a,b). The $Z_b \to \pi^\mp h_b(nP)$ (with $n = 1, 2$) processes were studied using one-dimensional fits to the $\pi^\mp h_b(nP)$ mass distributions, which were obtained by fitting for the $h_b(nP)$ yield in bins of $\pi^\mp h_b(nP)$ mass (Fig. 12c). The masses and widths of the $Z_b(10610)$ and $Z_b(10650)$ were consistent in all five reactions, and the combined significance of both Z_b states was over 10σ in each reaction. In 2015, the study of the $e^+e^- \to \pi^+\pi^-\Upsilon(1S, 2S, 3S)$ processes was extended to include a six-dimensional amplitude analysis [162]. The $J^P = 1^+$ hypothesis was favored for both the $Z_b(10610)$ and the $Z_b(10650)$.

A neutral version of the $Z_b(10610)$ was seen by Belle in 2013 in the related processes $e^+e^- \to \pi^0 Z_b(10610)$ with $Z_b(10610) \to \pi^0\Upsilon(2S, 3S)$, with a combined significance of 6.5σ [161]. The ratio of cross sections for the charged and neutral processes was consistent with expectations for an isovector $Z_b(10610)$. The statistics were not sufficient to observe the $Z_b(10610) \to \pi^0\Upsilon(1S)$ decay or the $Z_b(10650) \to \pi^0\Upsilon(1S, 2S, 3S)$ decays, but the upper limits were consistent with isospin expectations.

One of the most striking features of the $Z_b(10610)$ and $Z_b(10650)$ is that their masses are just above the thresholds needed to produce $B\bar{B}^*$ and $B^*\bar{B}^*$, respectively. This fact prompted a study of the processes $e^+e^- \to B^{(*)}\bar{B}^{(*)}\pi$ with center-of-mass energy near the $\Upsilon(5S)$ mass by the Belle experiment [163]. By fully reconstructing one B meson and the pion, Belle was able to observe the decays $Z_b(10610) \to B\bar{B}^*$ (where $B\bar{B}^*$ is shorthand for $B^+\bar{B}^{*0}$ and $\bar{B}^0B^{*+}$ and their charge conjugates) and $Z_b(10650) \to B^*\bar{B}^*$ (where $B^*\bar{B}^*$ is shorthand for $B^{*+}\bar{B}^{*0}$ and its charge conjugate), shown in

Fig. 12d. No evidence was found for the kinematically allowed $Z_b(10650) \to B\bar{B}^*$ decay, and no evidence was found for the process $e^+e^- \to B\bar{B}\pi$. Assuming the charged $Z_b(10610)$ and $Z_b(10650)$ decay only to $\pi^\pm\Upsilon(1S, 2S, 3S)$, $\pi^\pm h_b(1P, 2P)$, and $B\bar{B}^{(*)}$ (which is supported by the study of the inclusive $\Upsilon(5S)$ cross section [152]), branching fractions could be calculated. It was found that the open-bottom decays are roughly an order of magnitude larger than the closed-bottom decays.

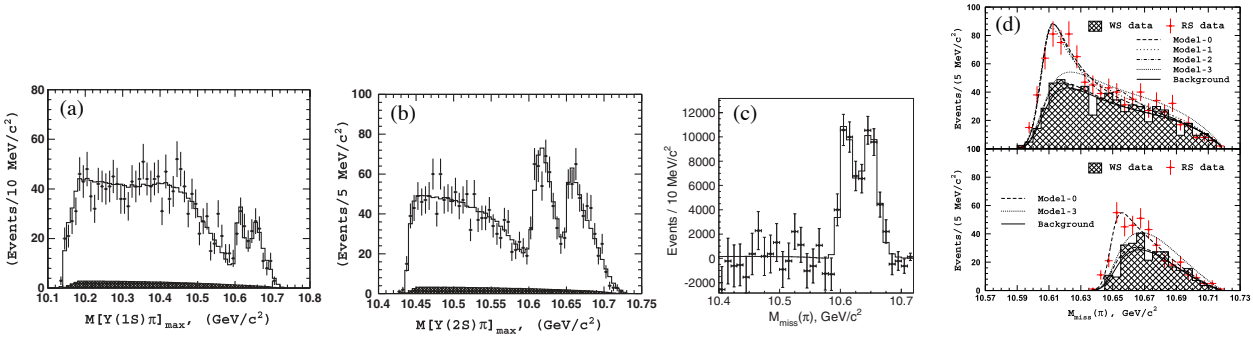

Figure 12: The Z_b states observed in e^+e^- annihilation in the bottomonium region. (a,b,c) Observation of the $Z_b(10610)$ and $Z_b(10650)$ in $e^+e^- \to \pi^\mp Z_b$ with the Z_b decaying to $\pi^\pm\Upsilon(1S)$ (a), $\pi^\pm\Upsilon(2S)$ (b), and $\pi^\pm h_b(1P)$ (c) [160]. (d) Observation of the $Z_b(10610)$ decaying to $(B\bar{B}^*)^\pm$ (top) and the $Z_b(10650)$ decaying to $(B^*\bar{B}^*)^\pm$ (bottom) [163]. All figures are from the Belle experiment.

2.5.4. Substructure in the Charmonium Region

While there are two Z_b states in the bottomonium region, one with mass near the $B\bar{B}^*$ threshold and one with mass near the $B^*\bar{B}^*$ threshold, there are analogous Z_c states in the charmonium region near the $D\bar{D}^*$ and $D^*\bar{D}^*$ thresholds, although with a few additional complications. Note that these Z_c states produced in e^+e^- annihilation are distinct from those produced in B decays (Sec. 2.4).

The first of the Z_c states discovered in e^+e^- annihilation was the $Z_c(3900)$. The $Z_c(3900)$ was simultaneously discovered by BESIII and Belle in 2013 in analyses of the process $e^+e^- \to \pi^+\pi^- J/\psi$ with center-of-mass energies near the $Y(4260)$ mass. The BESIII experiment used a single center-of-mass energy at 4.26 GeV [22]; the Belle experiment covered a wider range by using the initial-state radiation technique [23]. For both experiments, the $Z_c(3900)$ appeared as a peak in the mass spectrum of the $\pi^\pm J/\psi$ system, with a width of around 50 MeV (Fig. 13a). Only one-dimensional fits were performed, but studies of the $\pi^+\pi^-$ system were carried out to demonstrate that the $Z_c(3900)$ peak did not originate from kinematic reflections. Analogous to the $Z_b(10610)$ of bottomonium, the $Z_c(3900)$ is near the $D\bar{D}^*$ threshold. But unlike bottomonium, the $\pi^\pm J/\psi$ system showed no sign of a second state near the $D^*\bar{D}^*$ threshold (which is just above 4 GeV).

Shortly after the discovery of the $Z_c(3900)$, the BESIII experiment did observe a second state near the $D^*\bar{D}^*$ threshold, analogous to the $Z_b(10650)$ of bottomonium [156]. It was discovered in the process $e^+e^- \to \pi^+\pi^- h_c(1P)$, where three center-of-mass energies (4.23, 4.26, and 4.36 GeV) were analyzed near the $Y(4260)$ mass. The $Z_c(4020)$ was observed as a narrow peak (with a width of roughly 8 MeV) in the $\pi^\pm h_c(1P)$ mass spectrum (Fig. 13b). No evidence for the $Z_c(3900) \to \pi^\pm h_c(1P)$ could be found and only an upper limit could be set.

The BESIII experiment also studied the $Z_c(3900)$ and $Z_c(4020)$ in open-charm decays. Like the $Z_b(10610)$, the $Z_c(3900)$ was found to decay to $D\bar{D}^*$ in the process $e^+e^- \to D\bar{D}^*\pi$ (where $D\bar{D}^*$ stands for both $D^+\bar{D}^{*0}$ and $\bar{D}^0D^{*+}$ and their charge conjugates), both by reconstructing a single D meson (Fig. 13c) [154] and by reconstructing both D mesons [155]. The first of these analyses also demonstrated the J^P of the $Z_c(3900)$ to be 1^+. And, like the $Z_b(10650)$, the $Z_c(4020)$ was found in the process $e^+e^- \to D^*\bar{D}^*\pi$ decaying to $D^*\bar{D}^*$, where $D^*\bar{D}^*$ stands for $D^{*+}\bar{D}^{*0}$ and its charge conjugate (Fig. 13c) [158]. Also similar to bottomonium, the decays of the $Z_c(3900)$ and $Z_c(4020)$ to open charm are roughly an order of magnitude larger than their decays to closed charm. The masses and widths of the Z_c states as observed in their closed- and open-charm decays are not entirely consistent—the $Z_c(3900)$ is lighter and narrower in its open-charm decay, while the $Z_c(4020)$ is heavier and wider in its open-charm decay—but it is highly probable that the closed- and open-charm channels are related.

Neutral partners to the $Z_c(3900)$ and $Z_c(4020)$ were subsequently discovered in the neutral versions of all four reactions listed above. The $Z_c(3900)$ was found to decay to $\pi^0 J/\psi$ [31, 32] and $(D\bar{D}^*)^0$ [33]; the $Z_c(4020)$ was found to decay to $\pi^0 h_c(1P)$ [157] and $(D^*\bar{D}^*)^0$ [159]. In the analysis of the $Z_c(3900) \to \pi^0 J/\psi$ decay [32], the ratio of the cross section for $e^+e^- \to \pi^0 Z_c(3900)$ followed by $Z_c(3900) \to \pi^0 J/\psi$ to the cross section for $e^+e^- \to \pi^0\pi^0 J/\psi$ was measured at a number of different center-of-mass energies. The sizes of the data samples, however, were not sufficient to determine whether or not the $e^+e^- \to \pi^0 Z_c(3900)$ process proceeds through a $Y(4260)$.

A third Z_c state, the $Z_c(4055)$, was reported by the Belle Collaboration in the process $e^+e^- \to \pi^\pm Z_c$ with $Z_c \to \pi^\mp\psi(2S)$ for center-of-mass energies near the $Y(4360)$ [148]. Its mass and width are clearly inconsistent with both the $Z_c(3900)$ and the $Z_c(4020)$. These results also present a striking dissimilarity with the bottomonium system, where the parameters of the $Z_b(10610)$ and the $Z_b(10650)$ are consistent in all three reactions $e^+e^- \to \pi^+\pi^-\Upsilon(1S, 2S, 3S)$. The $Z_c(4055)$ requires further study.

It is interesting to note that neither the $Z_c(3900)$ nor the $Z_c(4055)$ has been seen in B decays. The $Z_c(3900)$ could have been seen in the decay $B \to K\pi J/\psi$, but instead the $Z_c(4200)$ and $Z_c(4430)$ were found (Sec. 2.4.4). Similarly, the $Z_c(4055)$ could have been seen in the decay $B \to K\pi\psi(2S)$, but instead the $Z_c(4240)$ and $Z_c(4430)$ were found (Sec. 2.4.1). The fact that the $Z_c(4055)$ and $Z_1(4050)$ (the latter produced in $B \to KZ_1$ and decaying to $\pi^\pm\chi_{c1}$, Sec. 2.4.4) have a similar mass and width must be coincidence. If the $Z_c(4055)$ were produced in B decays, like the $Z_1(4050)$, it would be seen in $B \to K\pi\psi(2S)$. And if the $Z_1(4050)$ were produced in e^+e^- annihilation like the $Z_c(4055)$, then in $e^+e^- \to \pi^\pm Z_1(4050)$ with $Z_1(4050) \to \pi^\mp\chi_{c1}$ and $\chi_{c1} \to \gamma J/\psi$ would produce a prominent $Z_1(4050)$ signal in $e^+e^- \to \gamma\pi^+\pi^- J/\psi$, which is not seen [52]. A search for the $Z_c(4020)$ in B decays has not yet been performed.

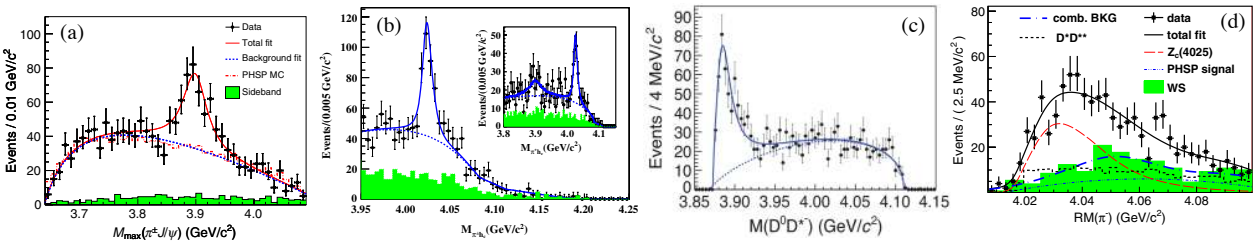

Figure 13: The Z_c states observed in e^+e^- annihilation in the charmonium region. (a) Observation of the $Z_c(3900)$ in $e^+e^- \to \pi^\mp Z_c$ with the Z_c decaying to $\pi^\pm J/\psi$ [22]. (b) Observation of the $Z_c(4020)$ in $e^+e^- \to \pi^\mp Z_c$ with the Z_c decaying to $\pi^\pm h_c(1P)$ [156]. (c) Observation of the $Z_c(3900)$ decaying to $(D\bar{D}^*)^\pm$ [154]. (d) Observation of the $Z_c(4020)$ decaying to $(D^*\bar{D}^*)^\pm$ [158]. All figures are from the BESIII experiment.

2.6. The Region Between 3.8 and 4.0 GeV

The majority of the exotic states discussed above exhibit properties that have clearly identified them as exotic: the $Z_c(4430)$ contains a $c\bar{c}$ pair and has an electric charge; the $Y(4260)$ has a mass that is incompatible with the predicted, and already discovered, $J^{PC} = 1^{--}$ quark-model states; the $X(3872)$ is extremely narrow and has a mass remarkably close to the $D^0\bar{D}^{*0}$ threshold. Other candidates for QCD exotica, especially in the region between 3.8 and 4.0 GeV, cannot be identified so obviously as exotic. The challenge in this region is to try to separate exotic candidates from quark-model states, many of which are yet to be identified. A few assignments appear to be straightforward: the $X(3823)$ is likely the $\psi_2(1D)$ ($n^{2s+1}L_J = 1^3D_2$) state of charmonium; and the $Z(3930)$ is likely the $\chi_{c2}(2P)$ state. But other assignments are not settled: the $X(3915)$ [which is likely the same as the $Y(3940)$] was previously identified as the $\chi_{c0}(2P)$ state, but this assignment is problematic; and the interpretation of the $X(3940)$ remains an outstanding issue. Here we provide a few notes on quark-model assignments.

(1) **The $X(3823)$ is the $\psi_2(1D)$.** The $X(3823)$ was seen by Belle in the process $B \to KX(3823)$ [124] and by BESIII in the process $e^+e^- \to \pi^+\pi^- X(3823)$ [164], where in both cases the $X(3823)$ decayed to $\gamma\chi_{c1}$. While the sizes of the data samples in these two measurements were not sufficient to determine the quantum numbers, the $J^{PC} = 2^{--}$ assignment is highly likely, based upon its close match to the quark-model predictions for the $\psi_2(1D)$ state of charmonium. First, the mass of the $X(3823)$ closely matches the quark-model predictions for the mass of the $\psi_2(1D)$ state, which is well constrained, given the identification of the $\psi(3770)$ with the related $\psi(1D)$ state. Second, the $X(3823)$ decays to $\gamma\chi_{c1}$, and the $\psi_2(1D)$ state is expected to have a large partial width to $\gamma\chi_{c1}$. Upper limits on the $X(3823)$ decay to $\gamma\chi_{c2}$ are also consistent with expectations for the $\psi_2(1D)$. Finally, the $X(3823)$ is narrow, as expected for a 2^{--} state, since the $D\bar{D}$ decay is forbidden by quantum numbers, and the $X(3823)$ has a mass below the $D\bar{D}^*$ threshold.

(2) **The $Z(3930)$ is the $\chi_{c2}(2P)$.** The $Z(3930)$ was seen by both Belle [168] and BaBar [169] in the process $\gamma\gamma \to Z(3930)$ with $Z(3930) \to D\bar{D}$ (Fig. 14a). Both measurements could conclusively determine the J^{PC} to be 2^{++}. Since the mass of the $Z(3930)$ is near the quark-model prediction for the $\chi_{c2}(2P)$, and since it decays to $D\bar{D}$ as is expected for the $\chi_{c2}(2P)$, the $\chi_{c2}(2P)$ assignment appears reasonable.

(3) **Is the $X(3915)$ [identified with the $Y(3940)$] the $\chi_{c0}(2P)$?** The $Y(3940)$ was seen by both Belle [106] and BaBar [122, 123] in the process $B \to KY(3940)$ with $Y(3940) \to \omega J/\psi$ (Fig. 8c). The initial mass measurement was near 3940 MeV (hence the name) [106], but subsequent measurements were near 3915 MeV [122, 123]. The $X(3915)$ was seen by Belle [166] and BaBar [167] in the process $\gamma\gamma \to X(3915)$ with $X(3915) \to \omega J/\psi$ (Fig. 14b). BaBar was also able to show that the J^{PC} is likely 0^{++} [167]. Since their masses and widths are consistent, and since they both decay to $\omega J/\psi$,

the $Y(3940)$ and $X(3915)$ are usually considered to be the same state [referred to as the $X(3915)$]. The $X(3915)$ was originally identified with the $\chi_{c0}(2P)$ state of charmonium, based on its mass and likely J^{PC}, but this assignment has a number of problems [207]. First, the mass difference between the $X(3915)$ and the $\chi_{c2}(2P)$ [or $Z(3930)$], 8.8 ± 3.2 MeV, is far smaller than the expected $\chi_{c0}(2P)$-$\chi_{c2}(2P)$ mass difference. Second, if the $X(3915)$ were the $\chi_{c0}(2P)$, then it should be seen in decays to $D\bar{D}$, which is expected to be the dominant mode. These $D\bar{D}$ decays would have been evident in the analysis of $B \to K D^0 \bar{D}^0$ by Belle [208] if $\mathcal{B}[X(3915) \to D^0 \bar{D}^0] > 1.2 \times \mathcal{B}[X(3915) \to \omega J/\psi]$ [207]. The $X(3915) \to D\bar{D}$ decay should also have been evident in the process $\gamma\gamma \to X(3915)$ with $X(3915) \to D\bar{D}$, which is not seen in Fig. 14a.

(4) **What is the $X(3940)$ [and the $X(4160)$]?** The $X(3940)$ was first reported by Belle in the process $e^+e^- \to J/\psi\, X(3940)$ with the $X(3940)$ decaying to anything [165]. A later analysis examined the processes $e^+e^- \to J/\psi\, D^{(*)}\bar{D}^{(*)}$, and the $X(3940)$ was seen only in the $D\bar{D}^*$ decay [41]. In addition, a peak named the $X(4160)$ was seen in $D^*\bar{D}^*$, and a broad excess of events was seen in $D\bar{D}$ (Fig. 14c). None of these peaks currently have clear interpretations.

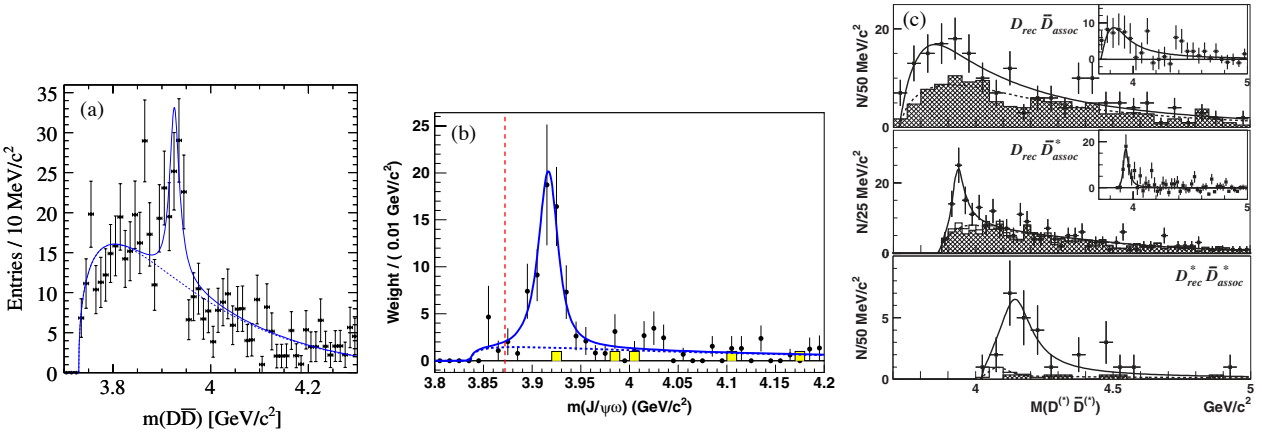

Figure 14: The XYZ around 3.9 GeV. (a) Observation of the $Z(3930)$ by BaBar in $\gamma\gamma \to Z$ with $Z \to D\bar{D}$ [169]. (b) Observation of the $X(3915)$ by BaBar in $\gamma\gamma \to X$ with $X \to \omega J/\psi$ [167]. (c) A study of $e^+e^- \to J/\psi + D\bar{D}, D\bar{D}^*, D^*\bar{D}^*$ at Belle [41]. The $D\bar{D}$ system (top) shows a broad excess of events; the $D\bar{D}^*$ system (middle) shows the $X(3940)$; the $D^*\bar{D}^*$ system (bottom) shows the $X(4160)$.

2.7. Results Waiting for Confirmation

The majority of the candidates for QCD exotica discussed above are experimentally on solid ground. Even many of the states that were controversial initially, such as the $Z_c(4430)$ and the $Y(4140)$, have become firmly established over the last several years. In this section we single out a few states, though, that remain unsettled and require confirmation.

LHCb, with its larger samples of B decays than those collected by the B factories, has confirmed the existence of a number of the states seen in B decays. There are a few more channels, however, that need to be revisited. The existence of the $Z_1(4050)$ and the $Z_2(4250)$ in $B \to K(\pi^\pm \chi_{c1})$, and the existence of the $Z_c(4200)$ and the $Z_c(4430)$ in $B \to K(\pi^\pm J/\psi)$, both reported by the Belle experiment but not seen by BaBar, remain somewhat controversial.

In the e^+e^- sector, the large number of Y states in the charmonium region needs to be investigated. While many features of the data are statistically significant, there is apparently little order from channel to channel. A more global analysis of the data is required to understand the effects of cross-channel scattering. Such an analysis could settle the existence or non-existence of a few of the Y states, such as the $Y(4230)$, and may help clarify the properties of the $Y(4260)$.

In $\gamma\gamma$ collisions, the $X(3915)$ (decaying to $\omega J/\psi$) is firmly established. The presumably related $X(4350)$, reported by Belle to decay to $\phi J/\psi$ [170], however, requires confirmation.

The issue of the $X(5568)$, recently reported by the D0 experiment in inclusive $p\bar{p}$ production at a center-of-mass energy of 1.96 TeV [175], also remains unsettled. Because it decays to $B_s\pi^\pm$, it could be a tetraquark state that contains four separate quark flavors, b, s, u, and d. It could be related to the electrically charged Z_c (containing $c\bar{c}$ and light quarks) or the Z_b (with $b\bar{b}$ and light quarks), but it differs in the fact that its mass is significantly below the threshold to decay to two open-(heavy)-flavor mesons, in this case a B and a K, while the Z_c and Z_b states have masses above the open-charm and open-bottom thresholds, respectively. The D0 experiment reported that a significant fraction (around 10%) of the B_s produced in the transverse momentum region between 10 and 30 GeV originated from $X(5568)$ decays. The LHCb experiment searched for the same state, but with pp collisions and with center-of-mass energies at 7 and 8 TeV, but found no evidence for it [209]. LHCb set an upper limit of around 2% for the fraction of B_s originating from $X(5568)$ decays for transverse momentum of the B_s above 10 GeV. The $X(5568)$ certainly deserves further study.

3. Theory Applications

3.1. Molecular Picture

We begin with the first theoretical picture proposed to describe the structure of hidden-flavor multiquark hadrons, that of hadronic molecules. The original proposal of charmed-meson molecules, as already noted, far predated [36, 37] the discovery [4] of the first confirmed exotic candidate, the $X(3872)$.

3.1.1. General Considerations: Binding Energy and Size

The only states thus far absolutely known to be hadronic molecules are the composite nuclei, lending hope that one may attempt to draw some useful insights from their attributes. The deuteron stands alone as the only confirmed two-hadron bound state, making it a suitable prototype for heavy-hadron molecules [210]. The essential properties of the deuteron for this purpose are (i) that its quantum numbers ($Q = 1$, $J^P = 1^+$, $I = 0$) are accessible to a bound state of a component proton and a neutron, (ii) the proximity of its mass $m_D \equiv 2m_N - B$ to the threshold for dissociation into $p + n$ (binding energy $B = 2.2$ MeV), which suggests a large characteristic size R for the state,

$$R \equiv \frac{\hbar}{\sqrt{2\mu B}} = 4.3 \text{ fm}\,, \tag{17}$$

where the reduced mass $\mu \simeq m_N/2$, and (iii) a large p-n spin-triplet (t) *scattering length* $a_t = 5.3$ fm in the corresponding channel, supporting its interpretation as a bound state [211]. Indeed, for sufficiently small B, the only length parameter describing the bound state is the scattering length, $R \to a$, a phenomenon known as *low-energy universality* [212].

In fact, the scattering length by itself provides only partial information on the structure of the state. A more incisive test comes through considering the next moment in the *effective-range expansion* of the low-momentum (k), s-wave ($\ell = 0$) scattering amplitude f_0, which is called the *effective range* r_0:

$$f_0 = \frac{1}{k \cot \delta_0(k) - ik} = \frac{1}{\frac{1}{a} + r_0 \frac{k^2}{2} - ik}\,. \tag{18}$$

For the deuteron channel, $r_0 = 1.75$ fm. Weinberg long ago derived a criterion [213] for determining in terms of a, r_0, and R whether a state is primarily extended (composite) or compact (elementary). The parameter connecting the observables is the wave function renormalization pole residue Z, which is 0 for purely composite particles like molecules and approaches 1 for an elementary state. The relations read

$$a = 2\left(\frac{1-Z}{2-Z}\right)R + O\left(\frac{1}{m}\right)\,, \quad r_0 = -\left(\frac{Z}{1-Z}\right)R + O\left(\frac{1}{m}\right)\,, \tag{19}$$

where m represents corrections due to the momentum scale of the binding interactions (*i.e.*, m is set to m_π if one-pion exchange is the primary binding mechanism). Noting that the deuteron satisfies $a_t > R$, and especially that $r_0 > 0$, Weinberg deduced that Z cannot be too close to 1, and indeed that the deuteron is dominated by its composite component since Z lies much closer to 0 than 1. In principle, such measurements for the heavy-quark exotics should become feasible in the future when near-threshold production experiments become possible and detailed *line shapes* of the production amplitudes for the states become available. At present, however, not even the sign of B for $X(3872)$ has been uniquely fixed.

As one further figure of merit for studies of hadronic molecules, the largest binding energies per nucleon for compound nuclei are < 9 MeV. Such numbers are obtained, for example, in nuclear shell models by starting with a basic attractive nucleon-nucleon potential of depth ≈ 50 MeV and then adding various corrections [214]. One therefore expects all true heavy-hadron molecules to lie not far below dissociation thresholds (tens of MeV or less) and to have large spatial extent [O(1–10 fm)].

3.1.2. Dynamics of Binding

Of course, bound states must also possess a dynamical mechanism that can provide a sufficiently attractive binding interaction. In the deuteron, the long-distance attraction necessary for this extended bound state to persist is provided largely, but not exclusively, through pion exchange. The detailed mechanism is a variant of the original Yukawa interaction, via a potential energy function of the form

$$V(r) = (\text{couplings} \times \text{spin-isospin-orbital structure}) \times \frac{e^{-\mu r}}{r} \times \left[1 + O\left(\frac{1}{\mu r}\right)\right]\,, \tag{20}$$

where μ is the mass of the exchanged meson. Contact [$\delta^{(3)}(\mathbf{r})$] terms are also frequently included as contributions to $V(r)$. At large r the pion, being the lightest meson, dominates. An intermediate-range attraction is interpreted as a two-π correlation or $J^P = 0^+$ σ-meson exchange, while a short-distance hard-core repulsion is interpreted as $J^P = 1^-$ ρ

or ω exchange. Potentials using this basic type of interaction are used to great effect in modeling complex nuclei, as in the Nijmegen [71], Bonn [72], and Argonne [73] potentials.

Needless to say, meson-exchange models, even for two-body systems, can become quite intricate and require a substantial number of parameters. Moreover, many species of compound nuclei have rather long lifetimes and well-measured properties (in particular, the deuteron is completely stable). In contrast, the heavy-quark exotic candidates all have very short lifetimes; the longest-lived one appears to be the $X(3872)$, whose width is only known as the bound < 1.2 MeV; a plausible width of, say, 100 keV corresponds to a lifetime of only 10^{-20} s. Not enough precision data is yet available to perform the same level of fitting to interaction potentials for heavy-quark exotics, even for the well-studied $X(3872)$. Nevertheless, the extreme closeness of the $X(3872)$ mass to the $D^0\bar{D}^{*0}$ threshold makes it extremely compelling to model as a molecule of these mesons [210].

It is also worth recalling that a $qq\bar{q}\bar{q}$ system can form a pair of color-singlet mesons in two ways, corresponding in the case of $c\bar{c}q\bar{q}$ systems like the $X(3872)$ to an open-charm meson pair, or to a pair of a charmonium and a light-quark meson. Indeed, the $X(3872)$ lies not only very close to the $D^0\bar{D}^{*0}$ threshold, but also to the thresholds for $J/\psi\,\rho^0_{\rm peak}$ (3872 MeV) and $J/\psi\,\omega$ (3880 MeV). However, molecules of the pure $(c\bar{c})(q\bar{q})$ type would necessarily be bound by the exchange of the much heavier $D^{(*)}$ mesons, which propagate shorter distances than π's and would have difficulty accounting for spatially extended bound states. It therefore appears much more natural for such states to have a rather larger open-charm than hidden-charm meson component, and therefore the open-charm decays are expected to dominate. For all exotics candidates for which open-charm modes have been seen, they do indeed provide the dominant decay channels, although several of the exotics still lack evidence for such decays despite dedicated searches and plenty of available phase space. One cannot eliminate the possibility of a substantial $(c\bar{c})(q\bar{q})$ component, or indeed, a pure charmonium $(c\bar{c})$ state if quantum numbers allow, to combine with a primarily open-charm hadron-pair molecule, and such a *coupled-channel analysis* may be essential to understanding the detailed structure of exotics such as the $X(3872)$.

One can also explore *quark exchange* as a binding mechanism, using a quark potential model. Indeed, one of the first analyses [215] of the $X(3872)$ contained both quark-exchange and pion-exchange potentials. Because of color confinement, one expects quark exchange to be a significant binding mechanism only at short distances, where the equivalent description in terms of meson exchanges (due to quark-hadron duality) might require the inclusion of multiple meson species. Moreover, quark exchanges with net non-singlet (octet) color charge are possible and cannot be expressed in terms in any number of (color-singlet) mesons, although the bound "mesons" in this case would themselves become colored objects.

Virtually every exotic candidate has been modeled as a hadronic molecule. Relevant thresholds appear in Figs. 1–2 as dashed or dotted lines, from which one can assess the ease or difficulty with which the molecular hypothesis can be supported. A few exotics lie remarkably close to hadron thresholds: the $X(3872)$ of course, and also the $X(3915)$ and possibly $X(3940)$ below $m_{D_s^+} + m_{D_s^-} = 3937$ MeV, $P_c(4380)$ below $m_{\Sigma_c^{*+}} + m_{D^0} = 4388$ MeV, and $P_c(4450)$ below $m_{\Sigma_c^+} + m_{D^{*0}} = 4461$ MeV [216]. Others are quite close to and lie just *above* thresholds, such as $Z_c^+(3900)$ above $m_{D^0} + m_{D^{*+}} = 3875$ MeV, $Z_c^+(4020)$ above $m_{D^{*0}} + m_{D^{*+}} = 4017$ MeV, $X(4630)$ above $\Lambda_c^+ + \bar{\Lambda}_c^- = 4573$ MeV, $Z_b(10610)$ above $m_{B^*} + m_B = 10604$ MeV, and $Z_b(10650)$ very slightly above $2m_{B^*} = 10650$ MeV. In these latter cases, the molecular hypothesis only works if one posits a mechanism to prevent the instantaneous fall-apart decay into the component hadrons, such as an intermediate-range potential barrier that must be tunneled through in order for decay to occur. Alternately, such states may be considered molecular resonances rather than true bound states [217]; a strong attraction between the component hadrons can persist above threshold, creating an enhancement exhibiting a width that nevertheless remains observably small. As the distance of the state from threshold increases, such objects gradually merge into ones better described as the threshold kinematical effects to be discussed in Sec. 3.5.

Lastly, one should note that the mass of the heavy quark Q influences the ease with which hadronic molecules can be formed. In particular, molecules containing $b\bar{b}$ should be more likely to form than those containing the lighter pair $c\bar{c}$ [76], since Fermi motion and other effects suppressed as $1/m_Q$ are rather larger in the charm case (in particular, when compared with the typical binding scales provided by m_π), and can be more effective in $c\bar{c}$ states in counteracting the binding obtained through light-meson exchanges.

3.1.3. Case Study: $X(3872)$ as a Molecule

As mentioned, virtually every heavy-quark exotic candidate has been considered in the molecular picture, which would make a full examination of the literature rather cumbersome for the purposes of this pedagogical summary. Instead, we present here a qualitative chronological overview of studies of the exotic state most likely to be a molecule by virtue of its proximity to a hadronic threshold, the $X(3872)$.

Despite intensive studies since 2003, the exact nature of the $J^{PC} = 1^{++}$ state $X(3872)$ still remains elusive. Its most remarkable feature remains its extreme closeness to the $D^0\bar{D}^{*0}$ threshold, $m_{X(3872)} - m_{D^{*0}} - m_{D^0} = +0.01 \pm 0.18$ MeV. In fact, the threshold $m_{D^{*+}} + m_{D^+}$ lies about 7 MeV higher, meaning that molecular $X(3872)$ should have a larger $D^0\bar{D}^{*0}$ than $D^+\bar{D}^{*-}$ component, thus manifestly breaking isospin in the $X(3872)$—a unique situation not previously encountered in hadronic physics. Nevertheless, no charged partner to the $X(3872)$ has turned up in a dedicated search [40], suggesting that it should be interpreted as a (largely) $I = 0$ state. Even so, it decays to both $J/\psi\,\pi^+\pi^-$ [112]—understood as the $I = 1$ state $J/\psi\,\rho^0$ due to the proximity of $m_{X(3872)}$ to the combination $m_{J/\psi} + m_{\rho^0,\,\rm peak}$—and to the $I = 0$ state

$J/\psi\,\omega$ [122, 167]. These features alone are enough to demonstrate that $X(3872)$ cannot simply be the yet-unobserved conventional charmonium state $\chi_{c1}(2P)$, which was anticipated on the basis of quark-potential models to lie several tens of MeV higher than 3872 MeV (note the cluster of [blue] dashed lines for $J^{PC} = 1^{++}$ in Fig. 1).

The first two analyses [215, 218] of $X(3872)$ as a $D^0\bar{D}^{*0}$ molecule included explicit quark degrees of freedom. The analysis of Ref. [215] also included $J/\psi\,\{\omega, \rho\}$ components; however, it was later found to underpredict the substantial radiative decay branching fractions to $J/\psi\,\gamma$ and $\psi(2S)\gamma$. Meanwhile, Ref. [218] predicted both $D^0\bar{D}^{*0}$ and $D^+\bar{D}^{*-}$ bound states, which the lack of $I = 1$ partners to the $X(3872)$ seems to preclude.

The first hadronic effective Lagrangian studies [219, 220] of $X(3872)$ as a bound state appeared in 2006–7, with the first chiral unitary calculations beginning in 2013 [221]. In the direction of purely hadronic-exchange potential models, the first calculation including σ exchange to represent intermediate-range attraction appeared in 2008 [222] and ρ exchange in 2009 [223]. While even the earliest calculations (*e.g.*, [215]) included both central and tensor interactions, the indispensability of including both s and d waves in the binding of the $D^0\bar{D}^{*0}$ pair via a tensor interaction—analogous to its necessary presence in the deuteron wave function in order to explain its nonzero electric quadrupole moment—was first noted in 2008 [224].

Calculations with separate treatment of the $D^0\bar{D}^{*0}$ and $D^+\bar{D}^{*-}$ and isospin breaking (*i.e.*, not just the charged and neutral $D^{(*)}$ mass differences, but the relative weight of these states in the $I = 0$ and $I = 1$ Hamiltonian eigenstates) began in 2009 [225].

State-of-the-art meson-exchange models for $X(3872)$ [226, 227] now include coupled-channel effects, isospin breaking, s-d mixing, and now also explicit $1/m_Q$ effects.

In contrast, in 2009 QCD sum rules calculations [228] were found to favor a much larger ($c\bar{c}$) component (97%) compared to the $D^0\bar{D}^{*0}$ component (3%) when the tiny width of the $X(3872)$ is taken into account. An $X(3872)$ with such a composition was found to satisfactorily accommodate its radiative decays [229], which can be quite challenging for pure meson-exchange models. In fact, an admixture for the $X(3872)$ favoring the $c\bar{c}$ component had been anticipated already in 2005 [230] on other grounds, as we discuss next. But the central message should already be clear: Although the technology for describing the $X(3872)$ as a primarily $D^0\bar{D}^{*0}$ molecule is quite mature, solid reasons exist for questioning this interpretation.

3.1.4. Prompt Production of the $X(3872)$

The suggestion that the $\chi_{c1}(2P)$ ($c\bar{c}$) component should dominate the $X(3872)$ wave function compared to the $D^0\bar{D}^{*0}$ component, despite its closeness to the $D^0\bar{D}^{*0}$ threshold, was emphasized in 2005 in Ref. [230], in part due to the (then) newly discovered fact [27, 171] that $X(3872)$ was produced in high-energy colliders with a rate comparable to that of ordinary charmonium $\psi(2S)$. This so-called *prompt production* (production at the primary collision point, as opposed to production through the subsequent decay of a b-containing hadron originally produced from the initial collision) of the $X(3872)$ [27, 28, 171, 173]—providing a cross section of about 30 nb—is surprisingly large and creates quite a problem for the molecular picture.

The essential physics is simple to describe, but its correct implementation remains controversial. If the $X(3872)$ is primarily a $D^0\bar{D}^{*0}$ molecule, then presumably the strongly bound $D^{(*)}$ hadrons must form first, and then *coalesce* into the weakly bound molecule. The component hadrons must have a sufficiently small relative momentum less than some $k_{\rm max}$ in order to have an opportunity to form a bound state, or else they simply fly off as free particles. One expects the probability of finding such correlated pairs to drop drastically for large beam energies such as those at the Tevatron and especially at the LHC, in particular for high values of transverse momentum p_T with respect to the beam.

Again drawing on the analogy between the deuteron and the $X(3872)$, one can ask about the rate of production of anti-deuterons in pp or $p\bar{p}$ collisions (whose component $\bar{p}\bar{n}$ baryons must clearly be produced in the collision). By modeling the coalescence in conjunction with standard hadronization Monte Carlo algorithms and limiting to $k_{\rm max} = 50$ MeV, Ref. [42] showed the prompt-production cross section to be only about 0.1 nb, hundreds of times smaller than the observed value. That this coalescence model produces the correct rate for antideuteron production (with $k_{\rm max} = 80$ MeV) was demonstrated in Ref. [231].

Hadronization is, however, a complicated process, and an analysis based on correlated free particles may not directly translate into their bound states. In particular, Ref. [232] argued that strong *final-state interactions* (FSI) between the hadrons are sufficient to allow $k_{\rm max}$ to be as high as 500 MeV and still form a bound state, making the large prompt production rate not so surprising. A rebuttal [43] argued that such strong FSI would produce unobserved results, like the generation of a $D_s\bar{D}_s^*$ molecule at the Tevatron, and that strong FSI did not appear to be needed for deuteron studies. The same collaboration also proposed an analysis [233] to consider the effect of multiple scattering of the D^0 and $\bar{D}^{*0}$ from pions in the interaction region in order to test how many $D^0\bar{D}^{*0}$ pairs can thereby be rescattered into a state of relative momentum $< k_{\rm max}$, and showed [231] that the prompt production rate of $X(3872)$ can be brought in this way closer to the experimental value—but again, to values still far below it, unless particularly strong FSI are included.

A direct comparison between prompt production of (anti)deuterons and $X(3872)$ at values of $p_T \approx 15$ GeV, at which the $X(3872)$ has already been seen at CMS [28], will illuminate the relative importance of FSI in the two processes and

will provide a more decisive probe of the structure of the $X(3872)$. Such experiments are well within the capabilities of the LHC, and these future measurements will provide crucial information for studies of exotics.

3.2. Hadrocharmonium Picture

3.2.1. Motivation and Origin

Some of the heavy-quark exotic candidates preferentially decay to conventional charmonium plus light hadrons, rather than to open-charm meson pairs ($D\bar{D}$ or $D\bar{D}^*$). In particular, the $J^{PC} = 1^{--}$ candidates $Y(4008)$, $Y(4230)$, $Y(4260)$, $Y(4360)$, and $Y(4660)$ (See Appendix A) fit into this category. Moreover, no open-charm decay of $Z_c^{\pm}(4430)$ has yet been seen, and it strongly prefers to decay to $\psi'\pi^{\pm}$ rather than to $J/\psi\,\pi^{\pm}$, and the $Y(4008)$ and $Y(4260)$ decay to $\pi^+\pi^- J/\psi$, while the $Y(4360)$ and $Y(4660)$ decay to $\pi^+\pi^-\psi'$: Some of the exotics clearly have specific preferred charmonium decay products.

These observations have a natural explanation if the exotic state can be described as a particular compact charmonium species embedded in a larger cloud of light-quark hadronic matter, an idea dating back to the proposal of *nuclear-bound quarkonium* in 1990 [234]. In this picture for exotics, the heavy $c\bar{c}$ pair can be supposed to act as a sort of nucleus for the system. This proposal was first qualitatively mentioned by Voloshin in the discussion of Ref. [18] in 2008, and developed into a model some months later in Ref. [44], where it was dubbed *hadrocharmonium*.

3.2.2. Structure and Binding

A first observation about the hadrocharmonium picture is that it is qualitatively distinct from a simple molecular picture of charmonium plus a light meson, in which the wave functions of the two hadrons have a somewhat suppressed spatial overlap, as in a diatomic molecule. In hadrocharmonium, the core is purported to live entirely within the light-quark cloud. Such a distinction should be kept in mind when considering the interpretation of calculations such as in Ref. [235], in which the $Y(4660)$ is proposed to be a $f_0(980)\psi'$ bound state.

The binding mechanism for hadrocharmonium [44] is a color van der Waals attraction between a compact, color-singlet $c\bar{c}$ core and a larger $q\bar{q}$ cloud interacting chiefly through the chromoelectric dipole ($E1$ multipole) interaction, the QCD analogue of the atomic van der Waals attraction. While this interaction is manifestly attractive, it does not guarantee the existence of bound states, especially because of the counteracting effect of the Fermi motion of the light degrees of freedom (mass labeled by M_X). As found in Ref. [44], a value of M_X exceeding 1 GeV, perhaps approaching 2 GeV, is necessary for the net effect of all interactions to give binding for the hadrocharmonium system. Interestingly, this result shows that hadrocharmonium with more highly excited light degrees of freedom is more likely to form and be observed. In the case of *hadrobottomonium*, the effect of Fermi motion decreases (since $m_b \simeq 3m_c$), but so does the strength of the chromoelectric dipole interaction, due to the smaller size of Υ states compared to ψ states; owing to these competing effects, hadrobottomonium states may still exist, but likely not as exact siblings to hadrocharmonium states. In particular, Ref. [44] anticipates hadrobottomonium states no lower than 11 GeV, too heavy to accommodate the known Z_b states (at 10610 and 10650 MeV).

3.2.3. Hadrocharmonium and Heavy-Quark Spin Symmetry

Owing to heavy-quark spin symmetry (HQSS) and the attendant hypothesis that the charmonium wave function is largely decoupled from the light degrees of freedom, one expects that any particular charmonium structure existing at the center of the hadrocharmonium state should leave its imprint on the final state. This restriction not only provides a natural explanation for the preference of particular states to decay to a particular charmonium state (*e.g.*, J/ψ for $Y(4008)$, $Y(4260)$, $Z_c(3900)$ *vs.* ψ' for $Y(4360)$, $Y(4660)$, $Z_c(4430)$ [44, 236] because the $J/\psi = \psi(1S)$ wave function is much more compact than that of the $\psi' = \psi(2S)$ [24, 25], but it also predicts that the open-charm decay modes should be relatively suppressed because of the dynamical difficulty of breaking up the compact $(c\bar{c})$ core and rearranging the constituents with $(c\bar{c})(q\bar{q})$ color structure into $(c\bar{q})(\bar{c}q)$. For the $Z_c(3900)$ this interpretation is problematic, as the $D\bar{D}^*$ mode appears to dominate its decay width [154].

In addition, HQSS predicts that the $c\bar{c}$ spin in hadrocharmonium is approximately conserved, so that states with a spin-triplet (-singlet) core should decay preferentially to ψ or χ_c (η_c or h_c). Experimental evidence that $Y(4260)$ and $Y(4360)$ decay not only to spin-triplet ψ states but spin-singlet h_c as well [156] inspired an extension of the hadrocharmonium hypothesis [47] that asserts the core can be a mixture of spin-singlet and spin-triplet $c\bar{c}$ and still satisfy HQSS.

In contrast, in a truly molecular model, the hadronic components have well-defined quantum numbers, and the HQSS predictions can be somewhat different. Following the aforementioned proposal of a $f_0(980)\psi'$ state in Ref. [235], the authors then predicted [237] the existence of an $f_0(980)\eta_c'$ bound state, using that ψ' and η_c' are degenerate states in the HQSS limit. A side-by-side comparison of the HQSS predictions of molecular, hadrocharmonium, and diquark pictures is presented in Ref. [81].

3.2.4. Can Hadrocharmonium Coexist with Other Pictures?

The question of whether hadrocharmonium states really occur in nature comes down to an assessment of the relative strength of valid competing dynamical effects. It seems extremely likely that, by allowing $\Lambda_{\rm QCD}$ and the heavy-quark mass m_Q to assume a variety of numerical values, one can find regimes in which hadronic molecular states occur and regimes in which hadroquarkonium states occur. These regimes may be distinct, or they may overlap, in which case the eigenstates of the hadronic QCD Lagrangian for a given set of parameters may be combinations of the two. Without being able to solve QCD for physical values of quark masses, one must rely on hints from data such as spectroscopy, decay modes and ratios, and in the future, detailed production line shapes.

One very interesting piece of data in this regard is the suggestion of a significant measured branching fraction for the radiative decay $Y(4260) \to \gamma X(3872)$ [52]. The $X(3872)$ was touted in Sec. 3.1 as the best candidate for a hadronic molecule (although not without some conceptual difficulties), while $Y(4260)$ was described in this section as a prime candidate for a hadrocharmonium state. If indeed they are connected by a prominent radiative transition, then one expects a high degree of similarity in the structure of their wave functions, and hence of what kinds of state they are. For example, the possibility that both are molecular-$c\bar{c}$ combinations is studied in Ref. [238].

3.3. Diquark Picture

3.3.1. General Considerations: Nature of Diquarks

The prediction by Eq. (4) of a attractive channel in which two color-**3** quarks can combine into a color-$\bar{\mathbf{3}}$ diquark (or two color-$\bar{\mathbf{3}}$ antiquarks into a color-**3** antidiquark) immediately suggests the possibility of composite but colored subcomponents inside of hadrons. This fact alone explains the rich history of diquark phenomenology [48], particularly for baryons. The diquark itself can be considered to be either a fairly compact object, with a size similar to that of an ordinary meson (a few tenths of a fm), or it can be considered merely as a correlated state between two quarks in a hadron. Since the quarks have spin $\frac{1}{2}$, the diquark (orbital) ground state can be scalar (spin 0) or vector (spin 1), and has positive parity.

While numerous papers dating as far back as the 1970s have examined the possibility of diquarks as constituents of exotic hadrons (including exotics containing heavy quarks), the modern studies of diquark models for heavy-quark exotics were originally inspired by certain peculiar behaviors of the light-quark scalar mesons $a_0(980)$ $(I = 1)$ and $f_0(980)$ $(I = 0)$ that cast doubt upon a naive $q\bar{q}$ interpretation for these states. For instance, their masses lie extremely close to the $K\bar{K}$ thresholds (hence little phase space is available for these channels), and yet their $K\bar{K}$ decay branching fractions are in the tens of percent [176]. Diquark-antidiquark models provide a natural explanation of this fact by suggesting that each diquark component in the $a_0(980)$ and $f_0(980)$ carries a valence s (or $\bar{s}$) quark [49]. A fresh look at more recent light-quark scalar meson data using the diquark model [239] inspired an extension of the approach [50] to the then-newly discovered heavy-quark exotics; this extension, to be discussed below, constitutes the basis of modern heavy-quark diquark models.

3.3.2. Heavy-Quark Diquark Models

The presence of heavy quarks in the exotic hadron has a number of interesting implications for its structure in diquark models. First, light-quark diquarks were predicted to be more strongly bound in the spin-0 than spin-1 channel, and hence the former ("good") diquarks are expected to be more successful in forming light hadrons than the latter ("bad") diquarks [240]. However, for a diquark that contains a heavy quark, the "good" and "bad" varieties differ only by the relative orientation of the heavy-quark spin, and operators sensitive to this spin are suppressed by powers of $1/m_Q$ according to heavy-quark spin symmetry (HQSS). Second, the characteristic size associated with a diquark may be identified with its Compton wavelength, which is inversely proportional to the reduced mass μ of its constituents. For a given light constituent mass m, μ can vary from $\frac{1}{2}m$ (for an equal-mass light-light system) up to m (for an infinitely heavy-light system). One thus expects a heavy-light diquark to be substantially smaller than a light-light diquark.

Diquark models tend to predict large numbers of states, particularly when compared with molecular hadron or hadrocharmonium models. This proliferation of states is the result of the nonzero net color charge of the diquarks, meaning that the overall system is bound by strong fundamental QCD forces rather than by the much weaker color-singlet van der Waals forces. As a result, one expects all quark spin and isospin combinations to produce a state, because the energy cost for exchanging up and down spins or exchanging u and d quarks is relatively small compared to the strong-interaction energy scales responsible for the overall binding of the state. In contrast, we have seen that molecular models are highly sensitive to the proximity of hadronic dissociation thresholds, as well as the spin and isospin of mesons assumed responsible for their binding. In particular, not every two-meson threshold is expected to produce a hadronic molecule. In the case of hadrocharmonium, we have seen that the spatial extent of the core charmonium wave function, which depends upon internal excitation quantum numbers, is significant in determining whether or not the state binds. One should not, however, infer from these observations that all diquark-antidiquark states are equivalent; the proximity of hadronic thresholds can have profound effects on the states, as discussed below.

The most common model for the diquark-antidiquark system[2] $(Qq_1)(\bar{Q}\bar{q}_2)$ uses an effective Hamiltonian that is dominated by spin and orbital interactions amongst the quarks. In the original model of Ref. [50], the Hamiltonian can be written as

$$H = m_{(Qq_1)} + m_{(\bar{Q}\bar{q}_2)} + H_{SS}^{qq} + H_{SS}^{q\bar{q}} + H_{SL} + H_L \,, \tag{21}$$

where $m_{(Qq_1)}$ and $m_{(\bar{Q}\bar{q}_2)}$ are the diquark masses. H_{SS}^{qq} represents spin-spin couplings between the two quarks (or the two antiquarks), and therefore refers to spin-spin couplings *within* either the diquark or the antidiquark:

$$H_{SS}^{qq} = 2\kappa_{(Qq_1)}\, \mathbf{s}_Q \cdot \mathbf{s}_{q_1} + 2\kappa_{(\bar{Q}\bar{q}_2)}\, \mathbf{s}_{\bar{Q}} \cdot \mathbf{s}_{\bar{q}_2} \,. \tag{22}$$

In contrast, $H_{SS}^{q\bar{q}}$ couples quarks to antiquarks, thereby providing interactions *between* the diquark and the antidiquark:

$$H_{SS}^{q\bar{q}} \;=\; 2\kappa_{Q\bar{q}_2}\, \mathbf{s}_Q \cdot \mathbf{s}_{\bar{q}_2} + 2\kappa_{Q\bar{Q}}\, \mathbf{s}_Q \cdot \mathbf{s}_{\bar{Q}} + 2\kappa_{q_1\bar{Q}}\, \mathbf{s}_{q_1} \cdot \mathbf{s}_{\bar{Q}} + 2\kappa_{q_1\bar{q}_2}\, \mathbf{s}_{q_1} \cdot \mathbf{s}_{\bar{q}_2} \,. \tag{23}$$

The remaining terms are the spin-orbit (H_{SL}) and purely orbital (H_L) contributions,

$$\begin{aligned} H_{SL} &= -2a[\mathbf{s}_{(Qq_1)} \cdot \mathbf{L} + \mathbf{s}_{(\bar{Q}\bar{q}_2)} \cdot \mathbf{L}] = -2a\, \mathbf{S} \cdot \mathbf{L} \,, \\ H_L &= \frac{B_c}{2} \mathbf{L}^2 \,. \end{aligned} \tag{24}$$

Here, $\mathbf{s}_{(Qq_1)} \equiv \mathbf{s}_Q + \mathbf{s}_{q_1}$ is the total diquark spin (and similarly for the antidiquark), and $\mathbf{S}$ represents the the total quark spin for the system. From this Hamiltonian, one then computes the mass eigenvalues for a full spectrum of four-quark states, using standard operator techniques.

The original model of Ref. [50] fit the $J^{PC} = 1^{++}$ $X(3872)$—the only exotic candidate known at the time—to the symmetric combination of $\{s_{(cq)} = 1,\, s_{(\bar{c}\bar{q})} = 0\}$ and $\{s_{(cq)} = 0,\, s_{(\bar{c}\bar{q})} = 1\}$ states, and predicted a number of other levels, such as a 1^{+-} state [the same quantum numbers as the $Z_c^0(3900)$ and $Z_c(4020)$] at the much lower mass of 3750 MeV. In 2014, the model was improved [51] by the inclusion of a significant dynamical assumption: Spin couplings between the diquark and the antidiquark are assumed to be negligible. In terms of the full Hamiltonian of Eq. (21), the contribution $H_{SS}^{q\bar{q}}$ of Eq. (23) is set to zero.

The model of Ref. [51] has many desirable features; for example, a number of the 1^{--} Y states naturally arise as relative $L = 1$ excitations of the diquark-antidiquark pair, meaning that the electric dipole radiative transition $Y(4260) \to \gamma X(3872)$ is natural in this picture [241], and the $Z_c^0(3900)$ arises as 1^{+-} partner to the $X(3872)$, the $\{s_{cq} = 1,\, s_{\bar{c}\bar{q}} = 0\}$ and $\{s_{cq} = 0,\, s_{\bar{c}\bar{q}} = 1\}$ states now appearing in the antisymmetric combination, while the $Z_c^0(4430)$ is the first radial excitation of $Z_c^0(3900)$. Nevertheless, the prediction of numerous yet-unobserved states is a key feature of this model; for example, a prominent 2^{++} state remains to be found. The analysis can be applied to the bottom sector as well, where it has been used, *e.g.*, to study the $Z_b(10610)$ and $Z_b(10650)$ [242]. It has also been applied to the $c\bar{c}s\bar{s}$ sector [243], where the troublesome 0^{++} $X(3915)$ [which, in contrast to the expectation for the pure $c\bar{c}$ state $\chi_{c0}(2P)$, lacks $D\bar{D}$ decays; see Sec. 2.6] is suggested to be the $c\bar{c}s\bar{s}$ ground state, and states that decay to $J/\psi\,\phi$ such as the $Y(4140)$ (Sec. 2.4.2) are naturally accommodated.

3.3.3. Dynamical Diquarks

For all its merits, the diquark picture in the Hamiltonian formalism does not provide detailed dynamics. One may, for example, relativize the light quarks [244], or incorporate a variant of the static Cornell potential [Eq. (2)] [245], or model the interaction using a static color flux tube [246], or introduce nonlocal (*e.g.*, Gaussian) vertex functions between the quarks [247].

However, one important feature not taken into account in these pictures is that the exotic states exist for only a very short time ($\sim 10^{-20}$ s or less), while the techniques described up to this point refer directly or indirectly to eigenstates of a Hamiltonian, which suggests a single time coordinate for the whole system and hence a single (approximate) common rest frame for the components. In reality, the diquark-antidiquark pair may be flying apart from their production point for the entire lifetime of the exotic hadron. Put another way, if one treats the exotic as some sort of molecule, it may not survive long enough to execute a single orbit.

The *dynamical diquark picture* introduced in Ref. [54] instead suggests that confinement is the primary binding mechanism for the exotic states. The diquark-antidiquark pair forms promptly at the production point, and rapidly separates due to the kinematics of the production process, whether via the decay of a heavy b-containing hadron or through a hadron collision process. Since the diquark and antidiquark are colored objects, they cannot separate asymptotically far apart; they create a *color flux tube* or *string* between them. Were sufficient energy available, the string would break as part of a conventional *fragmentation* process, producing an additional $q\bar{q}$ pair. In the case of the $(cq)(\bar{c}\bar{q})$ system, the first available threshold is $\Lambda_c + \bar{\Lambda}_c$ at 4573 MeV, and indeed the $X(4630)$ just above this threshold (Sec. 2.5.2) has only been seen so far in the baryonic decay mode.

[2]Hidden heavy flavor is implied here, but Q and $\bar{Q}$ need not be the same flavor.

Below the fragmentation threshold, the only available modes for decay require the quarks (in the diquark) and the antiquarks (in the antidiquark) to overlap with the wave function of a meson state; inasmuch as the diquark-antidiquark pair may have achieved a substantial separation ($r > 1$ fm) during the lifetime of the state, the overlap is suppressed by the exponentially small meson wave function tail at large r. The transition rate is therefore also suppressed, potentially explaining the measurably small exotic widths. Additionally, the large size of the diquark-antidiquark pair before coming to rest can explain the preference of more highly excited exotics like the $Z_c(4430)$ to decay into $\psi(2S)$, which is spatially much larger than the J/ψ [24, 25]. The production mechanism for $B^0 \to Z_c^-(4430)K^+$ is illustrated in Fig. 15.

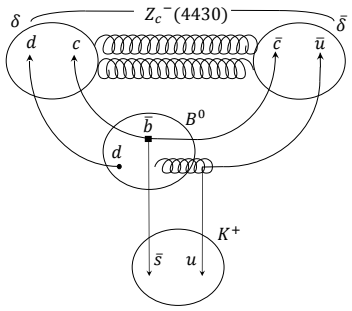

Figure 15: Illustration of the dynamical diquark picture mechanism for production of the $Z_c^-(4430)$ in the decay $B^0 \to Z_c^-(4430)K^+$ (the weak-interaction vertex indicated by a square), adapted from Ref. [54]. The diquark-antidiquark pair are denoted by δ and $\bar{\delta}$, and the color flux tube is indicated by gluon lines.

Despite these qualitative successes, it should be noted that the dynamical diquark picture has not yet been developed into a particular model with uniquely specified interactions. Necessary ingredients include modeling of the diquark formation and proper quantization of the flux tube glue, in order to obtain a specific spectrum and pattern of decays for the exotic states.

3.3.4. Pentaquarks from Diquarks

Both the conventional diquark picture and dynamical diquark picture can be used to study pentaquark states, including the recently discovered candidates $P_c(4380)$, $P_c(4450)$. In the conventional diquark picture [53], the pentaquark may be assembled as the bound state of three $\bar{\mathbf{3}}$ components, $\bar{c}(cq)(qq)$, a composition exploited, *e.g.*, in Refs. [248, 249, 250]. Alternately, pentaquarks can arise in the dynamical diquark model [55] via the sequential formation of compact color triplets through the attractive channels $\mathbf{3} \times \mathbf{3} \to \bar{\mathbf{3}}$ and $\bar{\mathbf{3}} \times \bar{\mathbf{3}} \to \mathbf{3}$ as a diquark-*triquark* system, $\bar{c}_{\bar{\mathbf{3}}}(qq)_{\bar{\mathbf{3}}} \to [\bar{c}(qq)]_{\mathbf{3}}$ plus $(cq)_{\bar{\mathbf{3}}}$, as was used in Ref. [251], and applied to hidden-strangeness system in Refs. [252, 253]. Whether or not the diquarks in exotics are sufficiently tightly bound to enter as elementary fields for use in QCD constituent counting rules and alter the energy scaling behavior of their production amplitudes is addressed in Ref. [254].

Significantly, the observation of opposite parities for the $P_c(4380)$ and $P_c(4450)$ requires one of the two states to contain a unit of orbital excitation. This fact is not difficult to accommodate in the diquark picture, where the broad $P_c(4380)$ can be a highly excited s-wave resonance ($J^P = \frac{3}{2}^-$), while the narrower $P_c(4450)$ can be a lower p-wave resonance ($J^P = \frac{5}{2}^+$).

3.3.5. Other Diquark Approaches

In addition to the Hamiltonian operator, quark model, and flux tube approaches, diquarks have also been employed as interpolating fields in QCD sum rule calculations and in lattice QCD simulations.

A very brief summary of the theory of QCD sum rules has been presented in Sec. 1.6.5, while a review of applications to the charmonium system through 2009 appears in Ref. [89]. QCD sum rules can incorporate diquark-antidiquark pair interpolating operators such as the $J^{PC} = 1^{+-}$ $\mathbf{3}$-$\bar{\mathbf{3}}$ current [255], an example of which is (C being the Dirac matrix representing charge conjugation):

$$J_{2\mu} = q_a^T C c_b (\bar{q}_a \gamma_\mu \gamma_5 C \bar{c}_b^T - \bar{q}_b \gamma_\mu \gamma_5 C \bar{c}_a^T) - q_a^T C \gamma_\mu \gamma_5 c_b (\bar{q}_a C \bar{c}_b^T - \bar{q}_b C \bar{c}_a^T) \,. \tag{25}$$

In Ref. [255], to give just one sample result, the 1^{++} $c\bar{c}q\bar{q}$ states are found to have masses about 4.0–4.2 GeV, somewhat higher than the $X(3872)$. Entire spectra may thus be computed once one has a complete set of interpolating operators. Other examples (both tetraquark and pentaquark states) appear in Refs. [256, 257, 258]. One must note, however, that QCD sum rules take their interpolating operators to be local, which in the current context means that the diquarks are pointlike.

A similar situation arises in lattice QCD simulations (briefly reviewed in Sec. 1.6.6). Here, calculations have been performed that include $D\bar{D}^*$, diquark-antidiquark, and $c\bar{c}$ interpolating operators. In the case of the $X(3872)$, the most

recent simulations [259, 260] include $J/\psi\,\omega$ and $J/\psi\,\rho$ as well. Of these simulations, only Ref. [260] includes diquark interpolating operators, but finds that the $X(3872)$ appears only if both $D\bar{D}^*$ and $c\bar{c}$ interpolators are included, *i.e.*, the diquark interpolators are unnecessary. This result is analogous to the structure for $X(3872)$ suggested in Sec. 3.1.3. Again, the interpolators in lattice simulations are nominally pointlike; introducing finite-size effects is possible, although rather costly in computational time, requiring the use of nontrivial link variables. Furthermore, the state-of-the-art calculations of Ref. [260] use $m_\pi = 266$ MeV; since the pion with its light mass may very well be crucial (See Sec. 1.6.2) to the successful formation of exotic states, the results of future simulations with smaller pion masses are eagerly awaited.

3.4. Hybrids

Although there is little doubt that hybrid mesons (and baryons) exist, not much else is known about these states. The main preliminary question concerns their observability; in particular, are they sufficiently long lived to be recognized as resonances? Assuming no unexpected experimental impediments to their production and observation, the main intellectual challenge will be discerning the degrees of freedom and their dynamics that are relevant to describing the spectrum, production, and decay of these novel states.

The absence of experimental input has led to a rather broad evolutionary landscape, with commensurately many ideas concerning the nature of soft glue. The chief historical ideas have been that soft glue forms some sort of string or flux tube, or that it is an effective constituent confined by a bag or potential. Alternatively, nonperturbative glue can be thought of in terms of collective, nonlocal degrees of freedom, or as a local quasiparticle degree of freedom.

The steadily improving capabilities of computational lattice gauge field theory lends hope that this situation will be improved. Ironically, lattice calculations have so far provided evidence for both pictures: The adiabatic gluonic surfaces discussed in Sec. 1.6.7 can be modeled reasonably well with a bag picture [261], while results from the Lattice Hadron Collaboration [262] provide compelling evidence that nonperturbative gluons can be thought of as chromomagnetic quasiparticles of quantum numbers $J^{PC} = 1^{+-}$ with an excitation energy of approximately 1 GeV. In this way, the lightest hybrid multiplet contains states with

$$J^{PC} = 1^{--} = (1^{+-})_{\text{glue}} \times (0^{-+})_{\text{quarks}}\,, \tag{26}$$

which corresponds to a vector hybrid with quarks in a spin singlet and in an s wave, and

$$J^{PC} = (0,1,2)^{-+} = (1^{+-})_{\text{glue}} \times (1^{--})_{\text{quarks}}\,, \tag{27}$$

which combines the "gluon" with quarks in a spin triplet and in an s wave.

An early lattice computation of the heavy hybrid-meson spectrum was made by the CP-PACS collaboration [263]. The authors worked with the Lagrangian of nonrelativistic QCD and ignored all spin-dependent operators. This assumption led to a degenerate multiplet of states with the quantum numbers given in Eq. (26). The computations yielded a charmonium hybrid multiplet 1.323(13) GeV above the spin-averaged charmonium ground state (near 4.39 GeV) and a bottomonium hybrid multiplet near 10.99 GeV.

More recently, the Hadron Spectrum Collaboration performed a large-scale unquenched calculation [262] that used a large variational basis, a fine temporal lattice spacing, two light dynamical quarks, a dynamical strange quark, and improved lattice actions to obtain a comprehensive charmonium spectrum. Despite these technical advances, the dynamical quarks were still heavy, yielding a pion mass of 396 MeV, and a J/ψ-η_c splitting of 80(2) MeV, which is too small compared to the experimental value of 113 MeV.

The authors of Ref. [262] also probed the internal structure of their hadrons by measuring state overlaps with various operators. Thus, for example, some vectors have significant overlaps with a quark-antiquark pair in a $^3S_1$ state, while others have larger overlap with $^3D_1$ operators. These overlaps only provide qualitative indications of state configurations because they are scale-dependent, and comparison to continuum matrix elements can be confounded by operator mixing.

This method can be used to determine states having large overlaps with operators of large gluonic content. The resulting states are indicated with red and blue boxes in Fig. 16 (darker grays, when the figure is viewed in a black-and-white representation). As can be seen, the red boxes form an approximate multiplet with the expected quantum numbers of Eq. (26). The thin (black) lines in the figure are experimental masses, and (green) boxes are calculations of predominantly conventional charmonium state masses. Notice that the agreement with $J^{PC} = 1^{--}$ worsens as one moves up the spectrum. In view of this deterioration, one might expect that an additional 100 MeV of uncertainty should be applied to the predicted hybrid masses presented in Table 4.

3.4.1. Transitions

Models of strong hybrid decays typically find a selection rule that forbids decay to pairs of identical s-wave mesons [264, 265, 266]. This constraint is sometimes extended to forbidding decay to any pairs of identical mesons [267]. Such a rule, leading to the absence of decay channels, often predicts hybrids to be narrow.

The first lattice calculation of a hadronic transition was made by the UKQCD collaboration for the case of heavy hybrids [268]. The static-quark limit imposes important constraints on the decay process, since the quark-antiquark

J^{PC}	Mass (MeV)	
0^{-+}	4195(13)	
1^{-+}	4217(16)	
1^{--}	4285(14)	
2^{-+}	4334(17)	
1^{+-}	4344(38)	4477(30)
0^{+-}	4386(9)	
2^{+-}	4395(40)	4509(18)
1^{++}	4399(14)	
0^{++}	4472(30)	
2^{++}	4492(21)	
3^{+-}	4548(22)	

Table 4: Charmonium hybrid mass predictions [262]. Masses are (`lattice mass`) - (`lattice` η_c) + (`expt.` η_c).

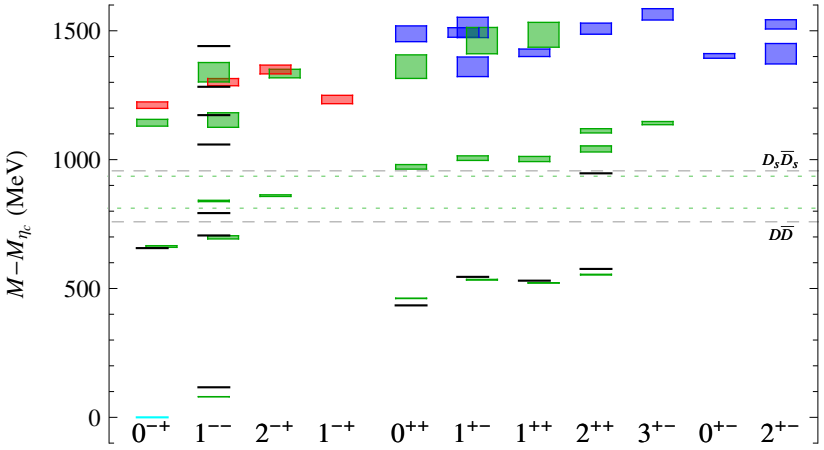

Figure 16: A lattice QCD calculation of charmonium states. (Figure reproduced with permission from Ref. [262].) Solid (black) lines are experimental masses, green boxes (the lighter grays in a black-and-white representation) refer to predominantly conventional charmonia, red boxes (the darker grays in the columns up to $J^{PC} = 1^{-+}$) are the lowest-lying hybrid multiplet; blue boxes (the darker grays in the columns starting at $J^{PC} = 0^{++}$) are the first excited hybrid multiplet. Box heights represent statistical uncertainty.

configuration must remain invariant. The authors focused on the decay of the exotic 1^{-+} state and determined that decay into s-wave mesons is forbidden (since production of the light-quark pair in a spin triplet is forbidden by conservation of gluonic parity and charge conjugation, while production of a spin singlet is forbidden by parity reflection in the quark-antiquark axis).

Furthermore, decay to an s-wave $(Q\bar{q})$ + p-wave $(q\bar{Q})$ configuration is forbidden because the p-wave excitation energy is typically greater than the hybrid excitation energy. Thus, the only allowed transition in the heavy-quark limit is a string de-excitation process in which a light flavor-singlet meson is produced.

The authors computed two such transitions, using unquenched QCD with light-quark masses near the strange quark mass. When the results are interpreted in terms of bottomonium, the authors obtained

$$\Gamma[b\bar{b}g(1^{-+}) \to \eta_b\,\eta(s\bar{s})] \sim 1 \text{ MeV}\,, \tag{28}$$

and

$$\Gamma[b\bar{b}g(1^{-+}) \to \chi_b\,\sigma(s\bar{s})] \sim 60 \text{ MeV}\,. \tag{29}$$

More recently, charmonium hybrid radiative transitions have been computed by the Hadron Spectrum Collaboration [269]. The calculation was made with a large operator basis in the quenched approximation. The renormalization constant required to compare the lattice matrix elements to physical ones was determined nonperturbatively by conserving charge at zero recoil. The resulting widths are presented in Table 5, where one sees quite acceptable agreement with experiment. Notice that the process $c\bar{c}g(1^{-+}) \to J/\psi\,\gamma$ is a magnetic dipole transition. With conventional charmonia, these transitions require a spin flip and are therefore suppressed for heavy quarks. In the case of hybrids, the extra "gluon" permits evading the suppression, and the transition can be large.

transition	$\Gamma_{\rm lattice}$ (keV)	$\Gamma_{\rm expt}$ (keV)
$\chi_{c0} \to J/\psi\gamma$	199(6)	131(14)
$\psi' \to \chi_{c0}\gamma$	26(11)	30(2)
$\psi'' \to \chi_{c0}\gamma$	265(66)	199(26)
$c\bar{c}g(1^{--}) \to \chi_{c0}\gamma$	< 20	
$J/\psi \to \eta_c\gamma$	2.51(8)	1.85(29)
$\psi' \to \eta_c\gamma$	0.4(8)	0.95 – 1.37
$\psi'' \to \eta_c\gamma$	10(11)	
$c\bar{c}g(1^{--}) \to \eta_c\gamma$	42(18)	
$c\bar{c}g(1^{-+}) \to J/\psi\gamma$	115(16)	

Table 5: Quenched lattice charmonia radiative decays [269].

3.4.2. Y(4260) as a Hybrid

The most popular candidate for a heavy hybrid meson is the $Y(4260)$ (we stress, however, that alternative models for this state exist as discussed above, such as hadrocharmonium and an $L = 1$ diquark-antidiquark state). As discussed in Section 2.5.2, the Y has been observed in the reaction $e^+e^- \to J/\psi\pi\pi$ by four different experiments and is evidently a $J^{PC} = 1^{--}$ charmoniumlike meson. With a mass of 4251(9) MeV, the state lies between quark model predictions for the 2D vector at 4168(24) MeV [expt. 4191(5) MeV] and the 4S vector at 4428(22) MeV [expt. 4421(4) MeV], and is therefore a prime candidate for an exotic state.

Several groups have noted the following features of the $Y(4260)$ [270, 271, 272]:

- The decay modes $J/\psi\,\sigma$, $J/\psi\,f_0$, $J/\psi\,a_0$ appear to dominate.
- $\Gamma[Y(4260) \to e^+e^-]$ is much smaller than for all other vector charmonia.
- $\Gamma[Y(4260) \to J/\psi\pi^+\pi^-]$ is much larger than for all other vector charmonia.
- The mass is about 1 GeV greater than the ground state η_c and J/ψ, as is expected for a gluonic excitation.

Close and Page [270] also argue that the decay selection rule implies a preferred decay to DD^{**} states, which lie 40 MeV above the Y mass. Rescattering (Sec. 3.5) is then postulated to yield the $J/\psi\,\pi\pi$ final state.

Subsequent lattice work [262] (discussed above) yielded an estimate of the vector charmonium hybrid mass of 4285 MeV, quite close to that of the Y. Furthermore, as just mentioned, lattice results strongly indicate that quarks should form a spin singlet in the low-lying vector hybrid. Since photons prefer to create quarks in a spin triplet, a spin flip is required to created the hybrid state. This observation neatly fits with the idea of an extra gluon being present in the state, but "costs" a factor of approximately $\langle p\rangle/m_c \sim \Lambda_{\rm QCD}/m_c \sim 0.1$ with respect to the creation of s-wave vector charmonia (Here, $\langle p\rangle$ is a typical momentum scale in the hybrid). Close and Page estimated the electronic width of the Y to be

$$5 \text{ eV} < \Gamma[Y(4260) \to e^+e^-] < 60 \text{ eV}\,. \tag{30}$$

Subsequent measurements have raised the lower limit to 9 eV. This width is 2–3 orders of magnitude smaller than those of the well-established conventional charmonium vectors, in rough agreement with the spin-flip suppression just noted.

Finally, Close and Page noted that the relatively large width, $\Gamma[Y(4260)] = 120(12)$ MeV, implies that decays to $D_1\bar{D}$, $D_1'\bar{D}$, and $D_0\bar{D}^*$ should be accessible. These decay modes feed $D^*\bar{D}\pi$ and $D\bar{D}\pi$ final states, which can be searched for. We remark that the current PDG [176] lists "not seen" for these modes, indicating that this expectation was incorrect.

If the $Y(4260)$ is indeed a hybrid (or predominantly a hybrid), the remainder of the low-lying multiplet should lie nearby. In particular, one expects a 0^{-+} hybrid at 4170 MeV, a 2^{-+} hybrid at 4310 MeV, and the quantum number-exotic 1^{-+} hybrid at 4190 MeV. The discovery of the latter meson would be a watershed moment in hadron spectroscopy, as it would be the first definitive sighting of this manifestly exotic, long-expected form of matter. After discovery, the next task will be a thorough exploration of the production and decay mechanisms that manifest in the hybrid spectrum. Finally, developing a robust models of these properties will lend insight into the behavior of QCD in a new regime.

3.5. Kinematical Effects

The relevance of "kinematical effects" to heavy exotic hadrons is slowly becoming more appreciated[3]. Before discussing the case of heavy mesons, we remind the reader of a long-standing controversy in the case of the light scalar f_0 and a_0 mesons.

[3]Although this nomenclature is traditional, it is regrettable, since channel coupling or the generation of self-energies is dynamical. Nevertheless, the term persists because it stresses that the relevant phenomena are not described solely by S-matrix poles.

3.5.1. Light Hadrons and Cusps

In the context of the constituent quark model, scalar mesons are considered as quark-antiquark states with $^{2S+1}L_J = {}^3P_0$ quantum numbers. This assignment is problematic because it leads to states that are heavier than the lightest s-wave states by a typical orbital excitation energy of several hundred MeV. Thus, the constituent quark model appears to identify the $f_0(1370)$, $f_0(1500)$, $a_0(1450)$, and $K_0(1430)$ as the lightest scalar nonet. The problem, of course, is that this identification leaves the $f_0(980)$, $a_0(980)$, and $f_0(500)$ as orphan states.

It should be stressed that this tension only exists in the context of nonrelativistic constituent quark models. Relativistic models, for example, typically have large spin-orbit forces in the light-quark sector, which can lead to light scalar mesons [273, 274]. Nevertheless, other issues remain: (i) The width of the f_0 is 40–100 MeV, much smaller than the 500–1000 MeV expected by scaling $\Gamma(b_1 \to \omega\pi)$; (ii) the near-degeneracy of the f_0 and a_0 suggests that they are nearly ideally mixed, but then $\Gamma(f_0 \to \pi\pi)/\Gamma(a_0 \to \eta\pi)$ should be around 4 (π vs. η light-quark Clebsch-Gordan coefficients), rather than the observed ratio of approximately 1; (iii) both states couple strongly to $K\bar{K}$, suggesting valence strange-quark content.

A popular alternative interpretation is that four-quark states $qq\bar{q}\bar{q}$ comprise the lowest scalar nonet. The quarks can either be in a symmetrical configuration, as in a bag model [49, 240], or asymmetrical, as in diquark models. In the diquark picture an "inverted" light-scalar nonet is built as follows:

$$\begin{aligned} [ud][\bar{u}\bar{d}] \qquad & f_0(500)\,, \\ [ud][\bar{d}\bar{s}],\ [ud][\bar{s}\bar{d}],\ [us][\bar{u}\bar{d}],\ [ds][\bar{d}\bar{u}] \qquad & \kappa(800)\,, \\ \frac{1}{\sqrt{2}}([su][\bar{s}\bar{u}] + [sd][\bar{s}\bar{d}]) \qquad & f_0(980)\,, \\ [su][\bar{s}\bar{d}],\ \frac{1}{\sqrt{2}}([su][\bar{s}\bar{u}] - [sd][\bar{s}\bar{d}]),\ [sd][\bar{s}\bar{u}] \qquad & a_0(980)\,. \end{aligned} \tag{31}$$

Yet another four-quark model assumes that states are predominantly composed of a meson-meson system. For example, the possibility that the $a_0(980)$ and $f_0(980)$ quartet is composed of $K\bar{K}$ bound states was examined in Ref. [275]. Similar applications in the light-quark sector abound: $f_1(1420)$ $(K^*\bar{K})$ [276], $f_2(2010)$ $(\phi\phi)$ [277] (p. VII.166), and $f_0(1770)$ $(K^*\bar{K}^*)$ [278].

Perhaps the most conservative resolution of the light-scalar issue relies on the strong coupling of scalar mesons to their decay channels to generate dynamical poles with masses below 1 GeV [64, 279, 280]. The dynamical states are not arranged according to their $q\bar{q}$ "seed" states, but according to the channels that dominate: $\pi\pi$ for the $f_0(500)$, $K\pi$ for the $\kappa(800)$, and $K\bar{K}$ for $f_0(980)$ and $a_0(980)$.

3.5.2. Heavy Hadrons and Cusps

Not surprisingly, all of these multiquark notions have found application in descriptions of the new heavy-quark exotic mesons. Bugg was the first to emphasize the possible importance of cusps for interpreting several heavy states [65]. Amongst these are the $X(3872)$ at the $D^0(1865)$-$D^{*0}(2007)$ threshold, $Z(4430)$ near the $D^*(2007)$-$D_1(2420)$ threshold, and $Y(4260)$, which is close to the $D(1865)$-$D_1(2420)$ threshold. All of these couplings are s wave. We remark that the same situation exists with baryons: the P_{11} $N(1710)$ and P_{13} $N(1720)$ are near the N-ω threshold, while the $\Lambda_c(2940)$ is near the $D^*(2007)$-N threshold.

Early applications of loop diagrams in heavy-meson physics concentrated on their effects on hadronic transitions [281, 282, 283, 284]. For example, Guo *et al.* [285, 286] examined the effects of virtual charmed-meson loops on strong transitions of charmonia and found that the loops significantly enhanced processes such as $\psi' \to \pi J/\psi$. We remark that, although these studies did not address cusp enhancements, they made the important point that the QCD multipole expansion does not incorporate the long-distance or long-time scales that can occur when intermediate hadrons are created and propagate. While this observation appears self-evident, it contradicts several decades of lore surrounding hadronic interactions that do not involve flavor exchange.

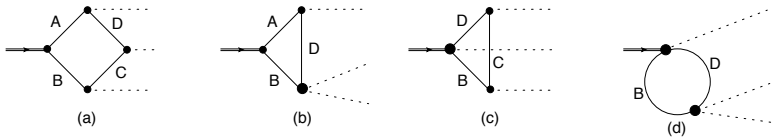

Figure 17: Various hadronic loop diagrams. Diagrams (b), (c), and (d) can be obtained from (a) by taking the limits $m_C \to \infty$, $m_A \to \infty$, and both, respectively.

The earliest explicit model that applied cusp effects to heavy exotics (to our knowledge) is due to Chen and Liu [287], who developed the "Initial Single Pion Emission" (ISPE) model to explain the $Z_b(10560)$ and $Z_b(10610)$ as cusp effects (although this terminology was not used). Ensuing work invoked the same mechanism to predict charmed-analogue states [subsequently discovered as the $Z_c(3900)$ and $Z_c(4020)$] [288]. The relevant diagrams correspond to (c) in Fig. 17, where, in the charm case, the initial meson is taken to be a heavy vector charmonium state [$\psi(4040)$], the intermediate particles (B,C,D) are D or D^* states, and the final state is $\pi\pi J/\psi$.

Subsequent work has employed several variants of loop diagrams to implement the cusp effect. These can be organized as shown in Fig. 17. At the one-loop level, all diagrams can be obtained from the box diagram (a) by integrating out various intermediate mesons (and rescaling appropriately). Thus, for example, the ISPE diagram is obtained in the large m_A (or m_B) limit. Other groups have considered diagram (b), which is obtained by taking m_C (or m_D) to be large. Taking m_A and m_C to infinity yields the bubble diagram (d). Of course other combinations can be taken (but appear to not be employed in the literature); these choices merge the box diagram to a four-point vertex, or have a bubble with a single particle on one side and a three-point vertex on the other. Vertex models are typically built from low-order effective Lagrangians (they are not effective field theories, in the sense of systematically including all allowed operators), or with the aid of heavy-quark or chiral symmetry. An important take-away point is that the cusp behavior obtained from all of these diagrams is similar.

The work of Wang *et al.* [289] is an example of an alternate analysis of the Z_c states that employs a formalism in this class of methods. The authors consider the reaction $Y(4260) \to \pi\pi J/\psi$ and postulate that the Y is a $D_1\bar{D}$ bound state. This choice leads naturally to the box diagrams of Fig. 17a. The authors also consider the case where $D^*\bar{D}$ interactions give rise to a $Z_c(3900)$ and include this contribution in their analysis of the BESIII data. The reasonably good fit to the data leads the authors to claim (i) there is "strong evidence that the mysterious $Y(4260)$ is a $\bar{D}D_1(2420) + D\bar{D}_1(2420)$ molecular state", and (ii) "for a more detailed description of the data the need for an explicit $Z_c(3900)$ pole seems to be necessary".

We remark that both of these conclusions seem to be overstatements of the results. It is only necessary for the $Y(4260)$ to couple to strongly to $\bar{D}D_1$ for their analysis to hold, which is expected for hybrids as well as molecular states. With regard to the claimed existence of a Z_c pole, their own analysis (presented in their Fig. 2) clearly shows that an explicit Z_c pole appears to *not* be needed to describe the data. Nevertheless, follow-up work by this group, discussed shortly, found further evidence in support of the resonance picture of the $Z_c(3900)$.

An application of the simplest nontrivial cusp diagram, Fig. 17d, appeared in 2014 [290]. In this work, it was noted that many of the recently discovered heavy charged states lie just *above* nearby open-flavor thresholds. These are $\bar{B}B^*$ [$Z_b(10610)$], $\bar{B}^*B^*$ [$Z_b(10650)$], $\bar{D}D^*$ [$Z_c(3900)$], and $\bar{D}^*D^*$ [$Z_c(4025)$]. While the proximity to thresholds suggests a molecular interpretation for states just below these thresholds, it would require unnatural dynamics to generate such poles above threshold. Even so, Ref. [21] argues otherwise.

The exotic bottomonium states were seen in Belle in $e^+e^- \to \Upsilon(5S) \to \Upsilon(nS)\pi^+\pi^-$ or $\Upsilon(5S) \to h_b(nP)\pi^+\pi^-$ in the final states $\Upsilon(nS)\pi^\pm$ or $h_c(nP)\pi^\pm$ (See Sec. 2.5). Axial-vector quantum numbers were heavily favored by an analysis of the angular distributions. In modeling these features, Ref. [290] noted that the $\Upsilon(5S)$ decays predominantly to $B^{(*)}\bar{B}^{(*)}$, which leads to an $\Upsilon(nS)\pi\pi$ amplitude that is roughly constant. The next most prolific decay mode of the $\Upsilon(5S)$ is to $B^{(*)}\bar{B}^{(*)}\pi$, which can rescatter via Fig. 17d to yield the $\Upsilon(nS)\pi\pi$ final state. Following tradition [64, 65], the imaginary part of the bubble was modeled with an exponential vertex form factor, and the entire bubble was reconstructed from the dispersion relation. Couplings and form factors scales were set by data in $\Upsilon(5S) \to \Upsilon(3S)\pi\pi$, and a surprisingly consistent description of *all* the data (13 peaks in 7 invariant mass distributions) followed.

The following general points were noted:

(i) Z "states" have $J^P = 1^+$;

(ii) Z "states" lie slightly above open-flavor thresholds;

(iii) Threshold partners produce effects of approximately the same width if they are observed in the same channel; however, these widths can differ in different channels. Such behavior is not expected with T-matrix poles;

(iv) Z_c "states" may appear in $\bar{B}^0 \to J/\psi\,\pi^0\pi^0$ and $B^\pm \to J/\psi\,\pi^\pm\pi^0$;

(v) Similarly, $\bar{B}_s \to J/\psi\,\varphi\varphi$ and $\bar{B}_0 \to J/\psi\,\varphi K$ should exhibit cusp effects at $D_s\bar{D}_s^*$ and $D_s^*\bar{D}_s^*$ thresholds, while $\bar{B}_0 \to J/\psi\,\eta K$ should display $D\bar{D}^*$, $D^*\bar{D}^*$, $D_s\bar{D}_s^*$, and $D_s^*\bar{D}_s^*$ cusp enhancements;

(vi) It should be possible to discern a rich spectrum of exotic "states" at higher center-of-mass energy in $J/\psi\,\pi\pi$. These include a $D_0\bar{D}_1$ state at 4740 MeV and $D_2\bar{D}_1$ enhancement at 4880 MeV;

(vii) $\Upsilon(5S) \to K\bar{K}\Upsilon(nS)$ should show enhancements at 10695 MeV ($B\bar{B}_s^*$ and $B^*\bar{B}_s$) and 10745 MeV ($B^*\bar{B}_s^*$).

Some aspects of this work were subsequently criticized. Reference [291] noted that the use of an exponential form factor in the dispersion relation violates causality. We remark that, while true, it has little bearing on the dispersion integral in which it is likely to be used. Gou *et al.* [292] argued that rescattering effects need to be summed, and that doing so necessarily forms a $Z_c(3900)$ resonance pole. The model employed by the authors includes a four-point $YJ/\psi\,\pi\pi$ vertex whose strength was fitted to the $Y(4260) \to D\bar{D}^*\pi$ distribution at high invariant mass. Fitting the same distribution at low invariant mass then required iterating $D\bar{D}^*$ bubble diagrams with sufficient strength to generate a $Z_c(3900)$ pole.

Nevertheless, it is clear the conclusion of Gou *et al.* is contingent upon the model used. In particular, it is natural

to attribute the enhancement in the $D\bar{D}^*\pi$ data near threshold to the threshold opening—as is common in hadronic physics. The latter point of view was pursued in Ref. [293], where a simple, causal, and unitarized nonrelativistic model was employed to describe the $Y \to D\bar{D}^*\pi$, $Y \to D^*\bar{D}^*\pi$, $Y \to J/\psi\,\pi\pi$, and $e^+e^- \to h_c\pi\pi$ data. No S-matrix poles were required to obtain very good agreement with experiment. This conclusion is supported by lattice gauge theory computations that report only weakly repulsive $(D^*\bar{D}^*)^\pm$ interactions in the $J^P = 1^+$ channel [294].

This topic has been revisited recently by Zhou and Xiao [295], who employed a unitarized coupled-channel approach similar to that of Törnqvist [64] to analyze the same Z_c data as above. The authors concluded that the $Z_c(3900)$ signal is related to the combined effect of a pair of near-threshold "shadow" poles and the $D\bar{D}^*$ threshold, in which a third-sheet pole might provide a dominant contribution. Similar work was also carried out by He [296] in a model that generated relevant interactions with boson exchange and employed a Bethe-Salpeter formalism to compute amplitudes.

It is disappointing, but not surprising, that conclusions concerning the dynamical origin of the Z_b and Z_c signals can depend strongly upon the model assumptions used to generate those conclusions. The way forward, of course, is to develop models that are sufficiently robust and well vetted against experimental results, such that the conclusions based upon them can be trusted.

Threshold enhancements and openings are generic features of hadronic systems, and one must therefore be cautious in claiming bound states where such effects are known to operate. Near-threshold enhancements can arise simply because hadrons are soft; thus, the $Y \to D\bar{D}^*\pi$ and $Y \to D^*\bar{D}^*\pi$ data are easily explained. Similarly, coupled-channel cusps should be regarded as a possible explanation for bumps seen in rescattering channels slightly above coupled-channel thresholds. If the "widths" of these enhancements vary strongly (as they do for the Z_c's) between pure threshold and rescattering processes, then one has an additional sign that nonresonant explanations should be considered. In particular, threshold bumps arise due to competing effects between form factors and phase space, whereas a rescattering enhancement width is mediated by form factors and a rescattering loop. One sees that (cusp-dominated) threshold bumps do not exhibit phase motion, while rescattering enhancements may have phase motion due to the associated bubble diagrams.

Indeed, both threshold effects and true resonant poles can coexist and interact; as was shown in Ref. [65], the presence of a threshold can, through self-energy diagrams, shift the position of the fundamental resonance closer to the threshold. It was noted in Ref. [297] that this "pole dragging" effect does not depend upon the origin of the pole, whether through meson molecules, diquark-antidiquark pairs, or intrinsic $q\bar{q}$ states.

3.5.3. Further Experimental Considerations

The LHCb collaboration recently reported the discovery of four states in the $J/\psi\,\phi$ invariant-mass distribution of $B^+ \to J/\psi\,\phi K^+$ [125] (See Sec. 2.4.2). Salient properties of these states are given in Table 6.

State	Mass (unct.) [MeV]	Width (unct.) [MeV]	J^{PC}
$Y(4140)$	4165.5(5,3)	83(21,16)	1^{++}
$Y(4274)$	4273.3(8,11)	56(11,10)	1^{++}
$X(4500)$	4506(11,13)	92(21,21)	0^{++}
$X(4700)$	4704(10,19)	120(31,35)	0^{++}

Table 6: Extracted $J/\psi\,\phi$ Breit-Wigner resonance properties [125].

The resonance parameters of Table 6 are based on standard Breit-Wigner phenomenology. However, motivated by point (v) above, the collaboration also fit the data with a cusp model of the $Y(4140)$. This amplitude model had one less parameter than the s-wave Breit-Wigner model and was able to fit the data better by 3σ (it has five fewer parameters than the full Breit-Wigner model and in this case fits the data better by 1.6σ). This success motivated the collaboration to construct a $D_sD_{s0}^*$ cusp model for the $Y(4274)$. It is perhaps not surprising that this choice did not perform better than the default amplitude model, since the s-wave quantum numbers are incorrect.

In the bottom sector, the relatively large rate for the reaction $\Upsilon(5S) \to h_b\pi\pi$ is somewhat mysterious, because a heavy-quark spin flip is required to make the transition from the $^3S_1$ Υ to the $^1P_1$ h_b bottomonium state. It is tempting to speculate that the spin flip is facilitated by the presence of light-quark degrees of freedom in the loop-diagram intermediate state that persist over long time scales. In effect, the virtual $B^{(*)}\bar{B}^{(*)}$ states permit the pions to carry off the spin component necessary to effect the required b-quark spin flip.

Lin *et al.* [298] have suggested that the coupling of the $Z_c(3900)$ to $\pi J/\psi$ can be exploited to search for this exotic state in photoproduction. The idea is that the virtual photon converts to a J/ψ via the vector-meson dominance mechanism, which then interacts with a nucleon by pion exchange, and creates an s-channel Z_c, which finally decays to $J/\psi\,\pi$. The cross section for $\gamma N \to ZN$ was estimated using a hadronic Lagrangian with dipole form factors, while the $Z_c\pi J/\psi$ coupling was taken from the measured width of the Z_c. The resulting cross section was predicted to peak at $\sqrt{s} \approx 7$ GeV, with a readily observable rate. In spite of these expectations, a measurement of $\mu N \to \mu J/\psi\,\pi N$ by the COMPASS collaboration [181] found no evidence for the $Z_c(3900)$. This somewhat problematical result may have a resolution in dynamical effects associated with the high center-of-mass energy (such as hadronic form factors or Pomeron exchange).

Finally, there appears to be a tension between e^+e^- and electroweak decay production mechanisms for a subset of exotic states. In particular, we note that the electroweak decay $\bar{B}^0 \to J/\psi\,\pi\pi$ has recently been measured by the LHCb Collaboration, and the distribution of events in $J/\psi\,\pi$ invariant mass was published [299]. A comparison of the analogous distribution from BESIII reveals a stark difference: Although the distributions stretch over nearly identical mass ranges, there is no sign of the $Z_c(3900)$ or $Z_c(4020)$ in the LHCb data. This result is difficult to understand, because other than quantum numbers, there seems to be little difference between $\gamma^* \to c\bar{c}$ ($Y(4260)$ decay where the $Z_c(3900)$ is seen, Sec. 2.5.4) and $b \to c\bar{c}d$ (B decay, where the Z_c is not seen).

4. Prospects

The search for and discovery of new QCD exotics has been one of the most productive areas of experimental particle physics in the past two decades. For example, of all the particles discovered so far at the Large Hadron Collider whose existence was not a foregone conclusion, all are QCD exotics with the exception of the Higgs boson. The fact that the rate of appearance of new experimental findings currently greatly outpaces theoretical explanations in this area [for instance, even the true structure of the $X(3872)$, the first and best studied example among the heavy-quark exotics, remains a mystery] is a state of affairs that has not occurred for many years in particle physics and provides an excellent indication of intellectual vitality in this field.

No obvious ceiling to the number of exotics yet to be discovered is known; there could be many dozens more remaining to be found. Moreover, the LHC experiments (particularly LHCb) and BESIII will continue to take data for several more years, the Belle II upgrade will soon be coming online, and in the future, detailed processes will be examined at GlueX (Jefferson Lab), COMPASS (CERN), and $\bar{\mathrm{P}}$ANDA at FAIR (GSI, Darmstadt). The great majority of exotics already observed appear in the hidden-charm $c\bar{c}$ and hidden-bottom $b\bar{b}$ tetraquark and $c\bar{c}$ pentaquark sectors. The flavor universality of QCD demands that, once the particular details of hadronic thresholds are taken into account, exotics should be possible in any combination of quark flavors. To date, the only exotic candidate with valence quark content other than $c\bar{c}$ and $b\bar{b}$ is the $X(5568)$ ($\bar{b}s\bar{d}u$), and its existence remains controversial (See Sec. 2.7). And yet, the $c\bar{c}$ sector was the first one in which the first unambiguous exotics candidates were found, despite decades of dedicated searches in the lighter-quark sectors. Is there a sense in which the existence of exotics, or at least the ability to distinguish them from backgrounds, requires the presence of heavy quarks? If it is the latter, then one can hope to glean some hints of exotics among states containing some (intermediate-mass) s quarks. The $D^*_{s0}(2317)$ discovered by BaBar in 2003 [300], for example, is surprising in having a much lighter mass than predicted for the expected $c\bar{s}$ state, and moreover decays through the isospin-violating mode $D_s\pi^0$. The state $Y(2175)$ [or $\phi(2170)$] was discovered by BaBar in 2007 [301] as a ϕf_0 resonance in the initial-state radiation process $e^+e^- \to \gamma_{\mathrm{ISR}}\phi\pi^+\pi^-$, the strange analogue of the one in which $Y(4260)$ was originally found (See Sec. 2.5.2). Now that the existence of heavy-quark exotics has been established, anomalous light-quark systems have come under greater scrutiny.

In the opposite direction of even more exotic hadrons, one can anticipate the production of states with manifestly exotic (for $q\bar{q}$) quantum numbers such as $J^{PC} = 1^{-+}$. In that case, if the state is neutral ($c\bar{c}q\bar{q}$), then one faces the enviable problem of trying to determine whether the states is a "conventional" hybrid exotic (See Sec. 3.4) or a tetraquark exotic. On the other hand, doubly heavy exotics (such as $cc\bar{q}\bar{q}$) lack heavy-quarkonium decay modes and should be rather straightforward to identify if they can be produced. Options for producing doubly heavy hadrons have been discussed in detail (*e.g.*, Ref. [302, 303]), and while not even the lowest conventional doubly heavy state [the $\Xi_c(ccq)$ baryon] has yet been confirmed, the prospects for producing such states are nevertheless considered bright. A key observation of [302] is that the chief complication in producing doubly-heavies, to produce two separate heavy $Q\bar{Q}$ pairs and induce a quark from each pair to coalesce, is already accomplished in B_c production. Copious B_c output (such as at LHCb) is therefore seen as a promising benchmark for producing doubly heavy hadrons. At an even higher level of exoticity are *hexaquarks* [304, 305], which can refer either to a bound state of 6 q's, or 3 q's plus 3 $\bar{q}$'s. Considering the comments on doubly heavies, presumably the latter type would be easier to produce with heavy quarks; indeed, it is possible that the $X(4630)$, with its strong coupling to $\Lambda_c\bar{\Lambda}_c$ (See Sec. 2.5.2), is such a state.

The differing status of experiment and theory with respect to our knowledge of the exotic candidates requires different intellectual approaches. Imminent experimental studies present tremendous opportunities for clarifying multiple issues (discovery of new states, confirmation of others, measurement of production and decay channels) in a systematic fashion: One can actually present these goals as a "to-do" list, as given below. Theoretical studies also present tremendous opportunities, in the sense that all known pictures have limits to their applicability, and none of them provide a plausible explanation for the whole set of exotic candidates. As discussed below, the direction of progress involves an honest assessment of the constraints on existing methods (does one really know what being a molecule means, which fields are truly important near hadronic thresholds, *etc.*), leading both to improvements rendering existing techniques more flexible and robust, and to the development entirely new theoretical approaches.

4.1. Experimental Issues and Prospects

As mentioned above, the goals for ongoing and future efforts in the experimental study of QCD exotica are comparatively straightforward. Here we simply list ten of the most important.

1. Search for qualitatively new classes of particles. There has been a growing list of robust experimental discoveries indicating potential candidates for QCD exotica. These include tetraquark candidates containing $c\bar{c}$ and light quarks [like the $Z_c(3900)$ and $Z_c(4430)$], pentaquark candidates containing $c\bar{c}$ and light quarks [the $P_c(4380)$ and $P_c(4450)$], and supernumerary states that are potentially hybrid mesons [like the $Y(4260)$]. However, pinning down these interpretations has proven difficult. Finding qualitatively new classes of particles could solidify emerging patterns (*e.g.*, peaks near thresholds) or reveal new ones. A few examples that could be revealing include: hexaquarks (either dibaryons or tri-mesons); double-heavy open-charm exotics (like $cc\bar{u}\bar{d}$); other tetraquark combinations [the $X(5568)$ is particularly intriguing and should obviously be studied further]; and states with exotic J^{PC}.
2. Search for new decay modes of the particles that have already been discovered. Once a particle is discovered in some production process (*e.g.*, B decays or e^+e^- annihilation), that same process can be used to search for new decay modes. So far, many particles have only been observed in a single decay mode. This result may, at least in part, be due to experimental commonplaces. For example, it is much easier to find decay modes containing a J/ψ (which is narrow and has a large dilepton branching fraction) than those with an η_c (which is wide and decays to multiple-hadron final states). As more data is collected, these less experimentally accessible decay modes should be explored. Judging from history, besides possibly establishing new decay modes, these searches are also likely to lead to the discovery of new particles. Furthermore, none of the discovered exotic states has yet to be seen to decay exclusively to light-quark final states, a result that might be due to a lack of data and comprehensive searches.
3. Identify the conventional mesons in the region between 3.8 and 4.0 GeV. This region serves as a crucial test for our understanding of conventional mesons above open-flavor thresholds, which is especially important if we hope to distinguish conventional mesons from exotic mesons using their observed properties. While the situation is currently complicated, there are a number of experimental measurements yet to be completed. For example, it seems the decay $\chi_{c2}(2P) \to D\bar{D}$ has been established, assuming the $Z(3930)$ is the $\chi_{c2}(2P)$. But can the $\chi_{c2}(2P)$ decay to $D\bar{D}^*$ be found? And what about the decay $\chi_{c0}(2P) \to D\bar{D}$? Besides open-charm decays, radiative decays (despite being much smaller) could also prove decisive.
4. Understand e^+e^- cross sections, both exclusive and inclusive, as a function of center-of-mass energy. As discussed in Section 2.5.2, e^+e^- cross sections in the charmonium region show a surprisingly diverse range of shapes. These shapes should be mapped more finely in the future. Will patterns start to emerge? Will possibly informative connections like the decay $Y(4260) \to \gamma X(3872)$ be established? Special attention should be paid to the open-charm cross sections, which are larger than the closed-charm cross sections, and which also display surprising structure. If possible, open-bottom cross sections should similarly be mapped.
5. Continue to establish the existence or nonexistence of resonances in B decays. The LHCb experiment has already resolved long-standing controversies in the $B \to K\pi\psi(2S)$ and $B \to K\phi J/\psi$ channels. Both revealed the existence of a number of states. Several more channels, however, remain controversial. The decays $B \to K\pi J/\psi$ and $B \to K\pi\chi_{c1}$ should be revisited with higher statistics. Other B and Λ_b decays should also be explored. Will the pattern of *pairs* of peaks continue?
6. Explore the differences between the Z_c in B decays and in e^+e^- annihilation. While many Z_c peaks have been seen in either B decays or e^+e^- annihilation, one of the most conspicuous puzzles is the fact that no Z_c peak has been seen in both. The $Z_c(3900)$, for example, discovered in $e^+e^- \to \pi^\mp Z_c$ with $Z_c \to \pi^\pm J/\psi$, is not seen in B decays to either $K(\pi J/\psi)$ or $\pi(\pi J/\psi)$. Searches with higher statistics should be performed. Similarly, the $Z_c(4430)$, discovered in $B \to KZ_c$ with $Z_c \to \pi^\pm\psi(2S)$ should be searched for in e^+e^- annihilation to $\pi^\mp Z_c$ with $Z_c \to \pi^\pm\psi(2S)$. This study requires higher statistics at higher center-of-mass energies than currently available.
7. Search for previously established particles in hadron production. Of all the candidates for QCD exotica, currently only the $X(3872)$, $Y(4140)$, and $X(5568)$ have been reported in prompt hadron production. Several other states, however, might also be experimentally accessible. Besides the $Y(4140)$, the $Y(4274)$, $X(4500)$, and $X(4700)$ might also be seen in *inclusive* $\phi J/\psi$ production. If they are not seen, why not? Several of the Z_c states could also have signatures allowing them to be observed in hadron production, such as $Z_c(3900) \to \pi^\pm J/\psi$ or $Z_c(4430) \to \pi^\pm\psi(2S)$.
8. Continue mining relatively unexplored production mechanisms, such as $\gamma\gamma$ collisions and $e^+e^- \to \psi + X$. While a lot of attention has been paid to B decays and e^+e^- annihilation, other production mechanisms should continue to be explored. In particular, $\gamma\gamma$ collisions and $e^+e^- \to \psi + X$ should be revisited with higher statistics.
9. Explore qualitatively new production mechanisms. New production mechanisms are desparately needed and may soon be available. At the upcoming $\bar{\text{P}}$ANDA experiment, a scan of $p\bar{p}$ cross sections would be extremely interesting. How would it compare to e^+e^- annihilation? At GlueX, the photoproduction of light-quark hybrid mesons will be studied. At COMPASS, the photoproduction of a variety of charmonium states is feasible and studies have just begun [181].

10. Consider more advanced phenomenological methods, such as coupled channels. While it is relatively straightforward for experiments to measure cross sections and to fit peaks, more advanced phenomenology becomes important when performing detailed Dalitz plot analyses or considering the effects of one channel coupling to another. There has been a lot of success in extending experimental studies in this direction. These efforts need to continue, and cooperation between experiment and theory remains essential.

4.2. Theoretical Issues and Prospects

Theory finds itself in an interesting predicament because the tools that have served so well for conventional hadronic states (*e.g.*, the quark model, chiral perturbation theory, lattice studies of static properties) seem to require new insights and extensions to maintain their applicability to the exotic states. The best-known theoretical methods require a clear separation between distinct distance/time/energy scales, but it is not clear how far apart the four (or five) quarks reside in these states, or even if they reach an equilibrium before the exotic state decays, so it is not clear what substructure degrees of freedom best represent the states. Moreover, quantum mechanics allows components of different structures but the same overall quantum numbers to mix; we have seen this proposal in the suggestion that the $X(3872)$ is a molecule plus conventional charmonium (Sec. 3.1). Similarly, the $J^{PC} = 1^{--}$ states such as the $Y(4260)$ provide an excellent place to look for the lowest hybrid (Sec. 3.4), but they may mix with $I = 0$ tetraquark states. Thus far, theoretical pictures tend to be at their most incisive when they are not as successful in explaining a given state, because they better indicate the limitations of the picture.

Indeed, among the generic problems with theory is that it can be focused too narrowly. For example, quark models may concentrate upon a specific flavor sector, which may be adequate when sufficient data exists in that sector, but often it does not; one should investigate models as broadly as possible to ensure a reasonable level of reliability. A related problem occurs for molecular models of states near thresholds that assume a particular meson pair AB forms a resonance, but that often do not posit any plausible mechanism for this binding. Under these conditions all possible meson pair thresholds can be thought to form a resonance or bound state! A similar situation occurs with threshold-cusp models associated with a channel AB. In this case, it is incumbent on the proposer to explain why the resulting cusp should dominate the process under consideration. Analogous observations apply to lattice gauge theory results that have not been obtained with a large interpolating-field basis (especially in the case of exotic spectroscopy, where multihadron interpolating fields must be considered), and to QCD sum rule calculations, which require careful validation against experiment to ensure robustness. These problems are compounded when the technique is applied to incomplete or ambiguous experimental results, such as is the case in some sectors of exotic spectroscopy.

Lattice QCD could be considered the arbiter of these questions, and the quality of these calculations is definitely improving (*e.g.*, the calculated pion mass is becoming ever closer to its physical value), but lattice simulations are at their best when dealing with compact, static, isolated states. The need to use a suitably large basis of interpolating operators to properly study exotic states has already been noted. Additionally, interpolating operators are typically pointlike; extended states require the simulation of link variables, which is computationally expensive. States with finite widths like exotics require a lattice technology that was originally developed for elastic scattering [306] and has been extended to multiparticle states [307], but has not yet been as well developed, particularly for heavy-quark states. Coupled-channel effects, which are clearly important for the heavy-quark exotics, have only recently received their first light-quark lattice simulations [308], but have not yet been studied for heavy-quark systems.

From the theoretical perspective, one of many experimental mysteries is the apparent difficulty of observing some exotic states in B decays, even though they have been seen in e^+e^- collisions. For example, the $Z_c(3900)$ and $Z_c(4020)$ are clearly revealed in $e^+e^- \to J/\psi(h_c)\,\pi\pi$. Nevertheless, the Dalitz plot for $\bar{B}^0 \to J/\psi\,\pi\pi$ has been measured by LHCb [299], and shows no hint of these states. In contrast, the $X(3823)$ [now believed to be the $\psi_2(1D)$] has been observed in both $B \to K\gamma\chi_{c1}$ and in $e^+e^- \to \pi\pi\gamma\chi_{c1}$. These findings are difficult to understand unless the production mechanism depends sensitively on the environment; if they withstand further experimental scrutiny, it becomes incumbent upon theorists to explain why these cases are different.

An analogous situation in the $\phi J/\psi$ channel where the LHCb collaboration found a quartet of new states in $B \to KY \to K\phi J/\psi$ [125]. A notable absence in the list is the $X(4350)$, which was observed in $\gamma\gamma \to \phi J/\psi$. One expects this state to have quantum numbers $J^P = 2^+$ or 0^+ and hence show up in p- or s-wave in B decays, respectively. Since the statistical significance of the $X(4350)$ is below 5σ (See App. A), it may disappear entirely, and models predicting it to exist become suspect.

There is also a curious dichotomy between exotics that decay to J/ψ and to $\psi(2S)$. In particular, the $Z_c(4055)$, $Y(4360)$, and $Z_c(4430)$ are produced in either e^+e^- or B decays, and so far appear only in $\psi(2S)\,\pi$ or $\psi(2S)\,\pi\pi$. In contrast, the $Y(4260)$ and $Z_c(4200)$ were discovered in the $J/\psi\,\pi\pi$ or $J/\psi\,\pi$ decay modes, respectively. Naively, one would expect all the states to couple to $\psi(nS)\,\pi(\pi)$ with weights approximately given by phase space and slowly varying couplings. Perhaps this conundrum is an example, among many, that points to novel dynamics, such as that proposed in Sec. 3.3.3.

5. Conclusions

An entirely new chapter of hadronic physics opened in 2003, with the discovery of the enigmatic $X(3872)$. It has since been joined by about 30 equally mysterious states, many believed to be tetraquarks or pentaquark resonances, while others might ultimately turn out instead to be prominent effects due to the opening of hadronic thresholds.

In this review we explored the history and techniques of the experiments that discovered, confirmed, and measured the mass, J^{PC}, and decay properties of these numerous states. Very often, the search to probe a known state led to the discovery of new ones.

We also examined in detail the leading theoretical pictures proposed for describing these states, finding that no single paradigm yet fits all of the candidate exotics. The eventual consensus picture may turn out to be one that is yet undiscovered, or a hybrid of those already proposed. In any case, the rate of theoretical work has not abated, with a new wave of excitement each time a new exotic candidate is discovered.

Many of the most prolific experiments uncovering these new results are still currently active, while a number of others designed to be sensitive to new production processes and/or new decay modes will come online in the next few years. The directions of both experimental and theoretical discovery can never be predicted, but only conjectured based upon past experience. In that light, the next several years should be just as rich, if not richer, in the volume of new experimental information and the creation of new theoretical ideas for these new classes of hadrons.

Acknowledgments

This work gratefully acknowledges support from the U.S. National Science Foundation under Grant No. 1403891 (R.F.L.) and the U.S. Department of Energy under Grant DE-FG02-05ER41374 (R.E.M.).

A. Glossary of Exotic States

A.1. $X(3823)$ *(or* $\psi_2(1D)$*)*

The $X(3823)$ was discovered by the Belle Collaboration in 2013 in the reaction $B \to KX$ with $X \to \gamma\chi_{c1}$ [124]. The BESIII Collaboration later found a peak consistent with the $X(3823)$ produced in $e^+e^- \to \pi^+\pi^- X$, again with $X \to \gamma\chi_{c1}$ [164]. The $X(3823)$ is likely the $\psi_2(1D)$ state of charmonium. See Sec. 2.6 for more detail.

A.2. $X(3872)$

Accidentally discovered by the Belle Collaboration in 2003 in the reaction $B \to KX$ with $X \to \pi^+\pi^- J/\psi$ [4], the $X(3872)$ was both the first of the XYZ states to be discovered and is the one that has been most studied. Nevertheless, like most of the XYZ states, there is no interpretation that is universally agreed upon. It has been produced in decays of the B meson [4, 109, 110, 111, 112, 113, 114, 115, 116, 117, 118, 119, 120, 121, 122, 140], in hadronic collisions [27, 28, 171, 172, 173, 178], and perhaps in radiative decays of the $Y(4260)$ [52]. Besides $\pi^+\pi^- J/\psi$, it has also been seen to decay to $\omega J/\psi$ [122], $D^*\bar{D}$ [115, 116, 117], $\gamma J/\psi$ [118, 119, 120, 121], and $\gamma\psi(2S)$ [118, 120]. Its unusual features include a mass that is currently indistinguishable from the $D^{*0}\bar{D}^0$ threshold (the current mass difference is 0.01 ± 0.18 MeV) and a narrow width (< 1.2 MeV). It is has no isospin partners and has $J^{PC} = 1^{++}$. See Sec. 2.3 for more discussion of its experimental properties.

A.3. $Z_c(3900)$

The $Z_c(3900)$ was simultaneously discovered in 2013 by the BESIII and Belle Collaborations in the process $e^+e^- \to \pi^\mp Z_c^\pm$ with $Z_c^\pm \to \pi^\pm J/\psi$. For the BESIII observation [22], the center-of-mass energy was fixed to 4.26 GeV. Belle [23] used initial-state radiation to cover the energy region from 4.15 to 4.45 GeV, corresponding to the region of the $Y(4260)$. It is not yet clear whether the production of the $Z_c(3900)$ is associated with the $Y(4260)$. The $Z_c(3900)$ has since been seen in decays to $\pi^0 J/\psi$ [31, 32] (Z_c^0) and in $D^*\bar{D}$ (both charged and neutral) [33, 154, 155]. It has only been produced in the reaction $e^+e^- \to \pi Z_c$. See Sec. 2.5.4 for more experimental details.

A.4. $X(3915)$ *(or* $\chi_{c0}(2P)$*)*

The $X(3915)$ was first seen by the Belle Collaboration in 2010 in the process $\gamma\gamma \to X$ with $X \to \omega J/\psi$ [166]. It was later confirmed by the BaBar Collaboration [167]. It appears as a clear peak with little background. Its J^{PC} is likely 0^{++}, so there is some possibility that it is the $\chi_{c0}(2P)$ state of charmonium, although this assignment is controversial. See Sec. 2.6 for more discussion.

A.5. $Y(3940)$

The $Y(3940)$ was first observed in 2005 by the Belle Collaboration in the process $B \to KY$ with $Y \to \omega J/\psi$ [106]. It was the second of the XYZ to be discovered [after the $X(3872)$]. It was later confirmed by the BaBar Collaboration in both 2008 [123] and 2010 [122], but with a mass around 3915 MeV. Due to its similar mass and width to the $X(3915)$, and since both states decay to $\omega J/\psi$, the $Y(3940)$ is usually identified with the $X(3915)$. See Sec. 2.6 for more details.

A.6. $Z(3930)$ *(or* $\chi_{c2}(2P)$*)*

The $Z(3930)$ was discovered in 2006 by the Belle Collaboration in the process $\gamma\gamma \to Z$ with $Z \to D\bar{D}$ [168]. It was confirmed in 2010 by the BaBar Collaboration in the same process [169]. Both collaborations measured $J^{PC} = 2^{++}$. It is often assumed to be the $\chi_{c2}(2P)$ state of charmonium. See Sec. 2.6 for more details.

A.7. $X(3940)$

The $X(3940)$ was first reported in 2007 by the Belle Collaboration in e^+e^- collisions near the $\Upsilon(4S)$ resonance. It appeared in $e^+e^- \to J/\psi X$, where the X either decayed inclusively or to $D^*\bar{D}$ [165]. A later analysis by Belle using a similar technique but with more data confirmed the $X(3940)$ decay to $D^*\bar{D}$ [41]. The same analysis also reported a $X(4160)$ state decaying to $D^*\bar{D}^*$ and a very broad excess of events near threshold in $D\bar{D}$. See Sec. 2.6 for more details.

A.8. $Z_c(4020)$

The $Z_c(4020)$ was discovered in 2013 by the BESIII Collaboration in the process $e^+e^- \to \pi^\mp Z_c^\pm$ with $Z_c^\pm \to \pi^\pm h_c$ [156]. The center-of-mass energies included 4.23, 4.26, and 4.36 GeV, and the production rate of the $Z_c(4020)$ apparently does not vary greatly over this energy range. It is thus unclear whether or not its production is associated with the $Y(4260)$, $Y(4360)$, or any other state produced in e^+e^- annihilation. The $Z_c(4020)$ has since been seen to decay to $\pi^0 h_c$ [157] and to both charged [158] and neutral [159] combinations of $D^*\bar{D}^*$. See Sec. 2.5.4 for more discussion.

A.9. $Z_1(4050)$ *and* $Z_2(4250)$

The $Z_1(4050)$ and $Z_2(4250)$ were reported in 2008 by the Belle Collaboration in the process $B \to KZ^\pm$ with $Z^\pm \to \pi^\pm \chi_{c1}$ [133]. Using a Dalitz plot analysis, the significance of each structure was reported to be more than 5σ. BaBar searched for the same structures in the same reaction but used a phenomenological method to describe the effects of possible resonances in the $K\pi$ subsystem [134]. They found no need for the $Z_1(4050)$ or $Z_2(4250)$ states, but with upper limits that are not inconsistent with the early measurements of Belle. See Sec. 2.4.4 for more discussion.

A.10. $Z_c(4055)$

The $Z_c(4055)$ was reported in 2015 by the Belle Collaboration in the reaction $e^+e^- \to \pi^\mp Z_c^\pm$ with $Z_c^\pm \to \pi^\pm \psi(2S)$ [148]. A wide range of e^+e^- energies was covered using the initial-state radiation of the beams. It appears that the $Z_c(4055)$ is only produced when the e^+e^- energies are near the $Y(4360)$ (between 4.0 and 4.5 GeV). When the energy is in the $Y(4660)$ region (between 4.5 and 4.9 GeV), no signal is apparent. See Sec. 2.5.4 for more discussion.

A.11. $Y(4140)$*,* $Y(4274)$*,* $X(4500)$*, and* $X(4700)$

The $Y(4140)$ was first reported in 2009 by the CDF Collaboration in the process $B \to KY$ with $Y \to \phi J/\psi$ [126]. A series of positive [129, 130] and negative [127, 128] searches using the same process followed, making the status of the $Y(4140)$ uncertain. In addition to the $Y(4140)$, the CDF and CMS Collaborations found evidence for a higher-mass structure, the $Y(4274)$ [130, 132], whose status was also uncertain. In 2016, the LHCb Collaboration used a much larger sample of events to decisively confirm the existence of both the $Y(4140)$ and the $Y(4274)$ [125, 131]. In the same analysis, LHCb also found evidence for two more structures, the $X(4500)$ and the $X(4700)$. See Sec. 2.4.2 for more detail.

A.12. $X(4160)$

The $X(4160)$ was reported by the Belle Collaboration in 2008 in the reaction $e^+e^- \to J/\psi X$ with $X \to D^*\bar{D}^*$, where the energy of the e^+e^- collisions was near the $\Upsilon(4S)$ resonance [41]. While the signal is significant ($> 5\sigma$), it is yet to be confirmed. The same reaction with $X \to D^*\bar{D}$ has so far produced only the $X(3940)$. See Sec. 2.6 for more discussion.

A.13. $Z_c(4200)$

The $Z_c(4200)$ was reported in 2014 by the Belle Collaboration in the process $B \to KZ_c^\pm$ with $Z_c^\pm \to \pi^\pm J/\psi$ [46]. Along with numerous K^* states, an amplitude analysis of the $K\pi^\pm J/\psi$ system showed evidence for both the $Z_c(4200)$ and the $Z_c(4430)$ [see the separate entry on the $Z_c(4430)$]. However, neither the $Z_c(4200)$ nor the $Z_c(4430)$ have yet been confirmed in this process. [BaBar reported a negative search for the $Z_c(4430)$ in $\pi^\pm J\psi$ [135], but this was before Belle first reported the $Z_c(4200)$]. See Sec. 2.4.4 for more details.

A.14. $Y(4230)$

The $Y(4230)$ was reported in 2015 by the BESIII Collaboration in the reaction $e^+e^- \to Y$ with $Y \to \omega\chi_{c0}$ [149]. Since BESIII only had large data sets at a few center-of-mass energies, the mass and width of the $Y(4230)$ could not be measured precisely. The energy dependence of the cross section for $e^+e^- \to \omega\chi_{c0}$ was, however, shown to be decisively different from the $Y(4260)$. There is some indication that a narrow peak around 4.23 GeV may also exist in the $e^+e^- \to \pi^+\pi^- h_c$ cross section [193]. See Sec. 2.5.2 for more details.

A.15. $Y(4260)$ *and* $Y(4008)$

The $Y(4260)$ was first observed by the BaBar Collaboration in 2005 in the reaction $e^+e^- \to Y$ with $Y \to \pi^+\pi^- J/\psi$ [29]. It was the third of the XYZ states to be discovered. It was later confirmed by CLEO-c [141] and by Belle [143] in the same reaction. CLEO-c [142] and BESIII [32] saw the same peak in $e^+e^- \to \pi^0\pi^0 J/\psi$. The Belle Collaboration reported a second peak, called the $Y(4008)$, just below the much larger $Y(4260)$ peak [23, 143]. The $Y(4008)$ peak was not confirmed by a BaBar analysis using the same method with a data set of similar size [144]. Establishing new decay modes of the $Y(4260)$ involves mapping other e^+e^- cross sections as a function of center-of-mass energy, which has proven difficult. See Sec. 2.5.2 for more discussion.

A.16. $X(4350)$

The $X(4350)$ was reported by the Belle Collaboration in 2010 in the reaction $\gamma\gamma \to X$ with $X \to \phi J/\psi$ [170]. Its significance is only at the level of 3.2σ and is in need of confirmation. See Sec. 2.7 for more detail.

A.17. $Y(4360)$ *and* $Y(4660)$

The $Y(4360)$ was discovered in 2007 by the BaBar Collaboration in the process $e^+e^- \to Y$ with $Y \to \pi^+\pi^-\psi(2S)$ [108]. This unexpected discovery was a byproduct of a search for the $Y(4260)$ decaying to $\pi^+\pi^-\psi(2S)$, which was not found. The Belle Collaboration soon confirmed the BaBar finding using the same process, but also found a second peak at higher mass, the $Y(4660)$ [146]. Both peaks have been confirmed with higher statistics by both the Belle [148] and BaBar Collaborations [147]. See Sec. 2.5.2 for more details.

A.18. $Z_c(4430)$ *and* $Z_c(4240)$

The $Z_c(4430)$ was first reported in 2008 by the Belle Collaboration in the process $B \to K Z_c^\pm$ with $Z_c^\pm \to \pi^\pm\psi(2S)$ [30]. As the first of the electrically charged XYZ states to be reported, it was the subject of much scrutiny. The initial report by Belle was based on a one-dimensional fit to the $\pi^\pm\psi(2S)$ invariant mass, but the data was later reanalyzed using more sophisticated amplitude analyses [136, 137]. The BaBar Collaboration, however, using a technique that allowed for $K\pi^\pm$ resonances in a model-independent way, could not confirm the $Z_c(4430)$ in either its reported decay of $\pi^\pm\psi(2S)$ or in the possible decay $\pi^\pm J/\psi$ [135]. Belle later also reported evidence for the $Z_c(4430)$ in $B \to K Z_c^\pm$ with $Z_c^\pm \to \pi^\pm J/\psi$ [also see the entry for the $Z_c(4200)$] [46]. In 2014, the LHCb Collaboration confirmed the existence of the $Z_c(4430)$ in $\pi^\pm\psi(2S)$ using a larger data set, and also observed a lighter and wider structure named the $Z_c(4240)$ [138, 139]. See Sec. 2.4.1 for more details.

A.19. $X(4630)$

The $X(4630)$ was seen in 2008 by the Belle Collaboration as a threshold enhancement in $e^+e^- \to X$ with $X \to \Lambda_c\bar{\Lambda}_c$ [150]. The $X(4630)$ is one of several peaks seen in exclusive e^+e^- cross sections, such as the $Y(4260)$ in $e^+e^- \to \pi\pi J/\psi$ and the $Y(4360)$ in $e^+e^- \to \pi\pi\psi(2S)$. The fact that it is named X rather than Y is thus somewhat of an anomaly. See Sec. 2.5.2 for more details.

A.20. $P_c(4380)$ *and* $P_c(4450)$

The $P_c(4380)$ and $P_c(4450)$ pentaquark candidates were reported in 2015 by the LHCb Collaboration in an amplitude analysis of the decay $\Lambda_b \to K^- J/\psi\, p$ [35]. In addition to a number of excited resonant Λ decays to K^-p, amplitudes corresponding to $P_c \to J/\psi p$ resonances were found to be necessary to describe the data. See Sec. 2.4.3 for more details.

A.21. $X(5568)$

The $X(5568)$ was reported in 2016 by the D0 Collaboration in inclusive hadronic ($p\bar{p}$) production of $B_s\pi^\pm$ [175]. It was not confirmed by the LHCb Collaboration in pp collisions at the LHC. While the data sets at LHCb are larger, the production mechanisms and energies are different. The state needs confirmation. See Sec. 2.7 for more details.

A.22. $Z_b(10610)$ *and* $Z_b(10650)$

The $Z_b(10610)$ and $Z_b(10650)$ were discovered in 2012 by the Belle Collaboration in e^+e^- annihilations near the $\Upsilon(5S)$ mass [160]. They were produced in the process $e^+e^- \to \pi^\mp Z_b^\pm$ and were found to decay through the five channels $\pi^\pm\Upsilon(1S, 2S, 3S)$ and $\pi^\pm h_b(1P, 2P)$, with consistent properties in each. Their J^P were measured to be 1^+ [162]. A neutral version of the $Z_b(10610)$ was later found in the process $e^+e^- \to \pi^0 Z_b$ with $Z_b \to \pi^0\Upsilon(2S, 3S)$ [161]. The open-bottom decays $Z_b(10610) \to B^*\bar{B}$ and $Z_b(10650) \to B^*\bar{B}^*$ were also reported by the Belle Collaboration [163]. See Sec. 2.5.3 for more discussion.

A.23. $Y_b(10888)$

The $Y_b(10888)$ was originally reported in 2010 by the Belle Collaboration in the process $e^+e^- \to Y_b$, with $Y_b \to \pi^+\pi^-\Upsilon(1S, 2S, 3S)$ [151]. This initial report found evidence for a deviation in mass between the peak in the $e^+e^- \to \pi^+\pi^-\Upsilon(1S, 2S, 3S)$ cross section and the peak in the inclusive e^+e^- cross section, the latter thought to be the $\Upsilon(5S)$. A later analysis found that the two peaks could be described with the same parameterization [152]. It is thus not clear that there is a $Y_b(10888)$ distinct from the $\Upsilon(5S)$, although the large closed-bottom cross sections are still a mystery. The energy dependences of the $e^+e^- \to \pi^+\pi^- h_b(1P, 2P)$ cross sections are consistent with those of the $e^+e^- \to \pi^+\pi^-\Upsilon(1S, 2S, 3S)$ cross sections [153]. See Sec. 2.5.1 for more details.

References

[1] M. Gell-Mann, *A Schematic Model of Baryons and Mesons*, Phys. Lett. **8** (1964) 214. doi:10.1016/S0031-9163(64)92001-3.

[2] G. Zweig, *An SU(3) Model for Strong Interaction Symmetry and Its Breaking. Version 1*, CERN Report CERN-TH-401 (1964).

[3] G. Zweig, *An SU(3) Model for Strong Interaction Symmetry and Its Breaking. Version 2*, in: D. Lichtenberg, S. P. Rosen (Eds.), Developments in the Quark Theory of Hadrons. Vol. 1. 1964–1978, 1964, p. 22.
URL http://inspirehep.net/record/4674/files/cern-th-412.pdf

[4] S.-K. Choi, *et al.*, *Observation of a Narrow Charmonium-like State in Exclusive $B^{\pm} \to K^{\pm}\pi^{+}\pi^{-}J/\psi$ Decays*, Phys. Rev. Lett. **91** (2003) 262001. arXiv:hep-ex/0309032, doi:10.1103/PhysRevLett.91.262001.

[5] E. Swanson, *The New Heavy Mesons: A Status Report*, Phys. Rept. **429** (2006) 243. arXiv:hep-ph/0601110, doi:10.1016/j.physrep.2006.04.003.

[6] S.-L. Zhu, *New Hadron States*, Int. J. Mod. Phys. E **17** (2008) 283. arXiv:hep-ph/0703225, doi:10.1142/S0218301308009446.

[7] S. Godfrey, S. Olsen, *The Exotic XYZ Charmonium-like Mesons*, Ann. Rev. Nucl. Part. Sci. **58** (2008) 51. arXiv:0801.3867, doi:10.1146/annurev.nucl.58.110707.171145.

[8] N. Drenska, R. Faccini, F. Piccinini, A. Polosa, F. Renga, C. Sabelli, *New Hadronic Spectroscopy*, Riv. Nuovo Cim. **33** (2010) 633. arXiv:1006.2741, doi:10.1393/ncr/i2010-10059-8.

[9] G. Pakhlova, P. Pakhlov, S. Eidelman, *Exotic Charmonium*, Phys. Usp. **53** (2010) 219, [Usp. Fiz. Nauk **180**, 225 (2010)]. doi:10.3367/UFNe.0180.201003a.0225.

[10] C.-Z. Yuan, *Recent Progress on the Study of the Charmoniumlike States*, Int. J. Mod. Phys. A **29** (2014) 1430046. arXiv:1404.7768, doi:10.1142/S0217751X14300464.

[11] A. Esposito, A. Guerrieri, F. Piccinini, A. Pilloni, A. Polosa, *Four-Quark Hadrons: an Updated Review*, Int. J. Mod. Phys. A **30** (2015) 1530002. arXiv:1411.5997, doi:10.1142/S0217751X15300021.

[12] S. Olsen, *A New Hadron Spectroscopy*, Front. Phys. **10** (2015) 101401. arXiv:1411.7738, doi:10.1007/S11467-014-0449-6.

[13] H.-X. Chen, W. Chen, X. Liu, S.-L. Zhu, *The Hidden-Charm Pentaquark and Tetraquark States*, Phys. Rept. **639** (2016) 1. arXiv:1601.02092, doi:10.1016/j.physrep.2016.05.004.

[14] A. Ali, *Multiquark Hadrons - A New Facet of QCD*, in: 14th Regional Conference on Mathematical Physics Islamabad, Pakistan, November 9–14, 2015, 2016. arXiv:1605.05954.

[15] N. Brambilla, *et al.*, *Heavy Quarkonium Physics*, CERN Yellow Report, arXiv:hep-ph/0412158.
URL http://www.qwg.to.infn.it

[16] E. Eichten, S. Godfrey, H. Mahlke, J. Rosner, *Quarkonia and Their Transitions*, Rev. Mod. Phys. **80** (2008) 1161. arXiv:hep-ph/0701208, doi:10.1103/RevModPhys.80.1161.

[17] E. Klempt, A. Zaitsev, *Glueballs, Hybrids, Multiquarks. Experimental Facts Versus QCD Inspired Concepts*, Phys. Rept. **454** (2007) 1. arXiv:0708.4016, doi:10.1016/j.physrep.2007.07.006.

[18] M. Voloshin, *Charmonium*, Prog. Part. Nucl. Phys. **61** (2008) 455. arXiv:0711.4556, doi:10.1016/j.ppnp.2008.02.001.

[19] N. Brambilla, *et al.*, *Heavy Quarkonium: Progress, Puzzles, and Opportunities*, Eur. Phys. J. **C71** (2011) 1534. arXiv:1010.5827, doi:10.1140/epjc/s10052-010-1534-9.

[20] G. Bodwin, E. Braaten, E. Eichten, S. Olsen, T. Pedlar, J. Russ, *Quarkonium at the Frontiers of High Energy Physics: A Snowmass White Paper*, in: Community Summer Study 2013: Snowmass on the Mississippi (CSS2013) Minneapolis, MN, USA, July 29-August 6, 2013, 2013, p. 1. arXiv:1307.7425.

[21] F.-K. Guo, C. Hanhart, Y. Kalashnikova, P. Matuschek, R. Mizuk, A. Nefediev, Q. Wang, J.-L. Wynen, *Interplay of Quark and Meson Degrees of Freedom in Near-Threshold States: A Practical Parametrization for Line Shapes*, Phys. Rev. D **93** (2016) 074031. arXiv:1602.00940, doi:10.1103/PhysRevD.93.074031.

[22] M. Ablikim, *et al.*, *Observation of a Charged Charmoniumlike Structure in $e^{+}e^{-} \to \pi^{+}\pi^{-}J/\psi$ at $\sqrt{s} = 4.26$ GeV*, Phys. Rev. Lett. **110** (2013) 252001. arXiv:1303.5949, doi:10.1103/PhysRevLett.110.252001.

[23] Z. Liu, *et al.*, *Study of $e^{+}e^{-} \to \pi^{+}\pi^{-}J/\psi$ and Observation of a Charged Charmoniumlike State at Belle*, Phys. Rev. Lett. **110** (2013) 252002. arXiv:1304.0121, doi:10.1103/PhysRevLett.110.252002.

[24] E. Eichten, K. Gottfried, T. Kinoshita, K. Lane, T.-M. Yan, *Charmonium: The Model*, Phys. Rev. D **17** (1978) 3090, [Erratum: Phys. Rev. D **21**, 313 (1980)]. doi:10.1103/PhysRevD.17.3090,10.1103/PhysRevD.21.313.

[25] E. Eichten, K. Gottfried, T. Kinoshita, K. Lane, T.-M. Yan, *Charmonium: Comparison with Experiment*, Phys. Rev. D **21** (1980) 203. doi:10.1103/PhysRevD.21.203.

[26] T. Barnes, S. Godfrey, E. Swanson, *Higher Charmonia*, Phys. Rev. D **72** (2005) 054026. arXiv:hep-ph/0505002, doi:10.1103/PhysRevD.72.054026.

[27] D. Acosta, *et al.*, *Observation of the Narrow State $X(3872) \to J/\psi\,\pi^{+}\pi^{-}$ in $\bar{p}p$ Collisions at $\sqrt{s} = 1.96$ TeV*, Phys. Rev. Lett. **93** (2004) 072001. arXiv:hep-ex/0312021, doi:10.1103/PhysRevLett.93.072001.

[28] S. Chatrchyan, *et al.*, *Measurement of the $X(3872)$ Production Cross Section via Decays to $J/\psi\,\pi\pi$ in pp Collisions at $\sqrt{s} = 7$ TeV*, JHEP **04** (2013) 154. arXiv:1302.3968, doi:10.1007/JHEP04(2013)154.

[29] B. Aubert, *et al.*, *Observation of a Broad Structure in the $\pi^{+}\pi^{-}J/\psi$ Mass Spectrum around 4.26 GeV/c^2*, Phys. Rev. Lett. **95** (2005) 142001. arXiv:hep-ex/0506081, doi:10.1103/PhysRevLett.95.142001.

[30] S.-K. Choi, *et al.*, *Observation of a Resonance-like Structure in the $\pi^{\pm}\psi'$ Mass Distribution in Exclusive $B \to K\pi^{\pm}\psi'$ decays*, Phys. Rev. Lett. **100** (2008) 142001. arXiv:0708.1790, doi:10.1103/PhysRevLett.100.142001.

[31] T. Xiao, S. Dobbs, A. Tomaradze, K. Seth, *Observation of the Charged Hadron $Z_c^{\pm}(3900)$ and Evidence for the Neutral $Z_c^{0}(3900)$ in $e^{+}e^{-} \to \pi\pi J/\psi$ at $\sqrt{s} = 4170$ MeV*, Phys. Lett. **B727** (2013) 366. arXiv:1304.3036, doi:10.1016/j.physletb.2013.10.041.

[32] M. Ablikim, *et al.*, *Observation of $Z_c(3900)^0$ in $e^{+}e^{-} \to \pi^{0}\pi^{0}J/\psi$*, Phys. Rev. Lett. **115** (2015) 112003. arXiv:1506.06018, doi:10.1103/PhysRevLett.115.112003.

[33] M. Ablikim, *et al.*, *Observation of a Neutral Structure near the $D\bar{D}^{*}$ Mass Threshold in $e^{+}e^{-} \to (D\bar{D}^{*})^{0}\pi^{0}$ at $\sqrt{s} = 4.226$ and 4.257 GeV*, Phys. Rev. Lett. **115** (2015) 222002. arXiv:1509.05620, doi:10.1103/PhysRevLett.115.222002.

[34] K. Olive, *et al.*, *Review of Particle Physics*, Chin. Phys. C **38** (2014) 090001. doi:10.1088/1674-1137/38/9/090001.

[35] R. Aaij, *et al.*, *Observation of $J/\psi\,p$ Resonances Consistent with Pentaquark States in $\Lambda_b^{0} \to J/\psi\,K^{-}p$ Decays*, Phys. Rev. Lett. **115** (2015) 072001. arXiv:1507.03414, doi:10.1103/PhysRevLett.115.072001.

[36] M. Voloshin, L. Okun, *Hadron Molecules and Charmonium Atom*, JETP Lett. **23** (1976) 333, [Pisma Zh. Eksp. Teor. Fiz. **23**, 369 (1976)].

[37] A. De Rújula, H. Georgi, S. Glashow, *Molecular Charmonium: A New Spectroscopy?*, Phys. Rev. Lett. **38** (1977) 317. doi:10.1103/PhysRevLett.38.317.

[38] H. Høgaasen, P. Sorba, *The Systematics of Possibly Narrow Quark States with Baryon Number One*, Nucl. Phys. **B145** (1978) 119. doi:10.1016/0550-3213(78)90417-0.

[39] H.-M. Chan, H. Høgaasen, *Baryonium States in Multi-Quark Spectroscopy*, Phys. Lett. **B72** (1977) 121. doi:10.1016/0370-2693(77)90077-6.

[40] B. Aubert, *et al.*, *Search for a Charged Partner of the $X(3872)$ in the B Meson Decay $B \to X^- K$, $X^- \to J/\psi\,\pi^-\pi^0$*, Phys. Rev. D **71** (2005) 031501. arXiv:hep-ex/0412051, doi:10.1103/PhysRevD.71.031501.

[41] P. Pakhlov, *et al.*, *Production of New Charmoniumlike States in $e^+e^- \to J/\psi\,D^{(*)}\bar{D}^{(*)}$ at $\sqrt{s} \sim 10$ GeV*, Phys. Rev. Lett. **100** (2008) 202001. arXiv:0708.3812, doi:10.1103/PhysRevLett.100.202001.

[42] C. Bignamini, B. Grinstein, F. Piccinini, A. Polosa, C. Sabelli, *Is the $X(3872)$ Production Cross Section at Tevatron Compatible with a Hadron Molecule Interpretation?*, Phys. Rev. Lett. **103** (2009) 162001. arXiv:0906.0882, doi:10.1103/PhysRevLett.103.162001.

[43] C. Bignamini, B. Grinstein, F. Piccinini, A. Polosa, V. Riquer, C. Sabelli, *More Loosely Bound Hadron Molecules at CDF?*, Phys. Lett. **B684** (2010) 228. arXiv:0912.5064, doi:10.1016/j.physletb.2010.01.037.

[44] S. Dubynskiy, M. Voloshin, *Hadro-Charmonium*, Phys. Lett. **B666** (2008) 344. arXiv:0803.2224, doi:10.1016/j.physletb.2008.07.086.

[45] A. Manohar, M. Wise, *Heavy Quark Physics*, Camb. Monogr. Part. Phys. Nucl. Phys. Cosmol. **10** (2000) 1.

[46] K. Chilikin, *et al.*, *Observation of a New Charged Charmoniumlike State in $\bar{B}^0 \to J/\psi\,K^-p^+$ decays*, Phys. Rev. D **90** (2014) 112009. arXiv:1408.6457, doi:10.1103/PhysRevD.90.112009.

[47] X. Li, M. Voloshin, *$Y(4260)$ and $Y(4360)$ as Mixed Hadrocharmonium*, Mod. Phys. Lett. A **29** (2014) 1450060. arXiv:1309.1681, doi:10.1142/S0217732314500606.

[48] M. Anselmino, E. Predazzi, S. Ekelin, S. Fredriksson, D. Lichtenberg, *Diquarks*, Rev. Mod. Phys. **65** (1993) 1199. doi:10.1103/RevModPhys.65.1199.

[49] R. Jaffe, *Multi-Quark Hadrons. 1. The Phenomenology of (2 Quark 2 Anti-Quark) Mesons*, Phys. Rev. D **15** (1977) 267. doi:10.1103/PhysRevD.15.267.

[50] L. Maiani, F. Piccinini, A. Polosa, V. Riquer, *Diquark-Antidiquarks with Hidden or Open Charm and the Nature of $X(3872)$*, Phys. Rev. D **71** (2005) 014028. arXiv:hep-ph/0412098, doi:10.1103/PhysRevD.71.014028.

[51] L. Maiani, F. Piccinini, A. Polosa, V. Riquer, *The $Z(4430)$ and a New Paradigm for Spin Interactions in Tetraquarks*, Phys. Rev. D **89** (2014) 114010. arXiv:1405.1551, doi:10.1103/PhysRevD.89.114010.

[52] M. Ablikim, *et al.*, *Observation of $e^+e^- \to \gamma X(3872)$ at BESIII*, Phys. Rev. Lett. **112** (2014) 092001. arXiv:1310.4101, doi:10.1103/PhysRevLett.112.092001.

[53] L. Maiani, A. Polosa, V. Riquer, *The New Pentaquarks in the Diquark Model*, Phys. Lett. **B749** (2015) 289. arXiv:1507.04980, doi:10.1016/j.physletb.2015.08.008.

[54] S. Brodsky, D. Hwang, R. Lebed, *Dynamical Picture for the Formation and Decay of the Exotic XYZ Mesons*, Phys. Rev. Lett. **113** (2014) 112001. arXiv:1406.7281, doi:10.1103/PhysRevLett.113.112001.

[55] R. Lebed, *The Pentaquark Candidates in the Dynamical Diquark Picture*, Phys. Lett. **B749** (2015) 454. arXiv:1507.05867, doi:10.1016/j.physletb.2015.08.032.

[56] C. Meyer, E. Swanson, *Hybrid Mesons*, Prog. Part. Nucl. Phys. **82** (2015) 21. arXiv:1502.07276, doi:10.1016/j.ppnp.2015.03.001.

[57] T. Barnes, *Quarks, Gluons, Bags, and Hadrons*, Ph.D. thesis, Caltech (1977).
URL http://resolver.caltech.edu/CaltechETD:etd-09142007-135116

[58] R. Jaffe, K. Johnson, *Unconventional States of Confined Quarks and Gluons*, Phys. Lett. **B60** (1976) 201. doi:10.1016/0370-2693(76)90423-8.

[59] J. Dudek, *The Lightest Hybrid Meson Supermultiplet in QCD*, Phys. Rev. D **84** (2011) 074023. arXiv:1106.5515, doi:10.1103/PhysRevD.84.074023.

[60] M. Berwein, N. Brambilla, J. Tarrús Castellà, A. Vairo, *Quarkonium Hybrids with Nonrelativistic Effective Field Theories*, Phys. Rev. D **92** (2015) 114019. arXiv:1510.04299, doi:10.1103/PhysRevD.92.114019.

[61] E. Wigner, *On the Behavior of Cross Sections Near Thresholds*, Phys. Rev. **73** (1948) 1002. doi:10.1103/PhysRev.73.1002.

[62] A. Baz', L. Okun', *On the Λ-Hyperon Creation Cross Section Near the Σ-Hyperon Creation Threshold*, Soviet Phys. JETP **8** (1959) 757, [Zh. ETF **35**, 757 (1959)].

[63] M. Naunenberg, A. Pais, *Correlations between Cusps in Differential Cross Sections and in Polarizations*, Phys. Rev. **123** (1961) 1058. doi:10.1103/PhysRev.123.1058.

[64] N. Törnqvist, *Understanding the Scalar Meson $q\bar{q}$ Nonet*, Z. Phys. **C68** (1995) 647. arXiv:hep-ph/9504372, doi:10.1007/BF01565264.

[65] D. Bugg, *How Resonances Can Synchronise with Thresholds*, J. Phys. **G35** (2008) 075005. arXiv:0802.0934, doi:10.1088/0954-3899/35/7/075005.

[66] D. Bugg, *An Explanation of Belle States $Z_b(10610)$ and $Z_b(10650)$*, Europhys. Lett. **96** (2011) 11002. arXiv:1105.5492, doi:10.1209/0295-5075/96/11002.

[67] A. De Rujula, H. Georgi, S. Glashow, *Hadron Masses in a Gauge Theory*, Phys. Rev. D **12** (1975) 147. doi:10.1103/PhysRevD.12.147.

[68] N. Isgur, G. Karl, *Hyperfine Interactions in Negative Parity Baryons*, Phys. Lett. **B72** (1977) 109. doi:10.1016/0370-2693(77)90074-0.

[69] N. Brambilla, A. Pineda, J. Soto, A. Vairo, *Effective Field Theories for Heavy Quarkonium*, Rev. Mod. Phys. **77** (2005) 1423. arXiv:hep-ph/0410047, doi:10.1103/RevModPhys.77.1423.

[70] H. Yukawa, *On the Interaction of Elementary Particles I*, Proc. Phys. Math. Soc. Jap. **17** (1935) 48, [Prog. Theor. Phys. Suppl.1,1(1935)]. doi:10.1143/PTPS.1.1.

[71] V. Stoks, R. Klomp, C. Terheggen, J. de Swart, *Construction of High Quality NN Potential Models*, Phys. Rev. C **49** (1994) 2950. arXiv:nucl-th/9406039, doi:10.1103/PhysRevC.49.2950.

[72] R. Machleidt, *The High Precision, Charge Dependent Bonn Nucleon-Nucleon Potential (CD-Bonn)*, Phys. Rev. C **63** (2001) 024001. arXiv:nucl-th/0006014, doi:10.1103/PhysRevC.63.024001.

[73] R. Wiringa, V. Stoks, R. Schiavilla, *An Accurate Nucleon-Nucleon Potential with Charge Independence Breaking*, Phys. Rev. C **51** (1995) 38. arXiv:nucl-th/9408016, doi:10.1103/PhysRevC.51.38.

[74] L. Glozman, D. Riska, *The Spectrum of the Nucleons and the Strange Hyperons and Chiral Dynamics*, Phys. Rept. **268** (1996) 263. arXiv:hep-ph/9505422, doi:10.1016/0370-1573(95)00062-3.

[75] N. Isgur, *Critique of a Pion Exchange Model for Interquark Forces*, Phys. Rev. D **62** (2000) 054026. arXiv:nucl-th/9908028, doi:10.1103/PhysRevD.62.054026.

[76] N. Törnqvist, *From the Deuteron to Deusons, an Analysis of Deuteron-like Meson Meson Bound States*, Z. Phys. **C61** (1994) 525. arXiv:hep-ph/9310247, doi:10.1007/BF01413192.

[77] N. Isgur, M. Wise, *Weak Decays of Heavy Mesons in the Static Quark Approximation*, Phys. Lett. **B232** (1989) 113. doi:10.1016/0370-2693(89)90566-2.

[78] N. Isgur, M. Wise, *Weak Transition Form-Factors Between Heavy Mesons*, Phys. Lett. **B237** (1990) 527. doi:10.1016/0370-2693(90)91219-2.

[79] B. Grinstein, *The Static Quark Effective Theory*, Nucl. Phys. **B339** (1990) 253. doi:10.1016/0550-3213(90)90349-I.

[80] H. Georgi, *An Effective Field Theory for Heavy Quarks at Low Energies*, Phys. Lett. **B240** (1990) 447. doi:10.1016/0370-2693(90)91128-X.

[81] M. Cleven, F.-K. Guo, C. Hanhart, Q. Wang, Q. Zhao, *Employing Spin Symmetry to Disentangle Different Models for the XYZ States*, Phys. Rev. D **92** (2015) 014005. arXiv:1505.01771, doi:10.1103/PhysRevD.92.014005.

[82] G. Ecker, *Chiral Perturbation Theory*, Prog. Part. Nucl. Phys. **35** (1995) 1. arXiv:hep-ph/9501357, doi:10.1016/0146-6410(95)00041-G.

[83] J. Oller, E. Oset, A. Ramos, *Chiral Unitary Approach to Meson-Meson and Meson-Baryon Interactions and Nuclear Applications*, Prog. Part. Nucl. Phys. **45** (2000) 157. arXiv:hep-ph/0002193, doi:10.1016/S0146-6410(00)00104-6.

[84] T. Truong, *Chiral Perturbation Theory and Final-State Theorem*, Phys. Rev. Lett. **61** (1988) 2526. doi:10.1103/PhysRevLett.61.2526.

[85] J. Oller, E. Oset, J. Peláez, *Nonperturbative Approach to Effective Chiral Lagrangians and Meson Interactions*, Phys. Rev. Lett. **80** (1998) 3452. arXiv:hep-ph/9803242, doi:10.1103/PhysRevLett.80.3452.

[86] J. Oller, E. Oset, *N/D Description of Two-Meson Amplitudes and Chiral Symmetry*, Phys. Rev. D **60** (1999) 074023. arXiv:hep-ph/9809337, doi:10.1103/PhysRevD.60.074023.

[87] G. Chew, S. Mandelstam, *Theory of Low-Energy Pion-Pion Interactions*, Phys. Rev. **119** (1960) 467. doi:10.1103/PhysRev.119.467.

[88] M. Shifman, A. Vainshtein, V. Zakharov, *QCD and Resonance Physics. Theoretical Foundations*, Nucl. Phys. **B147** (1979) 385. doi:10.1016/0550-3213(79)90022-1.

[89] M. Nielsen, F. Navarra, S. Lee, *New Charmonium States in QCD Sum Rules: A Concise Review*, Phys. Rept. **497** (2010) 41. arXiv:0911.1958, doi:10.1016/j.physrep.2010.07.005.

[90] K. Wilson, *Confinement of Quarks*, Phys. Rev. D **10** (1974) 2445. doi:10.1103/PhysRevD.10.2445.

[91] M. Creutz, L. Jacobs, C. Rebbi, *Monte Carlo Study of Abelian Lattice Gauge Theories*, Phys. Rev. D **20** (1979) 1915. doi:10.1103/PhysRevD.20.1915.

[92] M. Creutz, *Monte Carlo Study of Quantized $SU(2)$ Gauge Theory*, Phys. Rev. D **21** (1980) 2308. doi:10.1103/PhysRevD.21.2308.

[93] M. Born, R. Oppenheimer, *Zür Quantentheorie der Molekeln*, Ann. der Phys. **389** (1927) 457. doi:10.1002/andp.19273892002.

[94] L. Griffiths, C. Michael, P. Rakow, *Mesons with Excited Glue*, Phys. Lett. **B129** (1983) 351. doi:10.1016/0370-2693(83)90680-9.

[95] K. Juge, J. Kuti, C. Morningstar, *Ab Initio Study of Hybrid $\bar{b}gb$ Mesons*, Phys. Rev. Lett. **82** (1999) 4400. arXiv:hep-ph/9902336, doi:10.1103/PhysRevLett.82.4400.

[96] H. Ichie, V. Bornyakov, T. Streuer, G. Schierholz, *The Flux Distribution of the Three Quark System in $SU(3)$*, Nucl. Phys. Proc. Suppl. **119** (2003) 751. arXiv:hep-lat/0212024, doi:10.1016/S0920-5632(03)01654-2.

[97] T. Takahashi, H. Suganuma, Y. Nemoto, H. Matsufuru, *Detailed Analysis of the Three Quark Potential in $SU(3)$ Lattice QCD*, Phys. Rev. D **65** (2002) 114509. arXiv:hep-lat/0204011, doi:10.1103/PhysRevD.65.114509.

[98] F. Okiharu, R. Woloshyn, *A Study of Color Field Distributions in the Baryon*, Nucl. Phys. Proc. Suppl. **129** (2004) 745. arXiv:hep-lat/0310007, doi:10.1016/S0920-5632(03)02700-2.

[99] C. Alexandrou, P. De Forcrand, A. Tsapalis, *The Static Three Quark $SU(3)$ and Four Quark $SU(4)$ Potentials*, Phys. Rev. D **65** (2002) 054503. arXiv:hep-lat/0107006, doi:10.1103/PhysRevD.65.054503.

[100] A. Green, J. Lukkarinen, P. Pennanen, C. Michael, *A Study of Degenerate Four Quark States in $SU(2)$ Lattice Monte Carlo*, Phys. Rev. D **53** (1996) 261. arXiv:hep-lat/9508002, doi:10.1103/PhysRevD.53.261.

[101] P. Pennanen, A. Green, C. Michael, *Four-Quark Flux Distribution and Binding in Lattice $SU(2)$*, Phys. Rev. D **59** (1999) 014504. arXiv:hep-lat/9804004, doi:10.1103/PhysRevD.59.014504.

[102] N. Cardoso, P. Bicudo, *Color Fields of the Static Pentaquark System Computed in $SU(3)$ Lattice QCD*, Phys. Rev. D **87** (2013) 034504. arXiv:1209.1532, doi:10.1103/PhysRevD.87.034504.

[103] N. Cardoso, M. Cardoso, P. Bicudo, *Colour Fields Computed in $SU(3)$ Lattice QCD for the Static Tetraquark System*, Phys. Rev. D **84** (2011) 054508. arXiv:1107.1355, doi:10.1103/PhysRevD.84.054508.

[104] E. Braaten, C. Langmack, D. Smith, *Born-Oppenheimer Approximation for the XYZ Mesons*, Phys. Rev. D **90** (2014) 014044. arXiv:1402.0438, doi:10.1103/PhysRevD.90.014044.

[105] L. Antoniazzi, *et al.*, *Search for Hidden Charm Resonance States Decaying into J/ψ or ψ' Plus Pions*, Phys. Rev. D **50** (1994) 4258. doi:10.1103/PhysRevD.50.4258.

[106] K. Abe, *et al.*, *Observation of a Near-Threshold $\omega J/\psi$ Mass Enhancement in Exclusive $B \to K\omega J/\psi$ Decays*, Phys. Rev. Lett. **94** (2005) 182002. arXiv:hep-ex/0408126, doi:10.1103/PhysRevLett.94.182002.

[107] B. Aubert, *et al.*, *The $e^+e^- \to \pi^+\pi^-\pi^+\pi^-$, $K^+K^-\pi^+\pi^-$, and $K^+K^-K^+K^-$ Cross Sections at Center-of-Mass Energies 0.5* GeV–*4.5* GeV *Measured with Initial-State Radiation*, Phys. Rev. D **71** (2005) 052001. arXiv:hep-ex/0502025, doi:10.1103/PhysRevD.71.052001.

[108] B. Aubert, *et al.*, *Evidence of a Broad Structure at an Invariant Mass of* 4.32 GeV/c^2 *in the Reaction $e^+e^- \to \pi^+\pi^-\psi(2S)$ Measured at BaBar*, Phys. Rev. Lett. **98** (2007) 212001. arXiv:hep-ex/0610057, doi:10.1103/PhysRevLett.98.212001.

[109] R. Aaij, *et al.*, *Quantum Numbers of the $X(3872)$ State and Orbital Angular Momentum in Its $\rho^0 J/\psi$ Decay*, Phys. Rev. D **92** (2015) 011102. arXiv:1504.06339, doi:10.1103/PhysRevD.92.011102.

[110] S.-K. Choi, *et al.*, *Bounds on the Width, Mass Difference and other Properties of $X(3872) \to \pi^+\pi^- J/\psi$ Decays*, Phys. Rev. D **84** (2011) 052004. arXiv:1107.0163, doi:10.1103/PhysRevD.84.052004.

[111] R. Aaij, *et al.*, *Determination of the $X(3872)$ Meson Quantum Numbers*, Phys. Rev. Lett. **110** (2013) 222001. arXiv:1302.6269, doi:10.1103/PhysRevLett.110.222001.

[112] B. Aubert, *et al.*, *A Study of $B \to X(3872)\,K$, with $X(3872) \to J/\psi\,\pi^+\pi^-$*, Phys. Rev. D **77** (2008) 111101. arXiv:0803.2838, doi:10.1103/PhysRevD.77.111101.

[113] B. Aubert, *et al.*, *Study of the $B \to J/\psi\,K^-\pi^+\pi^-$ Decay and Measurement of the $B \to X(3872)\,K^-$ Branching Fraction*, Phys. Rev. D **71** (2005) 071103. arXiv:hep-ex/0406022, doi:10.1103/PhysRevD.71.071103.

[114] B. Aubert, *et al.*, *Study of $J/\psi\,\pi^+\pi^-$ States Produced in $B^0 \to J/\psi\,\pi^+\pi^-K^0$ and $B^- \to J/\psi\,\pi^+\pi^-K^-$*, Phys. Rev. D **73** (2006) 011101. arXiv:hep-ex/0507090, doi:10.1103/PhysRevD.73.011101.

[115] G. Gokhroo, *et al.*, *Observation of a Near-Threshold $D^0\bar{D}^0\pi^0$ Enhancement in $B \to D^0\bar{D}^0\pi^0 K$ Decay*, Phys. Rev. Lett. **97** (2006) 162002. arXiv:hep-ex/0606055, doi:10.1103/PhysRevLett.97.162002.

[116] B. Aubert, *et al.*, *Study of Resonances in Exclusive B Decays to $\bar{D}^{(*)}D^{(*)}K$*, Phys. Rev. D **77** (2008) 011102. arXiv:0708.1565, doi:10.1103/PhysRevD.77.011102.

[117] T. Aushev, *et al.*, *Study of the $B \to X(3872)\,(\to D^{*0}\bar{D}^0)K$ Decay*, Phys. Rev. D **81** (2010) 031103. arXiv:0810.0358, doi:10.1103/PhysRevD.81.031103.

[118] R. Aaij, *et al.*, *Evidence for the Decay $X(3872) \to \psi(2S)\gamma$*, Nucl. Phys. **B886** (2014) 665. arXiv:1404.0275, doi:10.1016/j.nuclphysb.2014.06.011.

[119] B. Aubert, *et al.*, *Search for $B^+ \to X(3872)\,K^+$, $X(3872) \to J/\psi\,\gamma$*, Phys. Rev. D **74** (2006) 071101. arXiv:hep-ex/0607050, doi:10.1103/PhysRevD.74.071101.

[120] B. Aubert, *et al.*, *Evidence for $X(3872) \to \psi(2S)\gamma$ in $B^\pm \to X(3872)\,K^\pm$ Decays, and a Study of $B \to c\bar{c}\gamma K$*, Phys. Rev. Lett. **102** (2009) 132001. arXiv:0809.0042, doi:10.1103/PhysRevLett.102.132001.

[121] V. Bhardwaj, *et al.*, *Observation of $X(3872) \to J/\psi\,\gamma$ and Search for $X(3872) \to \psi'\gamma$ in B Decays*, Phys. Rev. Lett. **107** (2011) 091803. arXiv:1105.0177, doi:10.1103/PhysRevLett.107.091803.

[122] P. del Amo Sanchez, *et al.*, *Evidence for the Decay $X(3872) \to J/\psi\,\omega$*, Phys. Rev. D **82** (2010) 011101. arXiv:1005.5190, doi:10.1103/PhysRevD.82.011101.

[123] B. Aubert, *et al.*, *Observation of $Y(3940) \to J/\psi\,\omega$ in $B \to J/\psi\,\omega K$ at BaBar*, Phys. Rev. Lett. **101** (2008) 082001. arXiv:0711.2047, doi:10.1103/PhysRevLett.101.082001.

[124] V. Bhardwaj, *et al.*, *Evidence of a New Narrow Resonance Decaying to $\chi_{c1}\gamma$ in $B \to \chi_{c1}\gamma K$*, Phys. Rev. Lett. **111** (2013) 032001. arXiv:1304.3975, doi:10.1103/PhysRevLett.111.032001.

[125] R. Aaij, *et al.*, *Observation of $J/\psi\,\phi$ Structures Consistent with Exotic States from Amplitude Analysis of $B^+ \to J/\psi\,\phi K^+$ Decays*, arXiv:1606.07895.

[126] T. Aaltonen, *et al.*, *Evidence for a Narrow Near-Threshold Structure in the $J/\psi\,\phi$ Mass Spectrum in $B^+ \to J/\psi\,\phi K^+$ Decays*, Phys. Rev. Lett. **102** (2009) 242002. arXiv:0903.2229, doi:10.1103/PhysRevLett.102.242002.

[127] R. Aaij, *et al.*, *Search for the $X(4140)$ State in $B^+ \to J/\psi\,\phi K^+$ Decays*, Phys. Rev. D **85** (2012) 091103. arXiv:1202.5087, doi:10.1103/PhysRevD.85.091103.

[128] J. Lees, *et al.*, *Study of $B^{\pm,0} \to J/\psi\,K^+K^-K^{\pm,0}$ and Search for $B^0 \to J/\psi\,\phi$ at BaBar*, Phys. Rev. D **91** (2015) 012003. arXiv:1407.7244, doi:10.1103/PhysRevD.91.012003.

[129] V. Abazov, *et al.*, *Search for the $X(4140)$ State in $B^+ \to J/\psi\,\phi K^+$ Decays with the D0 Detector*, Phys. Rev. D **89** (2014) 012004. arXiv:1309.6580, doi:10.1103/PhysRevD.89.012004.

[130] S. Chatrchyan, *et al.*, *Observation of a Peaking Structure in the $J/\psi\,\phi$ Mass Spectrum from $B^\pm \to J/\psi\,\phi K^\pm$ Decays*, Phys. Lett. **B734** (2014) 261. arXiv:1309.6920, doi:10.1016/j.physletb.2014.05.055.

[131] R. Aaij, *et al.*, *Amplitude Analysis of $B^+ \to J/\psi\,\phi K^+$ Decays*, arXiv:1606.07898.

[132] T. Aaltonen, *et al.*, *Observation of the $Y(4140)$ Structure in the $J/\psi\,\phi$ Mass Spectrum in $B^\pm \to J/\psi\,\phi K$ Decays*, arXiv:1101.6058.

[133] R. Mizuk, *et al.*, *Observation of Two Resonance-like Structures in the $\pi^+\chi_{c1}$ Mass Distribution in Exclusive $\bar{B}^0 \to K^-\pi^+\chi_{c1}$ Decays*, Phys. Rev. D **78** (2008) 072004. arXiv:0806.4098, doi:10.1103/PhysRevD.78.072004.

[134] J. Lees, *et al.*, *Search for the $Z_1(4050)^+$ and $Z_2(4250)^+$ States in $\bar{B}^0 \to \chi_{c1}K^-\pi^+$ and $B^+ \to \chi_{c1}K^0_S\pi^+$*, Phys. Rev. D **85** (2012) 052003. arXiv:1111.5919, doi:10.1103/PhysRevD.85.052003.

[135] B. Aubert, *et al.*, *Search for the $Z(4430)^-$ at BaBar*, Phys. Rev. D **79** (2009) 112001. arXiv:0811.0564, doi:10.1103/PhysRevD.79.112001.

[136] R. Mizuk, *et al.*, *Dalitz Analysis of $B \to K\pi^+\psi'$ Decays and the $Z(4430)^+$*, Phys. Rev. D **80** (2009) 031104. arXiv:0905.2869, doi:10.1103/PhysRevD.80.031104.

[137] K. Chilikin, *et al.*, *Experimental Constraints on the Spin and Parity of the $Z(4430)^+$*, Phys. Rev. D **88** (2013) 074026. arXiv:1306.4894, doi:10.1103/PhysRevD.88.074026.

[138] R. Aaij, *et al.*, *Observation of the Resonant Character of the $Z(4430)^-$ State*, Phys. Rev. Lett. **112** (2014) 222002. arXiv:1404.1903, doi:10.1103/PhysRevLett.112.222002.

[139] R. Aaij, *et al.*, *Model-Independent Confirmation of the $Z(4430)^-$ State*, Phys. Rev. D **92** (2015) 112009. arXiv:1510.01951, doi:10.1103/PhysRevD.92.112009.

[140] A. Bala, *et al.*, *Observation of $X(3872)$ in $B \to X(3872)\,K\pi$ Decays*, Phys. Rev. D **91** (2015) 051101. arXiv:1501.06867, doi:10.1103/PhysRevD.91.051101.

[141] Q. He, *et al.*, *Confirmation of the $Y(4260)$ Resonance Production in ISR*, Phys. Rev. D **74** (2006) 091104. arXiv:hep-ex/0611021, doi:10.1103/PhysRevD.74.091104.

[142] T. Coan, *et al.*, *Charmonium Decays of $Y(4260)$, $\psi(4160)$ and $\psi(4040)$*, Phys. Rev. Lett. **96** (2006) 162003. arXiv:hep-ex/0602034, doi:10.1103/PhysRevLett.96.162003.

[143] C.-Z. Yuan, *et al.*, *Measurement of $e^+e^- \to \pi^+\pi^- J/\psi$ Cross-Section via Initial State Radiation at Belle*, Phys. Rev. Lett. **99** (2007) 182004. arXiv:0707.2541, doi:10.1103/PhysRevLett.99.182004.

[144] J. Lees, *et al.*, *Study of the Reaction $e^+e^- \to J/\psi\,\pi^+\pi^-$ via Initial-State Radiation at BaBar*, Phys. Rev. D **86** (2012) 051102. arXiv:1204.2158, doi:10.1103/PhysRevD.86.051102.

[145] M. Ablikim, *et al.*, *Precise Measurement of the $e^+e^- \to \pi^+\pi^- J/\psi$ Cross Section at Center-of-Mass Energies from 3.77 to 4.60* GeV, arXiv:1611.01317.

[146] X. Wang, *et al.*, *Observation of Two Resonant Structures in $e^+e^- \to \pi^+\pi^-\psi(2S)$ via Initial State Radiation at Belle*, Phys. Rev. Lett. **99** (2007) 142002. arXiv:0707.3699, doi:10.1103/PhysRevLett.99.142002.

[147] J. Lees, *et al.*, *Study of the Reaction $e^+e^- \to \psi(2S)\pi^-\pi^-$ via Initial-State Radiation at BaBar*, Phys. Rev. D **89** (2014) 111103. arXiv:1211.6271, doi:10.1103/PhysRevD.89.111103.

[148] X. Wang, *et al.*, *Measurement of $e^+e^- \to \pi^+\pi^-\psi(2S)$ via Initial State Radiation at Belle*, Phys. Rev. D **91** (2015) 112007. arXiv:1410.7641, doi:10.1103/PhysRevD.91.112007.

[149] M. Ablikim, *et al.*, *Study of $e^+e^- \to \omega\chi_{cJ}$ at Center-of-Mass Energies from* 4.21 *to* 4.42 GeV, Phys. Rev. Lett. **114** (2015) 092003. arXiv:1410.6538, doi:10.1103/PhysRevLett.114.092003.

[150] G. Pakhlova, *et al.*, *Observation of a Near-Threshold Enhancement in the $e^+e^- \to \Lambda_c^+\Lambda_c^-$ Cross Section Using Initial-State Radiation*, Phys. Rev. Lett. **101** (2008) 172001. arXiv:0807.4458, doi:10.1103/PhysRevLett.101.172001.

[151] K.-F. Chen, *et al.*, *Observation of an Enhancement in $e^+e^- \to \Upsilon(1S)\pi^+\pi^-$, $\Upsilon(2S)\pi^+\pi^-$, and $\Upsilon(3S)\pi^+\pi^-$ Production around $\sqrt{s} =$* 10.89 GeV *at Belle*, Phys. Rev. D **82** (2010) 091106. arXiv:0810.3829, doi:10.1103/PhysRevD.82.091106.

[152] D. Santel, *et al.*, *Measurements of the $\Upsilon(10860)$ and $\Upsilon(11020)$ resonances via $\sigma(e^+e^- \to \Upsilon(nS)\pi^+\pi^-)$*, Phys. Rev. D **93** (2016) 011101. arXiv:1501.01137, doi:10.1103/PhysRevD.93.011101.

[153] A. Abdesselam, *et al.*, *Energy Scan of the $e^+e^- \to h_b(nP)\pi^+\pi^-$ ($n = 1, 2$) Cross Sections and Evidence for $\Upsilon(11020)$ Decays into Charged Bottomonium-like States*, Phys. Rev. Lett. **117** (2016) 142001. arXiv:1508.06562, doi:10.1103/PhysRevLett.117.142001.

[154] M. Ablikim, *et al.*, *Observation of a Charged $(D\bar{D}^*)^\pm$ Mass Peak in $e^+e^- \to \pi D\bar{D}^*$ at $\sqrt{s} =$* 4.26 GeV, Phys. Rev. Lett. **112** (2014) 022001. arXiv:1310.1163, doi:10.1103/PhysRevLett.112.022001.

[155] M. Ablikim, *et al.*, *Confirmation of a Charged Charmoniumlike State $Z_c(3885)^\mp$ in $e^+e^- \to \pi^\pm(D\bar{D}^*)^\mp$ with Double D Tag*, Phys. Rev. D **92** (2015) 092006. arXiv:1509.01398, doi:10.1103/PhysRevD.92.092006.

[156] M. Ablikim, *et al.*, *Observation of a Charged Charmoniumlike Structure $Z_c(4020)$ and Search for the $Z_c(3900)$ in $e^+e^- \to \pi^+\pi^- h_c$*, Phys. Rev. Lett. **111** (2013) 242001. arXiv:1309.1896, doi:10.1103/PhysRevLett.111.242001.

[157] M. Ablikim, *et al.*, *Observation of $e^+e^- \to \pi^0\pi^0 h_c$ and a Neutral Charmoniumlike Structure $Z_c(4020)^0$*, Phys. Rev. Lett. **113** (2014) 212002. arXiv:1409.6577, doi:10.1103/PhysRevLett.113.212002.

[158] M. Ablikim, *et al.*, *Observation of a Charged Charmoniumlike Structure in* $e^+e^- \to (D^*\bar{D}^*)^\pm\pi^\mp$ *at* $\sqrt{s} = 4.26$ GeV, Phys. Rev. Lett. **112** (2014) 132001. arXiv:1308.2760, doi:10.1103/PhysRevLett.112.132001.

[159] M. Ablikim, *et al.*, *Observation of a Neutral Charmoniumlike State* $Z_c(4025)^0$ *in* $e^+e^- \to (D^*\bar{D}^*)^0\pi^0$, Phys. Rev. Lett. **115** (2015) 182002. arXiv:1507.02404, doi:10.1103/PhysRevLett.115.182002.

[160] A. Bondar, *et al.*, *Observation of Two Charged Bottomonium-like Resonances in* $\Upsilon(5S)$ *Decays*, Phys. Rev. Lett. **108** (2012) 122001. arXiv:1110.2251, doi:10.1103/PhysRevLett.108.122001.

[161] P. Krokovny, *et al.*, *First Observation of the* $Z_b^0(10610)$ *in a Dalitz Analysis of* $\Upsilon(10860) \to \Upsilon(nS)\pi^0\pi^0$, Phys. Rev. D **88** (2013) 052016. arXiv:1308.2646, doi:10.1103/PhysRevD.88.052016.

[162] A. Garmash, *et al.*, *Amplitude Analysis of* $e^+e^- \to \Upsilon(nS)\pi^+\pi^-$ *at* $\sqrt{s} = 10.865$ GeV, Phys. Rev. D **91** (2015) 072003. arXiv:1403.0992, doi:10.1103/PhysRevD.91.072003.

[163] A. Garmash, *et al.*, *Observation of* $Z_b(10610)$ *and* $Z_b(10650)$ *Decaying to B Mesons*, Phys. Rev. Lett. **116** (2016) 212001. arXiv:1512.07419, doi:10.1103/PhysRevLett.116.212001.

[164] M. Ablikim, *et al.*, *Observation of the* $\psi(1^3D_2)$ *State in* $e^+e^- \to \pi^+\pi^-\gamma\chi_{c1}$ *at BESIII*, Phys. Rev. Lett. **115** (2015) 011803. arXiv:1503.08203, doi:10.1103/PhysRevLett.115.011803.

[165] K. Abe, *et al.*, *Observation of a New Charmonium State in Double Charmonium Production in* e^+e^- *Annihilation at* $\sqrt{s} \approx 10.6$ GeV, Phys. Rev. Lett. **98** (2007) 082001. arXiv:hep-ex/0507019, doi:10.1103/PhysRevLett.98.082001.

[166] S. Uehara, *et al.*, *Observation of a Charmonium-like Enhancement in the* $\gamma\gamma \to \omega J/\psi$ *Process*, Phys. Rev. Lett. **104** (2010) 092001. arXiv:0912.4451, doi:10.1103/PhysRevLett.104.092001.

[167] J. Lees, *et al.*, *Study of* $X(3915) \to J/\psi\,\omega$ *in Two-Photon Collisions*, Phys. Rev. D **86** (2012) 072002. arXiv:1207.2651, doi:10.1103/PhysRevD.86.072002.

[168] S. Uehara, *et al.*, *Observation of a* χ'_{c2} *Candidate in* $\gamma\gamma \to D\bar{D}$ *Production at Belle*, Phys. Rev. Lett. **96** (2006) 082003. arXiv:hep-ex/0512035, doi:10.1103/PhysRevLett.96.082003.

[169] B. Aubert, *et al.*, *Observation of the* $\chi_{c2}(2P)$ *Meson in the Reaction* $\gamma\gamma \to D\bar{D}$ *at BaBar*, Phys. Rev. D **81** (2010) 092003. arXiv:1002.0281, doi:10.1103/PhysRevD.81.092003.

[170] C. Shen, *et al.*, *Evidence for a New Resonance and Search for the* $Y(4140)$ *in the* $\gamma\gamma \to \phi J/\psi$ *Process*, Phys. Rev. Lett. **104** (2010) 112004. arXiv:0912.2383, doi:10.1103/PhysRevLett.104.112004.

[171] V. M. Abazov, *et al.*, *Observation and Properties of the* $X(3872)$ *Decaying to* $J/\psi\pi^+\pi^-$ *in* $p\bar{p}$ *collisions at* $\sqrt{s} = 1.96$ TeV, Phys. Rev. Lett. **93** (2004) 162002. arXiv:hep-ex/0405004, doi:10.1103/PhysRevLett.93.162002.

[172] T. Aaltonen, *et al.*, *Precision Measurement of the* $X(3872)$ *Mass in* $J/\psi\,\pi^+\pi^-$ *Decays*, Phys. Rev. Lett. **103** (2009) 152001. arXiv:0906.5218, doi:10.1103/PhysRevLett.103.152001.

[173] R. Aaij, *et al.*, *Observation of* $X(3872)$ *Production in pp Collisions at* $\sqrt{s} = 7$ TeV, Eur. Phys. J. **C72** (2012) 1972. arXiv:1112.5310, doi:10.1140/epjc/s10052-012-1972-7.

[174] V. Abazov, *et al.*, *Inclusive Production of the* $X(4140)$ *State in* $p\bar{p}$ *Collisions at D0*, Phys. Rev. Lett. **115** (2015) 232001. arXiv:1508.07846, doi:10.1103/PhysRevLett.115.232001.

[175] V. Abazov, *et al.*, *Evidence for a* $B_s^0\pi^\pm$ *state*, Phys. Rev. Lett. 117 (2016) 022003. arXiv:1602.07588, doi:10.1103/PhysRevLett.117.022003.

[176] K. Olive, *Review of Particle Physics*, Chin. Phys. **C40** (2016) 100001. doi:10.1088/1674-1137/40/10/100001.

[177] T. Pedlar, *et al.*, *Observation of the* $h_c(1P)$ *Using* e^+e^- *Collisions above* $D\bar{D}$ *Threshold*, Phys. Rev. Lett. **107** (2011) 041803. arXiv:1104.2025, doi:10.1103/PhysRevLett.107.041803.

[178] A. Abulencia, *et al.*, *Measurement of the Dipion Mass Spectrum in* $X(3872) \to J/\psi\pi^+\pi^-$ *Decays.*, Phys. Rev. Lett. **96** (2006) 102002. arXiv:hep-ex/0512074, doi:10.1103/PhysRevLett.96.102002.

[179] A. Abulencia, *et al.*, *Analysis of the Quantum Numbers* J^{PC} *of the* $X(3872)$, Phys. Rev. Lett. **98** (2007) 132002. arXiv:hep-ex/0612053, doi:10.1103/PhysRevLett.98.132002.

[180] G. Aad, *et al.*, *Observation of a New* χ_b *State in Radiative Transitions to* $\Upsilon(1S)$ *and* $\Upsilon(2S)$ *at ATLAS*, Phys. Rev. Lett. **108** (2012) 152001. arXiv:1112.5154, doi:10.1103/PhysRevLett.108.152001.

[181] C. Adolph, *et al.*, *Search for Exclusive Photoproduction of* $Z_c^\pm$ *(3900) at COMPASS*, Phys. Lett. **B742** (2015) 330. arXiv:1407.6186, doi:10.1016/j.physletb.2015.01.042.

[182] C. Adolph, *et al.*, *Observation of a New Narrow Axial-Vector Meson* $a_1(1420)$, Phys. Rev. Lett. **115** (2015) 082001. arXiv:1501.05732, doi:10.1103/PhysRevLett.115.082001.

[183] P. del Amo Sanchez, *et al.*, *Observation of* $\eta_c(1S)$ *and* $\eta_c(2S)$ *Decays to* $K^+K^-\pi^+\pi^-\pi^0$ *in Two-Photon Interactions*, Phys. Rev. D **84** (2011) 012004. arXiv:1103.3971, doi:10.1103/PhysRevD.84.012004.

[184] J. Lees, *et al.*, *Dalitz Plot Analysis of* $\eta_c \to K^+K^-\eta$ *and* $\eta_c \to K^+K^-\pi^0$ *in Two-Photon Interactions*, Phys. Rev. D **89** (2014) 112004. arXiv:1403.7051, doi:10.1103/PhysRevD.89.112004.

[185] B. Aubert, *et al.*, *Measurements of the Absolute Branching Fractions of* $B^\pm \to K^\pm X(c\bar{c})$, Phys. Rev. Lett. **96** (2006) 052002. arXiv:hep-ex/0510070, doi:10.1103/PhysRevLett.96.052002.

[186] K. Chen, *et al.*, *Observation of Anomalous* $\Upsilon(1S)\pi^+\pi^-$ *and* $\Upsilon(2S)\pi^+\pi^-$ *Production Near the* $\Upsilon(5S)$ *Resonance*, Phys. Rev. Lett. **100** (2008) 112001. arXiv:0710.2577, doi:10.1103/PhysRevLett.100.112001.

[187] I. Adachi, *et al.*, *First Observation of the P-Wave Spin-Singlet Bottomonium States* $h_b(1P)$ *and* $h_b(2P)$, Phys. Rev. Lett. **108** (2012) 032001. arXiv:1103.3419, doi:10.1103/PhysRevLett.108.032001.

[188] B. Aubert, *et al.*, *Measurement of the* $e^+e^- \to b\bar{b}$ *Cross Section between* $\sqrt{s} = 10.54$ GeV *and 11.20* GeV, Phys. Rev. Lett. **102** (2009) 012001. arXiv:0809.4120, doi:10.1103/PhysRevLett.102.012001.

[189] M. Ablikim, *et al.*, *Determination of the* $\psi(3770)$*,* $\psi(4040)$*,* $\psi(4160)$ *and* $\psi(4415)$ *Resonance Parameters*, eConf C070805 (2007) 02, [Phys. Lett. **B660**, 315 (2008)]. arXiv:0705.4500, doi:10.1016/j.physletb.2007.11.100.

[190] X. H. Mo, G. Li, C. Yuan, K. He, H. Hu, J. Hu, P. Wang, Z. Wang, *Determining the Upper Limit of* Γ*(ee) for the* $Y(4260)$, Phys. Lett. **B640** (2006) 182. arXiv:hep-ex/0603024, doi:10.1016/j.physletb.2006.07.060.

[191] C. Yuan, *et al.*, *Observation of* $e^+e^- \to K^+K^-J/\psi$ *via Initial State Radiation at Belle*, Phys. Rev. D **77** (2008) 011105. arXiv:0709.2565, doi:10.1103/PhysRevD.77.011105.

[192] C. Shen, *et al.*, *Updated Cross Section Measurement of* $e^+e^- \to K^+K^-J/\psi$ *and* $K_S^0K_S^0J/\psi$ *via Initial State Radiation at Belle*, Phys. Rev. D **89** (2014) 072015. arXiv:1402.6578, doi:10.1103/PhysRevD.89.072015.

[193] C.-Z. Yuan, *Evidence for Resonant Structures in* $e^+e^- \to \pi^+\pi^-h_c$, Chin. Phys. **C38** (2014) 043001. arXiv:1312.6399, doi:10.1088/1674-1137/38/4/043001.

[194] M. Ablikim, *et al.*, *Observation of* $e^+e^- \to \eta J/\psi$ *at Center-of-Mass Energy* $\sqrt{s} = 4.009$ GeV, Phys. Rev. D **86** (2012) 071101. arXiv:1208.1857, doi:10.1103/PhysRevD.86.071101.

[195] X. Wang, Y. Han, C. Yuan, C. Shen, P. Wang, *Observation of* $\psi(4040)$ *and* $\psi(4160)$ *Decay into* $\eta J/\psi$, Phys. Rev. D **87** (2013) 051101.

arXiv:1210.7550, doi:10.1103/PhysRevD.87.051101.
[196] M. Ablikim, *et al.*, *Measurement of the $e^+e^- \to \eta J/\psi$ Cross Section and Search for $e^+e^- \to \pi^0 J/\psi$ at Center-of-Mass Energies between* 3.810 *and* 4.600 GeV, Phys. Rev. D **91** (2015) 112005. arXiv:1503.06644, doi:10.1103/PhysRevD.91.112005.
[197] M. Ablikim, *et al.*, *Observation of $e^+e^- \to \omega\chi_{c1,2}$ Near $\sqrt{s} = 4.42$ and* 4.6 GeV, Phys. Rev. D **93** (2016) 011102. arXiv:1511.08564, doi:10.1103/PhysRevD.93.011102.
[198] D. Cronin-Hennessy, *et al.*, *Measurement of Charm Production Cross Sections in e^+e^- Annihilation at Energies between* 3.97 *and* 4.26 GeV, Phys. Rev. D **80** (2009) 072001. arXiv:0801.3418, doi:10.1103/PhysRevD.80.072001.
[199] B. Aubert, *et al.*, *Study of the Exclusive Initial-State Radiation Production of the $D\bar{D}$ System*, Phys. Rev. D **76** (2007) 111105. arXiv:hep-ex/0607083, doi:10.1103/PhysRevD.76.111105.
[200] B. Aubert, *et al.*, *Exclusive Initial-State-Radiation Production of the $D\bar{D}$, $D^*\bar{D}^*$, and $D^*\bar{D}^*$ Systems*, Phys. Rev. D **79** (2009) 092001. arXiv:0903.1597, doi:10.1103/PhysRevD.79.092001.
[201] P. del Amo Sanchez, *et al.*, *Exclusive Production of $D_s^+D_s^-$, $D_s^{*+}D_s^-$, and $D_s^{*+}D_s^{*-}$ via e^+e^- Annihilation with Initial-State-Radiation*, Phys. Rev. D **82** (2010) 052004. arXiv:1008.0338, doi:10.1103/PhysRevD.82.052004.
[202] K. Abe, *et al.*, *Measurement of the Near-Threshold $e^+e^- \to D^{(*)\pm}D^{(*)\mp}$ Cross Section Using Initial-State Radiation*, Phys. Rev. Lett. **98** (2007) 092001. arXiv:hep-ex/0608018, doi:10.1103/PhysRevLett.98.092001.
[203] G. Pakhlova, *et al.*, *Measurement of the Near-Threshold $e^+e^- \to D\bar{D}$ Cross Section Using Initial-State Radiation*, Phys. Rev. D **77** (2008) 011103. arXiv:0708.0082, doi:10.1103/PhysRevD.77.011103.
[204] G. Pakhlova, *et al.*, *Observation of $\psi(4415) \to D\bar{D}_2^*(2460)$ Decay Using Initial-State Radiation*, Phys. Rev. Lett. **100** (2008) 062001. arXiv:0708.3313, doi:10.1103/PhysRevLett.100.062001.
[205] G. Pakhlova, *et al.*, *Measurement of the $e^+e^- \to D^0D^{*-}\pi^+$ Cross Section Using Initial-State Radiation*, Phys. Rev. D **80** (2009) 091101. arXiv:0908.0231, doi:10.1103/PhysRevD.80.091101.
[206] G. Pakhlova, *et al.*, *Measurement of $e^+e^- \to D_s^{(*)+}D_s^{(*)-}$ Cross Sections Near Threshold Using Initial-State Radiation*, Phys. Rev. D **83** (2011) 011101. arXiv:1011.4397, doi:10.1103/PhysRevD.83.011101.
[207] S. Olsen, *Is the $X(3915)$ the $\chi_{c0}(2P)$?*, Phys. Rev. D **91** (2015) 057501. arXiv:1410.6534, doi:10.1103/PhysRevD.91.057501.
[208] J. Brodzicka, *et al.*, *Observation of a New D_{sJ} Meson in $B^+ \to \bar{D}^0D^0K^+$ decays*, Phys. Rev. Lett. **100** (2008) 092001. arXiv:0707.3491, doi:10.1103/PhysRevLett.100.092001.
[209] R. Aaij, *et al.*, *Search for Structure in the $B_s^0\pi^\pm$ Invariant Mass Spectrum*, Phys. Rev. Lett. **117** (2016) 152003. arXiv:1608.00435, doi:10.1103/PhysRevLett.117.152003.
[210] N. Törnqvist, *Isospin Breaking of the Narrow Charmonium State of Belle at* 3872 MeV *as a Deuson*, Phys. Lett. **B590** (2004) 209. arXiv:hep-ph/0402237, doi:10.1016/j.physletb.2004.03.077.
[211] J. Sakurai, J. Napolitano, *Modern Quantum Physics*, Addison-Wesley, Boston, USA, 2011.
[212] E. Braaten, M. Kusunoki, *Low-Energy Universality and the New Charmonium Resonance at* 3870 MeV, Phys. Rev. D **69** (2004) 074005. arXiv:hep-ph/0311147, doi:10.1103/PhysRevD.69.074005.
[213] S. Weinberg, *Evidence That the Deuteron Is Not an Elementary Particle*, Phys. Rev. **137** (1965) B672. doi:10.1103/PhysRev.137.B672.
[214] K. Krane, *Introductory Nuclear Physics*, Wiley, New York, USA, 1987.
[215] E. Swanson, *Short Range Structure in the $X(3872)$*, Phys. Lett. **B588** (2004) 189. arXiv:hep-ph/0311229, doi:10.1016/j.physletb.2004.03.033.
[216] M. Karliner, J. Rosner, *New Exotic Meson and Baryon Resonances from Doubly-Heavy Hadronic Molecules*, Phys. Rev. Lett. **115** (2015) 122001. arXiv:1506.06386, doi:10.1103/PhysRevLett.115.122001.
[217] L. Zhao, L. Ma, S.-L. Zhu, *Spin-Orbit Force, Recoil Corrections, and Possible $B\bar{B}^*$ and $D\bar{D}^*$ Molecular States*, Phys. Rev. D **89** (2014) 094026. arXiv:1403.4043, doi:10.1103/PhysRevD.89.094026.
[218] C.-Y. Wong, *Molecular States of Heavy-Quark Mesons*, Phys. Rev. C **69** (2004) 055202. arXiv:hep-ph/0311088, doi:10.1103/PhysRevC.69.055202.
[219] M. AlFiky, F. Gabbiani, A. Petrov, *$X(3872)$: Hadronic Molecules in Effective Field Theory*, Phys. Lett. **B640** (2006) 238. arXiv:hep-ph/0506141, doi:10.1016/j.physletb.2006.07.069.
[220] S. Fleming, M. Kusunoki, T. Mehen, U. van Kolck, *Pion Interactions in the $X(3872)$*, Phys. Rev. D **76** (2007) 034006. arXiv:hep-ph/0703168, doi:10.1103/PhysRevD.76.034006.
[221] P. Wang, X. Wang, *Study on $X(3872)$ from Effective Field Theory with Pion Exchange Interaction*, Phys. Rev. Lett. **111** (2013) 042002. arXiv:1304.0846, doi:10.1103/PhysRevLett.111.042002.
[222] Y.-R. Liu, X. Liu, W.-Z. Deng, S.-L. Zhu, *Is $X(3872)$ Really a Molecular State?*, Eur. Phys. J. **C56** (2008) 63. arXiv:0801.3540, doi:10.1140/epjc/s10052-008-0640-4.
[223] X. Liu, Z.-G. Luo, Y.-R. Liu, S.-L. Zhu, *$X(3872)$ and Other Possible Heavy Molecular States*, Eur. Phys. J. **C61** (2009) 411. arXiv:0808.0073, doi:10.1140/epjc/s10052-009-1020-4.
[224] C. Thomas, F. Close, *Is $X(3872)$ a Molecule?*, Phys. Rev. D **78** (2008) 034007. arXiv:0805.3653, doi:10.1103/PhysRevD.78.034007.
[225] I. Lee, A. Faessler, T. Gutsche, V. Lyubovitskij, *$X(3872)$ as a Molecular DD^* State in a Potential Model*, Phys. Rev. D **80** (2009) 094005. arXiv:0910.1009, doi:10.1103/PhysRevD.80.094005.
[226] N. Li, S.-L. Zhu, *Isospin Breaking, Coupled-Channel Effects and Diagnosis of $X(3872)$*, Phys. Rev. D **86** (2012) 074022. arXiv:1207.3954, doi:10.1103/PhysRevD.86.074022.
[227] L. Zhao, L. Ma, S.-L. Zhu, *The Recoil Correction and Spin-Orbit Force for the Possible $B^*\bar{B}^*$ and $D^*\bar{D}^*$ States*, Nucl. Phys. **A942** (2015) 18. arXiv:1504.04117, doi:10.1016/j.nuclphysa.2015.06.010.
[228] R. D. Matheus, F. Navarra, M. Nielsen, C. Zanetti, *QCD Sum Rules for the $X(3872)$ as a Mixed Molecule-Charmonium State*, Phys. Rev. D **80** (2009) 056002. arXiv:0907.2683, doi:10.1103/PhysRevD.80.056002.
[229] M. Nielsen, C. Zanetti, *Radiative Decay of the $X(3872)$ as a Mixed Molecule-Charmonium State in QCD Sum Rules*, Phys. Rev. D **82** (2010) 116002. arXiv:1006.0467, doi:10.1103/PhysRevD.82.116002.
[230] M. Suzuki, *The $X(3872)$ Boson: Molecule or Charmonium*, Phys. Rev. D **72** (2005) 114013. arXiv:hep-ph/0508258, doi:10.1103/PhysRevD.72.114013.
[231] A. Guerrieri, F. Piccinini, A. Pilloni, A. Polosa, *Production of Tetraquarks at the LHC*, Phys. Rev. D **90** (2014) 034003. arXiv:1405.7929, doi:10.1103/PhysRevD.90.034003.
[232] P. Artoisenet, E. Braaten, *Production of the $X(3872)$ at the Tevatron and the LHC*, Phys. Rev. D **81** (2010) 114018. arXiv:0911.2016, doi:10.1103/PhysRevD.81.114018.
[233] A. Esposito, F. Piccinini, A. Pilloni, A. Polosa, *A Mechanism for Hadron Molecule Production in $pp(\bar{p})$ Collisions*, J. Mod. Phys. **4** (2013) 1569. arXiv:1305.0527, doi:10.4236/jmp.2013.412193.
[234] S. Brodsky, I. Schmidt, G. de Téramond, *Nuclear-Bound Quarkonium*, Phys. Rev. Lett. **64** (1990) 1011. doi:10.1103/PhysRevLett.64.1011.

[235] F.-K. Guo, C. Hanhart, U.-G. Meißner, *Evidence That the $Y(4660)$ Is a $f_0(980)\psi'$ Bound State*, Phys. Lett. **B665** (2008) 26. arXiv:0803.1392, doi:10.1016/j.physletb.2008.05.057.

[236] M. Voloshin, $Z_c(3900)$—*What Is Inside?*, Phys. Rev. D **87** (2013) 091501. arXiv:1304.0380, doi:10.1103/PhysRevD.87.091501.

[237] F.-K. Guo, C. Hanhart, U.-G. Meißner, *Implications of Heavy-Quark Spin Symmetry on Heavy-Meson Hadronic Molecules*, Phys. Rev. Lett. **102** (2009) 242004. arXiv:0904.3338, doi:10.1103/PhysRevLett.102.242004.

[238] Y. Dong, A. Faessler, T. Gutsche, V. Lyubovitskij, *Radiative Decay $Y(4260) \to X(3872) + \gamma$ Involving Hadronic Molecular and Charmonium Components*, Phys. Rev. D **90** (2014) 074032. arXiv:1404.6161, doi:10.1103/PhysRevD.90.074032.

[239] L. Maiani, F. Piccinini, A. Polosa, V. Riquer, *A New Look at Scalar Mesons*, Phys. Rev. Lett. **93** (2004) 212002. arXiv:hep-ph/0407017, doi:10.1103/PhysRevLett.93.212002.

[240] R. Jaffe, *Exotica*, Phys. Rept. **409** (2005) 1. arXiv:hep-ph/0409065, doi:10.1016/j.physrep.2004.11.005.

[241] H.-X. Chen, L. Maiani, A. Polosa, V. Riquer, $Y(4260) \to \gamma + X(3872)$ in the Diquarkonium Picture, Eur. Phys. J. **C75** (2015) 550. arXiv:1510.03626, doi:10.1140/epjc/s10052-015-3781-2.

[242] A. Ali, C. Hambrock, W. Wang, *Tetraquark Interpretation of the Charged Bottomonium-like States $Z_b^{\pm}(10610)$ and $Z_b^{\pm}(10650)$ and Implications*, Phys. Rev. D **85** (2012) 054011. arXiv:1110.1333, doi:10.1103/PhysRevD.85.054011.

[243] R. Lebed, A. Polosa, $\chi_{c0}(3915)$ *As the Lightest $c\bar{c}s\bar{s}$ State*, Phys. Rev. D **93** (2016) 094024. arXiv:1602.08421, doi:10.1103/PhysRevD.93.094024.

[244] D. Ebert, R. Faustov, V. Galkin, *Excited Heavy Tetraquarks with Hidden Charm*, Eur. Phys. J. **C58** (2008) 399. arXiv:0808.3912, doi:10.1140/epjc/s10052-008-0754-8.

[245] S. Patel, M. Shah, P. Vinodkumar, *Mass Spectra of Four-Quark States in the Hidden Charm Sector*, Eur. Phys. J. **A50** (2014) 131. arXiv:1402.3974, doi:10.1140/epja/i2014-14131-9.

[246] C. Deng, J. Ping, H. Huang, F. Wang, *Systematic Study of Z_c^+ Family from a Multiquark Color Flux-Tube Model*, Phys. Rev. D **92** (2015) 034027. arXiv:1507.06408, doi:10.1103/PhysRevD.92.034027.

[247] F. Goerke, T. Gutsche, M. Ivanov, J. Körner, V. Lyubovitskij, P. Santorelli, *Four-Quark Structure of $Z_c(3900)$, $Z(4430)$ and $X_b(5568)$ States*, Phys. Rev. D94 (2016) 094017. arXiv:1608.04656, doi:10.1103/PhysRevD.94.094017.

[248] V. Anisovich, M. Matveev, J. Nyiri, A. Sarantsev, A. Semenova, *Nonstrange and Strange Pentaquarks with Hidden Charm*, Int. J. Mod. Phys. **A30** (2015) 1550190. arXiv:1509.04898, doi:10.1142/S0217751X15501900.

[249] G.-N. Li, X.-G. He, M. He, *Some Predictions of Diquark Model for Hidden Charm Pentaquark Discovered at the LHCb*, JHEP **12** (2015) 128. arXiv:1507.08252, doi:10.1007/JHEP12(2015)128.

[250] R. Ghosh, A. Bhattacharya, B. Chakrabarti, *The Masses of $P_c^*(4380)$ and $P_c^*(4450)$ in the Quasi Particle Diquark Model*, arXiv:1508.00356.

[251] R. Zhu, C.-F. Qiao, *Pentaquark States in a Diquark-Triquark Model*, Phys. Lett. **B756** (2016) 259. arXiv:1510.08693, doi:10.1016/j.physletb.2016.03.022.

[252] R. Lebed, *Diquark Substructure in ϕ Photoproduction*, Phys. Rev. D **92** (2015) 114006. arXiv:1510.01412, doi:10.1103/PhysRevD.92.114006.

[253] R. Lebed, *Do the P_c^+ Pentaquarks Have Strange Siblings?*, Phys. Rev. D **92** (2015) 114030. arXiv:1510.06648, doi:10.1103/PhysRevD.92.114030.

[254] S. Brodsky, R. Lebed, *QCD Dynamics of Tetraquark Production*, Phys. Rev. D **91** (2015) 114025. arXiv:1505.00803, doi:10.1103/PhysRevD.91.114025.

[255] W. Chen, S.-L. Zhu, *The Vector and Axial-Vector Charmonium-like States*, Phys. Rev. D **83** (2011) 034010. arXiv:1010.3397, doi:10.1103/PhysRevD.83.034010.

[256] Z.-G. Wang, T. Huang, *Analysis of the $X(3872)$, $Z_c(3900)$ and $Z_c(3885)$ as Axial-Vector Tetraquark States with QCD Sum Rules*, Phys. Rev. D **89** (2014) 054019. arXiv:1310.2422, doi:10.1103/PhysRevD.89.054019.

[257] Z.-G. Wang, T. Huang, *The $Z_b(10610)$ and $Z_b(10650)$ as Axial-Vector Tetraquark States in the QCD Sum Rules*, Nucl. Phys. **A930** (2014) 63. arXiv:1312.2652, doi:10.1016/j.nuclphysa.2014.08.084.

[258] Z.-G. Wang, *Analysis of $P_c(4380)$ and $P_c(4450)$ as Pentaquark States in the Diquark Model with QCD Sum Rules*, Eur. Phys. J. **C76** (2016) 70. arXiv:1508.01468, doi:10.1140/epjc/s10052-016-3920-4.

[259] S. Prelovsek, L. Leskovec, *Evidence for $X(3872)$ from DD^* Scattering on the Lattice*, Phys. Rev. Lett. **111** (2013) 192001. arXiv:1307.5172, doi:10.1103/PhysRevLett.111.192001.

[260] M. Padmanath, C. Lang, S. Prelovsek, $X(3872)$ *and* $Y(4140)$ *Using Diquark-Antidiquark Operators with Lattice QCD*, Phys. Rev. D **92** (2015) 034501. arXiv:1503.03257, doi:10.1103/PhysRevD.92.034501.

[261] K. Juge, J. Kuti, C. Morningstar, *Fine Structure of the QCD String Spectrum*, Phys. Rev. Lett. **90** (2003) 161601. arXiv:hep-lat/0207004, doi:10.1103/PhysRevLett.90.161601.

[262] L. Liu, G. Moir, M. Peardon, S. Ryan, C. Thomas, P. Vilaseca, J. Dudek, R. Edwards, B. Joo, D. Richards, *Excited and Exotic Charmonium Spectroscopy from Lattice QCD*, JHEP **07** (2012) 126. arXiv:1204.5425, doi:10.1007/JHEP07(2012)126.

[263] T. Manke, *et al.*, *Hybrid Quarkonia on Asymmetric Lattices*, Phys. Rev. Lett. **82** (1999) 4396. arXiv:hep-lat/9812017, doi:10.1103/PhysRevLett.82.4396.

[264] P. Page, *Why Hybrid Meson Coupling to Two S Wave Mesons Is Suppressed*, Phys. Lett. **B402** (1997) 183. arXiv:hep-ph/9611375, doi:10.1016/S0370-2693(97)00438-3.

[265] N. Isgur, R. Kokoski, J. Paton, *Gluonic Excitations of Mesons: Why They Are Missing and Where to Find Them*, Phys. Rev. Lett. **54** (1985) 869, [AIP Conf. Proc. 132, 242 (1985)]. doi:10.1103/PhysRevLett.54.869,10.1063/1.35357.

[266] A. Le Yaouanc, L. Oliver, O. Pène, J. C. Raynal, S. Ono, $q\bar{q}g$ Hybrid Mesons in $\psi \to \gamma$ + Hadrons, Z. Phys. **C28** (1985) 309. doi:10.1007/BF01575740.

[267] P. Page, E. Swanson, A. Szczepaniak, *Hybrid Meson Decay Phenomenology*, Phys. Rev. D **59** (1999) 034016. arXiv:hep-ph/9808346, doi:10.1103/PhysRevD.59.034016.

[268] C. McNeile, C. Michael, P. Pennanen, *Hybrid Meson Decay from the Lattice*, Phys. Rev. D **65** (2002) 094505. arXiv:hep-lat/0201006, doi:10.1103/PhysRevD.65.094505.

[269] J. Dudek, R. Edwards, C. Thomas, *Exotic and Excited-State Radiative Transitions in Charmonium from Lattice QCD*, Phys. Rev. D **79** (2009) 094504. arXiv:0902.2241, doi:10.1103/PhysRevD.79.094504.

[270] F. Close, P. Page, *Gluonic Charmonium Resonances at BaBar and Belle?*, Phys. Lett. **B628** (2005) 215. arXiv:hep-ph/0507199, doi:10.1016/j.physletb.2005.09.016.

[271] E. Kou, O. Pène, *Suppressed Decay into Open Charm for the $Y(4260)$ Being an Hybrid*, Phys. Lett. **B631** (2005) 164. arXiv:hep-ph/0507119, doi:10.1016/j.physletb.2005.09.013.

[272] S.-L. Zhu, *The Possible Interpretations of $Y(4260)$*, Phys. Lett. **B625** (2005) 212. arXiv:hep-ph/0507025, doi:10.1016/j.physletb.2005.08.068.

[273] N. Ligterink, E. Swanson, *A Coulomb Gauge Model of Mesons*, Phys. Rev. C **69** (2004) 025204. arXiv:hep-ph/0310070, doi:10.1103/PhysRevC.69.025204.

[274] M. Koll, R. Ricken, D. Merten, B. Metsch, H. Petry, *A Relativistic Quark Model for Mesons with an Instanton Induced Interaction*, Eur. Phys. J. **A9** (2000) 73. arXiv:hep-ph/0008220, doi:10.1007/PL00013675.

[275] J. Weinstein, N. Isgur, $K\overline{K}$ *Molecules*, Phys. Rev. D **41** (1990) 2236. doi:10.1103/PhysRevD.41.2236.

[276] D. Caldwell, *A Possible Solution to the e / Iota Puzzle*, Mod. Phys. Lett. **A2** (1987) 771. doi:10.1142/S0217732387000963.

[277] J. Hernández, *et al.*, *Review of Particle Properties*, Phys. Lett. **B239** (1990) 1, [Erratum: Phys. Lett. **B253**, 524 (1991)]. doi:10.1016/0370-2693(91)91762-K.

[278] K. Dooley, E. Swanson, T. Barnes, *A Prediction of Spin 0 and 2 Vector Meson Molecules: A New Model of the* $f_2(1720)$, Phys. Lett. **B275** (1992) 478. doi:10.1016/0370-2693(92)91620-0.

[279] E. van Beveren, T. Rijken, K. Metzger, C. Dullemond, G. Rupp, J. Ribeiro, *A Low Lying Scalar Meson Nonet in a Unitarized Meson Model*, Z. Phys. **C30** (1986) 615. arXiv:0710.4067, doi:10.1007/BF01571811.

[280] R. Kaminski, L. Lesniak, J. Maillet, *Relativistic Effects in the Scalar Meson Dynamics*, Phys. Rev. D **50** (1994) 3145. arXiv:hep-ph/9403264, doi:10.1103/PhysRevD.50.3145.

[281] G. Li, Q. Zhao, B.-S. Zou, *Isospin Violation in* ϕ, J/ψ, $\psi' \to \omega\pi^0$ *via Hadronic Loops*, Phys. Rev. D **77** (2008) 014010. arXiv:0706.0384, doi:10.1103/PhysRevD.77.014010.

[282] G. Li, Y.-J. Zhang, Q. Zhao, *Study of Isospin Violating* ϕ *Excitation in* $e^+e^- \to \omega\pi^0$, J. Phys. **G36** (2009) 085008. arXiv:0803.3412, doi:10.1088/0954-3899/36/8/085008.

[283] C. Hanhart, B. Kubis, J. Peláez, *Investigation of* a_0-f_0 *Mixing*, Phys. Rev. D **76** (2007) 074028. arXiv:0707.0262, doi:10.1103/PhysRevD.76.074028.

[284] M. Lutz, M. Soyeur, *Radiative and Isospin-Violating Decays of* D_s*-Mesons in the Hadrogenesis Conjecture*, Nucl. Phys. **A813** (2008) 14. arXiv:0710.1545, doi:10.1016/j.nuclphysa.2008.09.003.

[285] F.-K. Guo, C. Hanhart, G. Li, U.-G. Meißner, Q. Zhao, *Novel Analysis of the Decays* $\psi' \to h_c\pi^0$ *and* $\eta_c' \to \chi_{c0}\pi^0$, Phys. Rev. D **82** (2010) 034025. arXiv:1002.2712, doi:10.1103/PhysRevD.82.034025.

[286] F.-K. Guo, C. Hanhart, G. Li, U.-G. Meißner, Q. Zhao, *Effect of Charmed Meson Loops on Charmonium Transitions*, Phys. Rev. D **83** (2011) 034013. arXiv:1008.3632, doi:10.1103/PhysRevD.83.034013.

[287] D.-Y. Chen, X. Liu, $Z_b(10610)$ *and* $Z_b(10650)$ *Structures Produced by the Initial Single Pion Emission in the* $\Upsilon(5S)$ *Decays*, Phys. Rev. D **84** (2011) 094003. arXiv:1106.3798, doi:10.1103/PhysRevD.84.094003.

[288] D.-Y. Chen, X. Liu, *Predicted Charged Charmonium-Like Structures in the Hidden-Charm Dipion Decay of Higher Charmonia*, Phys. Rev. D **84** (2011) 034032. arXiv:1106.5290, doi:10.1103/PhysRevD.84.034032.

[289] Q. Wang, C. Hanhart, Q. Zhao, *Decoding the Riddle of* $Y(4260)$ *and* $Z_c(3900)$, Phys. Rev. Lett. **111** (2013) 132003. arXiv:1303.6355, doi:10.1103/PhysRevLett.111.132003.

[290] E. Swanson, Z_b *and* Z_c *Exotic States as Coupled Channel Cusps*, Phys. Rev. D **91** (2015) 034009. arXiv:1409.3291, doi:10.1103/PhysRevD.91.034009.

[291] A. Szczepaniak, *Triangle Singularities and XYZ Quarkonium Peaks*, Phys. Lett. **B747** (2015) 410. arXiv:1501.01691, doi:10.1016/j.physletb.2015.06.029.

[292] F.-K. Guo, C. Hanhart, Q. Wang, Q. Zhao, *Could the Near-Threshold XYZ States Be Simply Kinematic Effects?*, Phys. Rev. D **91** (2015) 051504. arXiv:1411.5584, doi:10.1103/PhysRevD.91.051504.

[293] E. Swanson, *Cusps and Exotic Charmonia*, Int. J. Mod. Phys. **E25** (2016) 1642010. arXiv:1504.07952, doi:10.1142/S0218301316420106.

[294] Y. Chen, *et al.*, *Low-Energy Scattering of* $(D^*\bar{D}^*)^\pm$ *System and the Resonance-like Structure* $Z_c(4025)$, Phys. Rev. D **92** (2015) 054507. arXiv:1503.02371, doi:10.1103/PhysRevD.92.054507.

[295] Z.-Y. Zhou, Z. Xiao, *Distinguishing Near-Threshold Pole Effects from Cusp Effects*, Phys. Rev. D **92** (2015) 094024. arXiv:1505.05761, doi:10.1103/PhysRevD.92.094024.

[296] J. He, *The* $Z_c(3900)$ *as a Resonance from the* $D\bar{D}^*$ *Interaction*, Phys. Rev. D **92** (2015) 034004. arXiv:1505.05379, doi:10.1103/PhysRevD.92.034004.

[297] S. Blitz, R. Lebed, *Tetraquark Cusp Effects from Diquark Pair Production*, Phys. Rev. D **91** (2015) 094025. arXiv:1503.04802, doi:10.1103/PhysRevD.91.094025.

[298] Q.-Y. Lin, X. Liu, H.-S. Xu, *Charged Charmoniumlike State* $Z_c(3900)^\pm$ *via Meson Photoproduction*, Phys. Rev. D **88** (2013) 114009. arXiv:1308.6345, doi:10.1103/PhysRevD.88.114009.

[299] R. Aaij, *et al.*, *Measurement of the Resonant and CP Components in* $\overline{B}^0 \to J/\psi\,\pi^+\pi^-$ *Decays*, Phys. Rev. D **90** (2014) 012003. arXiv:1404.5673, doi:10.1103/PhysRevD.90.012003.

[300] B. Aubert, *et al.*, *Observation of a Narrow Meson Decaying to* $D_s^+\pi^0$ *at a Mass of* 2.32 GeV/c^2, Phys. Rev. Lett. **90** (2003) 242001. arXiv:hep-ex/0304021, doi:10.1103/PhysRevLett.90.242001.

[301] B. Aubert, *et al.*, *A Structure at* 2175 MeV *in* $e^+e^- \to \phi f_0(980)$ *Observed via Initial-State Radiation*, Phys. Rev. D **74** (2006) 091103. arXiv:hep-ex/0610018, doi:10.1103/PhysRevD.74.091103.

[302] M. Karliner, *Doubly Heavy Exotic Mesons and Baryons and How to Look for Them*, Acta Phys. Polon. **B47** (2016) 117. doi:10.5506/APhysPolB.47.117.

[303] S. Koshkarev, V. Anikeev, *Production of the Doubly Charmed Baryons—The Double Intrinsic Charm Approach,* arXiv:1605.03070.

[304] R. Jaffe, *Perhaps a Stable Dihyperon*, Phys. Rev. Lett. **38** (1977) 195, [Erratum: Phys. Rev. Lett. **38**, 617 (1977)]. doi:10.1103/PhysRevLett.38.195.

[305] V. Matveev, P. Sorba, *Is Deuteron a Six Quark System?*, Lett. Nuovo Cim. **20** (1977) 435. doi:10.1007/BF02790723.

[306] M. Lüscher, *Two Particle States on a Torus and Their Relation to the Scattering Matrix*, Nucl. Phys. **B354** (1991) 531. doi:10.1016/0550-3213(91)90366-6.

[307] M. Hansen, S. Sharpe, *Multiple-Channel Generalization of Lellouch-Lüscher Formula*, Phys. Rev. D **86** (2012) 016007. arXiv:1204.0826, doi:10.1103/PhysRevD.86.016007.

[308] J. Dudek, R. Edwards, C. Thomas, D. Wilson, *Resonances in Coupled* πK-ηK *Scattering from Quantum Chromodynamics*, Phys. Rev. Lett. **113** (2014) 182001. arXiv:1406.4158, doi:10.1103/PhysRevLett.113.182001.